

AD-A128 955

GPS (GLOBAL POSITIONING SYSTEM) ERROR BUDGETS ACCURACY
AND APPLICATIONS C. (U) FEDERAL ELECTRIC CORP
VANDENBERG AFB CA SYSTEMS PERFORMANCE A.

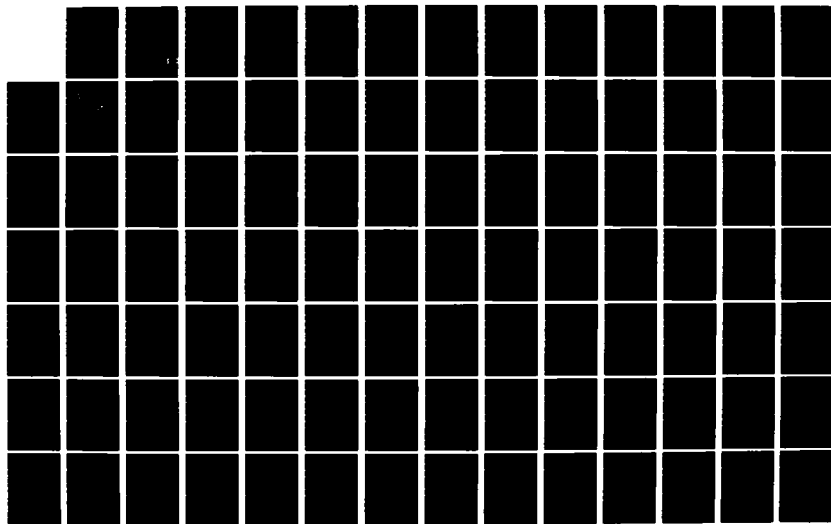
1/2

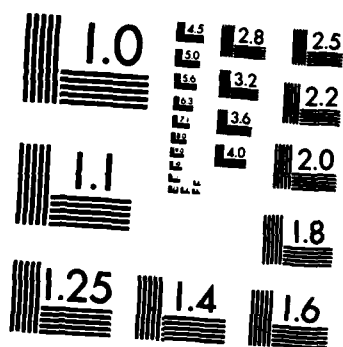
UNCLASSIFIED

R A BROOKS ET AL. DEC 82 A5300-T-82-33

F/G 17/7

NL





MICROCOPY RESOLUTION TEST CHART
NATIONAL BUREAU OF STANDARDS-1963-A

DA 128955

**GPS ERROR BUDGETS, ACCURACY,
AND
APPLICATIONS CONSIDERATIONS
FOR
TEST AND TRAINING RANGES**

SYSTEMS PERFORMANCE ANALYSIS DEPARTMENT

FEDERAL ELECTRIC CORPORATION

WTR Division, Vandenberg Air Force Base, California 93437

DECEMBER 1982

FINAL REPORT

**APPROVED FOR PUBLIC RELEASE
DISTRIBUTION UNLIMITED**

Prepared for

WESTERN SPACE AND MISSILE CENTER (AFSC)

Vandenberg Air Force Base, California 93437


**DTIC
ELECTE
JUN 06 1983**

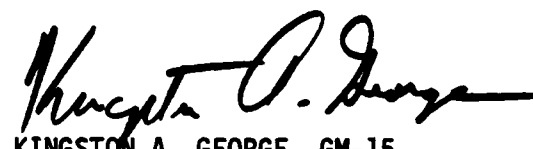
E

DTIC FILE COPY


83 06 03 01 2

This final report was submitted by Systems Performance Analysis Department, Federal Electric Corporation - ITT, WTR Division, P.O. Box 5728, Vandenberg Air Force Base, CA 93437, under Contract F04703-81-C-0101 with the Western Space and Missile Center, Vandenberg Air Force Base, CA 93437. Operations Research Analyst, Mr. J. McConnell, WSMC/XRQA, was the Division Project Engineer-in-Charge. This technical report has been reviewed and is approved for publication.


JOHN B. McCONNELL GS-13
Project Engineer


KINGSTON A. GEORGE GM-15
Chief, Requirements and
Analysis Division

FOR THE COMMANDER


WAYNE J. CRAFT, Colonel, USAF
Director of Plans, Programs & Requirements

REPORT DOCUMENTATION PAGE		READ INSTRUCTIONS BEFORE COMPLETING FORM
1. REPORT NUMBER WSMC TR 82- 2	2. GOVT ACCESSION NO. AD-A128955	3. RECIPIENT'S CATALOG NUMBER
4. TITLE (and Subtitle) GPS Error Budgets, Accuracy, and Applications Considerations for Test and Training Ranges		5. TYPE OF REPORT & PERIOD COVERED Final December 1982
7. AUTHOR(s) Dr. Richard A. Brooks, et al.		6. PERFORMING ORG. REPORT NUMBER AS300-T-82-33 ^v
9. PERFORMING ORGANIZATION NAME AND ADDRESS Systems Performance Analysis Department, AS300 Federal Electric Corporation - III WTR Division, P.O. Box 5728 Vandenberg Air Force Base, CA 93437		8. CONTRACT OR GRANT NUMBER(s) Western Space & Missile Center Contract No. F4703-81-C-0101
11. CONTROLLING OFFICE NAME AND ADDRESS Western Space and Missile Center XRQA Vandenberg Air Force Base, CA 93437		10. PROGRAM ELEMENT, PROJECT, TASK AREA & WORK UNIT NUMBERS Task No. AI015
14. MONITORING AGENCY NAME & ADDRESS (if different from Controlling Office) Same as above		12. REPORT DATE December 1982 Final
		13. NUMBER OF PAGES
		15. SECURITY CLASS. (of this report) Unclassified
		15a. DECLASSIFICATION/DOWNGRADING SCHEDULE N/A
16. DISTRIBUTION STATEMENT (of this Report) Unlimited Distribution		
17. DISTRIBUTION STATEMENT (of the abstract entered in Block 20, if different from Report) N/A		
18. SUPPLEMENTARY NOTES None		
19. KEY WORDS (Continue on reverse side if necessary and identify by block number) NAVSTAR Global Positioning System (GPS) Range Applications Time, Space, Position Information (TSPI) Instrumentation Test and Training Range Instrumentation		
20. ABSTRACT (Continue on reverse side if necessary and identify by block number) A Triservices study, currently in progress, will develop representative test and training range instrumentation configurations based on NAVSTAR Global Positioning System (GPS) technology, evaluate performance capabilities, and develop cost information. The Air Force Western Space and Missile Center (WSMC) Vandenberg AFB, California is the lead organization. During the early phase of the study a collection of GPS documentation was established for reference purposes. This documentation along with experience from other GPS projects		

20. ABSTRACT (continued)

at WSMC provided the basis for the report. This report provides information that should be useful to range analysts developing and evaluating GPS-based instrumentation concepts at the test and training ranges. Some of the subjects are not thoroughly developed and may require further work. Subjects addressed include definition of performance evaluation terms, Doppler data processing, use of pseudo-satellite ground stations, two and three dimensional solutions, receiver and translator configurations, and vehicle dynamics effects on receiver operation.

PREFACE

A Triservices study, currently in progress, will develop representative test and training range instrumentation configurations compatible with the NAVSTAR Global Positioning System (GPS), evaluate performance capabilities, and develop cost information. The Air Force Western Space and Missile Center, Vandenberg AFB, California provided the study chairman and has responsibility for other GPS oriented projects. During the early phase of the study a collection of GPS articles and documents was established for reference purposes. Those documents and experience from WSMC projects provided the information herein. Due to the need to expedite availability of this information to range analysts responsible for developing and evaluating GPS compatible instrumentation configurations for their particular situations, some of the subjects are not thoroughly developed and further work is necessary. Definition of performance evaluation terms and Doppler data processing refinements are well developed. Significant subjects included in the applications considerations section include use of pseudo-satellite ground stations to supplement the satellite constellation, methods and effects of two dimensional solutions, receiver and translator configurations, and effects of vehicle dynamics on receiver operation and results.

Accession For	
NTIS GRA&I	<input checked="" type="checkbox"/>
DTIC TAB	<input type="checkbox"/>
Unannounced	<input type="checkbox"/>
Justification	
By	
Distribution/	
Availability Codes	
Dist	Avail and/or Special
A	



ACKNOWLEDGEMENT

Various individuals contributed to the content of this document. Dr. Richard A. Brooks (FEC consultant) developed the report outline and contributed Sections 2.0, 3.0 and subsections 4.10 and 4.11 as well as technical review of other sections. Robert L. Baker was the SPAD Task Manager; he obtained the reference material and contributed Section 1 and subsection 4.5. Hugh A. Eakin contributed subsections 4.6 and 4.9 and performed the editorial rewrite required to improve report coherency. Subsections 4.1 and 4.7 were contributed by Joe C. Warnock and George R. McKelvey respectively. Subsection 4.8 was contributed by Steven A. Cresswell and subsections 4.3 and 4.4 by Dr. Morgan Kuo and with Mr. Cresswell, subsection 4.2. The graphics were prepared by Greg S. Boyland and William F. Cackler and last but not least, the manuscript was prepared by Beulah A. Kirkham.

TABLE OF CONTENTS

<u>SECTION</u>	<u>TITLE</u>	<u>PAGE</u>
	PREFACE	<i>i</i>
	ACKNOWLEDGEMENT	<i>ii</i>
	LIST OF FIGURES	<i>v</i>
	LIST OF TABLES	<i>vii</i>
1.0	INTRODUCTION	1.0-1
	1.1 GPS Development and Operation	1.1-1
	1.2 Document Organization and Summary	1.2-1
2.0	ERROR BUDGETS	2.0-1
	2.1 Pseudo-Range Noise Error	2.0-6
	2.2 Pseudo-Range Ionospheric Delay Compensation	2.0-7
	2.3 Nominal Real-Time Error Budget	2.0-9
	2.4 Pseudo-Doppler Range Noise Error and Ionospheric Delay Compensation	2.0-11
	2.5 Ideal Post-Test Error Budget	2.0-13
	2.6 Summary of Error Budget Properties	2.0-15
3.0	ACCURACY MEASURES	3.0-1
	3.1 Three Dimensional Error Probability Distribution	3.0-4
	3.2 Two Dimensional Error Probability Distribution	3.0-7
	3.3 One Dimensional Error Probability Distribution	3.0-9
	3.4 Dilution of Precision	3.0-9
	3.5 Accuracy Measure Relationships	3.0-10
	3.6 Error Probability Relationships to Accuracy Measures	3.0-13
4.0	APPLICATIONS CONSIDERATIONS	4.0-1
	4.1 Real-Time versus Post-Test	4.1-1
	4.2 Relative versus Absolute and Small Arena versus Global Navigation Issues	4.2-1
	4.3 Satellite Constellations Current and Planned	4.3-1
	4.4 2 versus 3 Dimensional Navigation	4.4-1
	4.5 Pseudo-Satellites	4.5-1
	4.6 Effects of Vehicle Dynamics on Receiver Operation	4.6-1
	4.7 The GPS Receiver versus Translator for Mobile and/or Stationary Applications	4.7-1 ~

TABLE OF CONTENTS (CONTINUED)

<u>SECTION</u>	<u>PAGE</u>
4.9 Standard User Hardware Characteristics	4.9-1
4.10 Filtering and Smoothing	4.10-1
4.11 Doppler Processing	4.11-1
5.0 CONCLUSIONS AND RECOMMENDATIONS	5.0-1
BIBLIOGRAPHY	<i>vii</i>
APPENDICES	A-1
GLOSSARY	<i>xiii</i>

LIST OF FIGURES

<u>FIGURE</u>		<u>PAGE</u>
1.1	Three Basic Segments of Global Positioning System	1.1-2
1.2	GPS Receiver Simplified Block Diagram	1.1-6
2.1	Doppler Smoothing Technique	2.0-3
3.1	Distribution of 3 Dimensional Radial Errors Normalized by Sigma S	3.0-15
3.2	Distribution of 3 Dimensional Radial Errors Normalized by SEP	3.0-16
3.3	Distribution of 3 Dimensional Radial Errors Normalized by Sigma P	3.0-17
3.4	Distribution of 2 Dimensional Radial Errors Normalized by Sigma C	3.0-18
3.5	Distribution of 2 Dimensional Radial Errors Normalized by CEP	3.0-19
3.6	Distribution of 2 Dimensional Radial Errors Normalized by Sigma H	3.0-20
3.7	EEP for 3 Dimensions (Effective)	3.0-21
3.8	EEP for 2 Dimensions (Effective)	3.0-22
3.9	EEP for 1 Dimension (Effective)	3.0-23
4.2.1	Horizontal and Vertical Errors	4.2-3
4.2.2	Relationship of Obliquity Factor to Surface Elevation Angle	4.2-5
4.2.3	Mean Ionospheric Delay and Envelope of Delay Variations vs Time of Day During March	4.2-5
4.2.4	Spatial Variation of Pseudo-Range Error Due to Space and Control Segments	4.2-6
4.2.5	Temporal Variation of Pseudo-Range Error Due to Space and Control Segments	4.2-7
4.3.1	NAVSTAR/GPS 6-Plane, 18-Satellite Configuration	4.3-2
4.3.2	Three-Dimensional Navigation at Yuma	4.3-7
4.3.3	Three-Dimensional Navigation at Grand Bahama	4.3-7
4.3.4	Three-Dimensional Navigation at Cold Lake	4.3-8
4.3.5	Two-Dimensional Navigation at Yuma	4.3-8
4.3.6	Geometric Method to Select Optimum Satellite Constellation	4.3-10
4.4.1(a)	Relationship of PDOP and HDOP with A Priori Altitude Uncertainty in 3 Dimensional Navigation	4.4-7
4.4.1(b)	Relationship of PDOP and HDOP with A Priori Altitude Uncertainty in 3 Dimensional Navigation	4.4-8

LIST OF FIGURES (CONTINUED)

<u>FIGURE</u>	<u>PAGE</u>
4.4.1(c) Relationship of PDOP and HDOP with A Priori Altitude Uncertainty in 3 Dimensional Navigation	4.4-8
4.4.1(d) Relationship of PDOP and HDOP with A Priori Altitude Uncertainty in 3 Dimensional Navigation	4.4-9
4.4.2(a) Relationship of HDOP with Altitude Uncertainty in 2 Dimensional Navigation	4.4-11
4.4.2(b) Relationship of HDOP with Altitude Uncertainty in 2 Dimensional Navigation	4.4-12
4.4.2(c) Relationship of HDOP with Altitude Uncertainty in 2 Dimensional Navigation	4.4-13
4.4.2(d) Relationship of HDOP with Altitude Uncertainty in 2 Dimensional Navigation	4.4-14
4.4.3 2D and 3D Constellation Value (CV) During Buildup	4.4-15
4.5.1 ICBM Pseudo-Satellite Operation	4.5-3
4.7.1 GPS Satellite C/A Code Signal Generation Simplified Block Diagram	4.7-3
4.7.2 Simplified Spread Spectrum Receiver Block Diagram	4.7-4
4.7.3 Receiving and Recording GPS Signals Using Standard Telemetry Equipment	4.7-6
4.7.4(a) Analog Playback	4.7-8
4.7.4(b) Digital Playback	4.7-8
4.7.5 GPS Relay Techniques Simplified Block Diagram	4.7-12
4.7.6 Transmitter Power and Transmitter Final Battery Penalties For Equivalent Singal-to-noise Performance at the Receiver Site	4.7-18
4.7.7 Examples of Potential Translator Applications	4.7-22

LIST OF TABLES

<u>TABLE</u>		<u>PAGE</u>
1.1	GPS Satellite Signal Characteristics	1.1-3/1.1-4
2.1	GPS System Specification Error Budget	2.0-5
2.2	Received Signal Levels (Specification)	2.0-6
2.3	Carrier-To-Noise Density Ratios	2.0-6
2.4	Pseudo-Ranging Noise Errors (RMS)	2.0-7
2.5	RMS Noise Errors Before and After Dual Frequency Ionospheric Delay Compensation	2.0-9
2.6	GPS Real-Time Error Budget	2.0-10
2.7	Pseudo-Doppler Range RMS Noise Errors Before and After Ionospheric Delay Compensation	2.0-12
2.8	RMS Noise Errors for Pseudo-Delta Range and Pseudo-Range Rate	2.0-13
2.9	GPS Post-Test Error Budget	2.0-14
2.10	Error Effects for Various Navigation Modes	2.0-16
3.1	3 Dimensional Accuracy Relations	3.0-12
3.2	2 Dimensional Accuracy Relations	3.0-12
4.2.1	GPS Error Budget (Absolute and Relative Navigation)	4.2-2
4.3.1	Navigation Availability with Four Satellites	4.3-3
4.3.2	Navigation Availability with Five Satellite Constellation	4.3-4
4.3.3	Navigation Availability with Six Satellite Constellation	4.3-5
4.3.4	Total GPS Daily Coverage	4.3-6
4.3.5	Anticipated Worldwide User Position Error Distribution	4.3-11
4.7.1	Comparisons of Relay and Receiver Systems	4.7-10
4.7.2	GPS Receiver Requirement Comparisons	4.7-13
4.7.3	Comparison of Relay System Characteristics	4.7-20
4.9.1	Accuracy Equations for GPS Receiver Types (Based on 18 Satellite Configuration)	4.9-7

1.0 INTRODUCTION

Use of the Global Positioning System (GPS) for Army, Navy and Air Force test and training ranges' Time, Space and Position Information (TSPI) requirements provides potential improvements in accuracy and mobility and less cost to the nation in comparison to current range instrumentation systems. This document was prepared to provide members of the Triservices ranges' test and evaluation community with an orientation to GPS, examination of the error sources affecting GPS performance, discussion of accuracy measures developed to assess GPS performance, and a variety of GPS applications and related issues of interest to the range analyst and planner. Means of evaluating accuracy of results using the GPS capability and complementing it to improve local accuracy or extend test periods for particular ranges' scenarios are discussed.

GPS will be fully operational in the late 1980's with an array of 18 satellites that create, in effect, an accurate RF three dimensional grid all over the world and extending thousands of miles above the surface. GPS overcomes previous navigation systems limitations of insufficient accuracy, limited area, and two dimensional results. The use of GPS is not restricted to number of participants, weather conditions, visibility, or location (except for range requirements such as data link line-of-sight). Common use of GPS technology will allow standardization of data processing and interfaces.

1.1 GPS Development and Operation

The GPS program has been in existence for approximately fourteen years. It was begun when the United States Air Force, Army, Marine Corps, Navy and Defense Mapping Agency combined their technical resources to develop a highly accurate space-based navigation system. The development of GPS is being managed by a Joint Program Office (JPO) at the Air Force Systems Command, Space Division, in Los Angeles. The management team consists of DoD, DoT and NATO personnel.

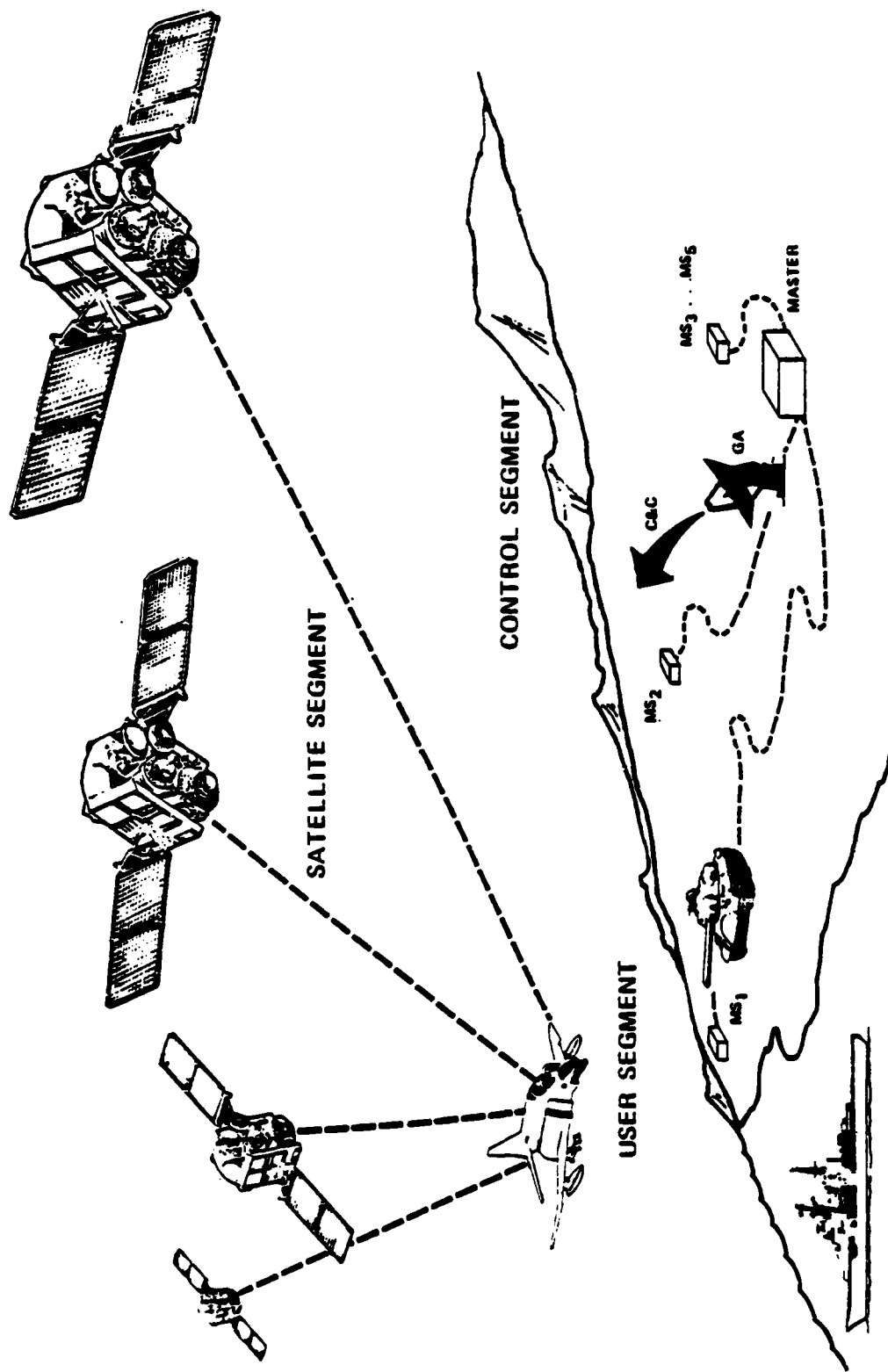
The GPS program is being conducted through three successive phases. During Phase I, GPS performance and feasibility were validated. Currently in Phase II, GPS operational effectiveness is being validated. In Phase III, production and deployment of GPS will be accomplished.

The GPS comprises three major segments: Space, Control and User as shown in Figure 1.1.

The Space Segment will consist of a number of NAVSTAR satellites. Each satellite transmits an L_1 (1575.42 MHz) and an L_2 (1227.6 MHz) signal. L_1 is modulated by a Precise (P) signal and a Clear/Acquisition (C/A) signal. L_2 is modulated by either a P or C/A signal. Superimposed on these spread spectrum signals is a navigation message containing ephemeris, clock and atmospheric propagation correction data. Table 1.1 summarizes satellite signal characteristics. Each satellite is positioned in a 10,900 nautical mile circular orbit (with period equal to 12 sidereal hours) at an inclination of 55 degrees. In the fully operational configuration, there are 18 satellites in six orbital planes with three satellites in each plane. This configuration is designed to provide a minimum of four satellites in view to any user, thereby ensuring worldwide coverage.

The Control Segment includes a number of Monitor Stations and Ground Antennas located throughout the world, together with a Master Control Station. The Monitor Stations each contain a GPS receiver which passively tracks all NAVSTARs within view and collects orbital data. The Master Control Station processes the data collected by the Monitor stations and estimates orbital elements, clock parameters and atmospheric propagation corrections for each

THREE BASIC SEGMENTS OF GLOBAL POSITIONING SYSTEM



- MONITOR STATION
 - SATELLITE POSITION DATA
 - SATELLITE TIME DATA
- MASTER STATION
 - DATA PROCESSING FOR SATELLITE
 - EPHEMERIS AND CLOCK MODEL
 - PARAMETERS
- GROUND ANTENNA
 - NAV DATA REFRESH AND C&C

- ARMY
- NAVY
- AIR FORCE
- USMC
- NATO
- CIVIL SECTOR
 - GENERAL AVIATION
 - MARINE
 - SCIENTIFIC
 - NASA

"PSEUDORANGE" (CIRCUIT PROPAGATION DELAY)

$$\rho = \sqrt{(x_u - x_s)^2 + (y_u - y_s)^2 + (z_u - z_s)^2} + c \Delta t_{\text{user}}$$

1 2 3 4

FIGURE 1.1

GPS SATELLITE SIGNALS CHARACTERISTICS

TABLE 1.1

	CODES		SIGNAL LEVEL (dBW)	CENTER FREQUENCY (MHz)
	C/A	P		
L1	K	K	-163/-160	1575.42
L2	S	N	-166	1227.60

K - CONSTANTLY TRANSMITTED.
 N - NORMALLY TRANSMITTED.
 S - SELECTABLE (NOT SIMULTANEOUSLY)

"P" (PRECISION) CODE:

SEVEN DAY SEGMENT OF 267 DAY

CODE SEQUENCE.

10.23 MHz RATE.

SPECIAL ACQUISITION PROCEDURE REQUIRED.

PROVIDES ACCURATE PSEUDO-RANGE AND

PSEUDO-RANGE RATE DATA.

"C/A" (CLEAR ACCESS) CODE:

1 MSEC REPETITION PERIOD.

1.023 MHz RATE.

EASY ACQUISITION

LOWER ACCURACY.

GPS SATELLITE SIGNALS CHARACTERISTICS (CONT.)

TABLE 1.1 (CONT.)

CODE FUNCTIONS:	NAVIGATION MESSAGE:
1. SPACE VEHICLE IDENTIFICATION.	50 bps NRZ MODULATION.
o SAME PRN CODE GENERATORS	5-6 SECOND SUBFRAME LENGTH.
USED IN ALL SATELLITES.	
o EACH SATELLITE USES A SEPARATE	PROVIDES
SEGMENT.	- HEALTH AND STATUS
2. PSEUDO-RANGE MEASUREMENTS	- HAND-OVER-WORD
	- CLOCK CORRECTION PARAMETERS
	- ORBIT EPHEMERIDES
	- ATMOSPHERIC PROPAGATION DELAY
	CORRECTIONS

NAVSTAR satellite. These estimates are used to update the navigation message of each satellite, and the updated messages are transmitted to the satellites via the Ground Antennas.

The User Segment consists of individual User Equipment (UE) sets and support equipment. Each UE set passively receives data transmitted by NAVSTAR satellites and provides navigation and time information to a host vehicle. Receiver operation is illustrated in Figure 1.2.

The concept of GPS rests on the principle of trilateration. That is, when the positions of three points (suitably located) are known together with the distance (or range) from each to a fourth point, then the position of the fourth point can be determined. In GPS, the positions of the NAVSTAR satellites are contained in their respective navigation messages. The User infers range to a given satellite by measuring the propagation time of the encoded radio signal transmitted by the satellite. The user inferred range obtained by conversion of measured propagation time is called pseudo-range. Because of the clock offset, the user requires pseudo-ranges from at least four (vice three) satellites to estimate his three dimensional position and clock error relative to GPS time.

In a completely analogous manner, the user obtains pseudo-range rates and extracts his velocity and the drift rate of his clock relative to GPS time by measuring the received (Doppler shifted) frequencies of the carrier signals from four (or more) NAVSTAR satellites.

GPS RECEIVER SIMPLIFIED BLOCK DIAGRAM

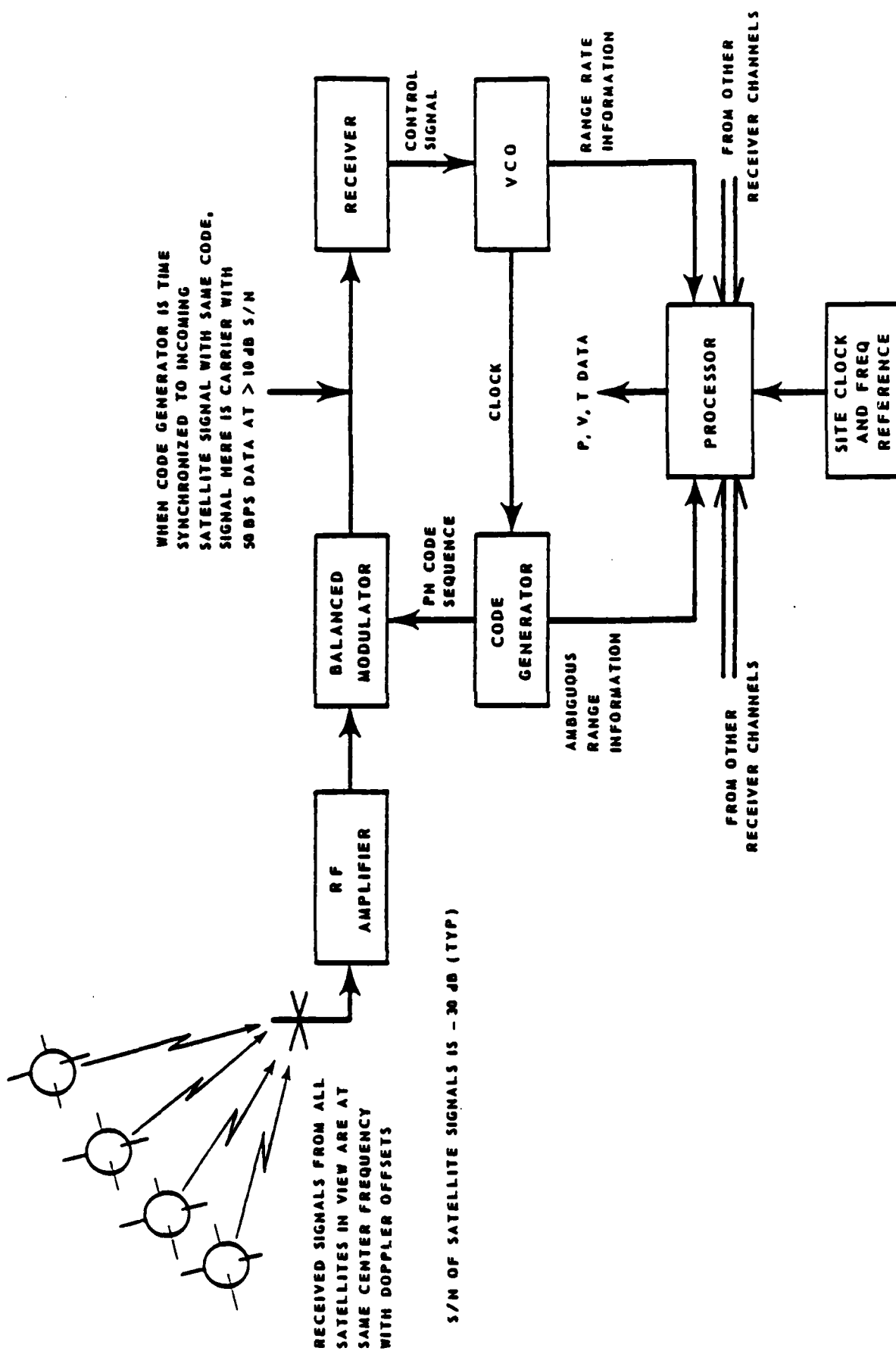


FIGURE 1.2

1.2 Document Organization and Summary

Sections 2.0 and 3.0 develop accuracy evaluation concepts and Section 4.0 contains several applications considerations. In Section 2.0, the effects of various GPS error sources are discussed with the objective of establishing an error budget for GPS satellite to receiver range measurements. Two error budgets (one for real-time and one for post-test uses) are developed and the GPS error specification is presented. The contributors to the error budgets are allocated by responsibility to the Space Segment, the Control Segment, or the User Segment. Although the error sources in each segment are subject to some manipulation, attention is focused primarily on error sources which are most directly affected by the user.

The User Segment errors are strongly dependent on link margin (Signal-to-Noise Ratio), code selection, method of ionospheric delay compensation, and whether effective use is made of the available Doppler measurement data. Because of this strong dependence, the main thrust of Section 2.0 deals with these issues.

The definition, relationship and interpretation of various accuracy measures that can be used to assess GPS navigation and time-transfer performance are presented in Section 3.0. There exists a variety of accuracy measures currently used to assess the performance of navigation and weapons systems. These measures include such entities as Root-Sum-Square (RSS) quantities, spherical and circular standard error, and spherical and circular error probable. The proliferation of such measures raises questions regarding their respective interpretation and mutual relationships. In Section 3.0, various commonly used accuracy measures are defined. The assumption of Gaussian probability distribution is invoked to enable quantitative interpretation of each such measure and its relation to other measures. The main thrust of Section 3.0 is to provide the analyst with some guidelines which will enable proper selection and calculation of the appropriate accuracy measure for his particular application.

Section 4.0 contains eleven subsections dealing with a variety of considerations for GPS Range applications. An attempt is made to relate the interacting effects of the various subsections and of the previous sections.

Subsection 4.1 amplifies the limitations to real-time data processing and possible refinements for post-test processing. Subsection 4.2 addresses relative and absolute accuracy considerations and applications. "Relative" implies that the position, velocity and time data of test participant(s) with respect to each other is the significant information as compared to "absolute" which requires data in a global coordinate system. Relative is primarily applicable to small arena or local scenarios. Global scenarios might use relative techniques for some requirements such as propulsion and guidance system performance evaluation and for scoring.

Subsection 4.3 provides information about the current and future number of satellites available. Two effects of major importance for Range tests are the periods when a sufficient number of satellites are above the horizon and the accuracy of the results due to their positions relative to the test participants. Determination of test participants' TSPI using the current GPS satellites is restricted to a few periods of a few hours per day. Length of the periods depends to some extent on the number of parameters to be estimated and user latitude and longitude. Subsection 4.4 continues the discussion of accuracy considerations with the emphasis on two and three dimensional solutions.

Complementing the current GPS satellite array with compatible ground stations can extend test periods, make testing independent of the satellites, improve accuracy and line-of-sight considerations, and/or provide range C^3 capabilities. Subsection 4.5 provides considerations of this concept referred to as "pseudo-satellites" or "inverted GPS".

Test vehicle dynamics induce tracking errors and can inhibit acquisition of data with traditional range instrumentation. GPS technology is subject to the same problems but in different manners than the range analyst is accustomed to evaluating. Subsection 4.6 identifies these problems and presents information about their effects. Methods of "aiding" signal acquisition and track are reviewed.

Subsection 4.7 discusses uses of GPS receiver and translator configurations. WSMC experience includes use of GPS receivers during two Minuteman ICBM launches and development of a GPS translator equipped sonobuoy array for

reentry vehicle scoring. A missile-borne translator is also being evaluated. Section 4.7 discusses receiver aiding and various approaches to translator designs.

Raw measurement data rather than navigation solution results are preferable for test and training range data processing in order to evaluate the output and/or apply more sophisticated processing techniques. Section 4.8 discusses these needs from the standpoint of making provision in user equipment under development for these data requirements. Another consideration the range analyst must take into account is the ability to record and/or transmit the data since operational equipment modifications are frequently forbidden or restricted.

Subsection 4.9 continues discussions of GPS receivers being developed with descriptions of their characteristics and specifications, wherever possible.

Section 4.10 discusses applications of Kalman Filter/Smoother (KFS) techniques to GPS measurements and the complementary benefits of GPS data and inertial navigation system data.

Subsection 4.11 continues the discussion of GPS data processing and develops subtle concepts in Doppler data processing.

2.0 ERROR BUDGETS

For each operational combination of a code (C/A or P), a link (L_1, L_2, \dots) and a Space Vehicle (SV) within view of a properly equipped GPS user, there exist two types of measurements available to the user. These measurement types are, respectively, pseudo-time delay and pseudo-Doppler shift of a signal propagating from the SV to the user receiver.

When the pseudo-time delay is scaled by the speed of light, a pseudo-range measurement is obtained. Denoting this measurement by \tilde{R} , it follows that

$$\tilde{R} = R + CT_U + \epsilon_R \quad ,$$

where R is the range (from the indicated location of the SV to the true location of the user receiver), C is the speed of light, T_U is the user clock offset relative to GPS time, and ϵ_R is the combined error in the pseudo-range measurement from all sources.

In a somewhat similar fashion, the pseudo-Doppler shift cycles can be counted over an arbitrary time interval and converted to an incremental pseudo-Doppler range measurement.

Introducing the increment notation

$$[X]_{t_1}^{t_2} = X(t_2) - X(t_1) \quad ,$$

The incremental pseudo-Doppler range measurement over time interval $[t_1, t_2]$ is expressed by

$$[\tilde{r}]_{t_1}^{t_2} = [R]_{t_1}^{t_2} + C[T_U]_{t_1}^{t_2} + [\epsilon_r]_{t_1}^{t_2} \quad ,$$

where R , T_U and C have the same meaning as before, and ϵ_r is the combined error in the pseudo-Doppler range measurement from all sources.

There exist numerous methods of processing pseudo-range and pseudo-Doppler range measurements to perform various navigation functions. Some of these methods will be explored in detail in a later section. Here the more important

methods are examined in brief.

The most direct method of GPS navigation is to utilize four or more pseudo-range measurements (from suitable SVs) and solve for user position and time offset. And in a similar fashion, it is possible to solve for user velocity and frequency offset by utilizing four or more incremental pseudo-Doppler range measurements which have been approximately differentiated to obtain pseudo-range rates.

Another method (applicable primarily to post-test processing) consists of two steps. First the pseudo-range and incremental pseudo-Doppler range measurements are differenced and averaged to obtain a more accurate initial value of pseudo-range to each SV. Then the smoothed initial value of pseudo-range is added to the incremental pseudo-Doppler range measurements for each SV to obtain high precision pseudo-range measurements at a high data rate. This technique (developed in Section 4.11) is illustrated in Figure 2.1.

Furthermore, in addition to the above navigation methods (which are absolute or global in nature), there exist two differential navigation methods.

Relative navigation is defined as the determination of the coordinate differences (in a suitable frame of reference) between two different users at a common set of times. Delta navigation is defined as the determination of the coordinate differences between two or more locations occupied by a single user at different times.

In any method of navigation, the consideration of accuracy performance is generally a matter of major concern. The assessment of navigation performance is a two step process. The first step, which is the main subject of this section, consists of categorization, characterization, and quantification of the various error contributors in the user measurement equations. The second step, which is the subject of Section 3.0, consists of quantification of the process of error propagation through the user algorithms together with the definition and calculation of appropriate accuracy measures for the purpose of performance analysis.

The end result of the first of the two steps in navigation performance analysis is a budget for user measurement errors. This error budget usually provides estimates of the RMS values of the various error contributors, as well as the

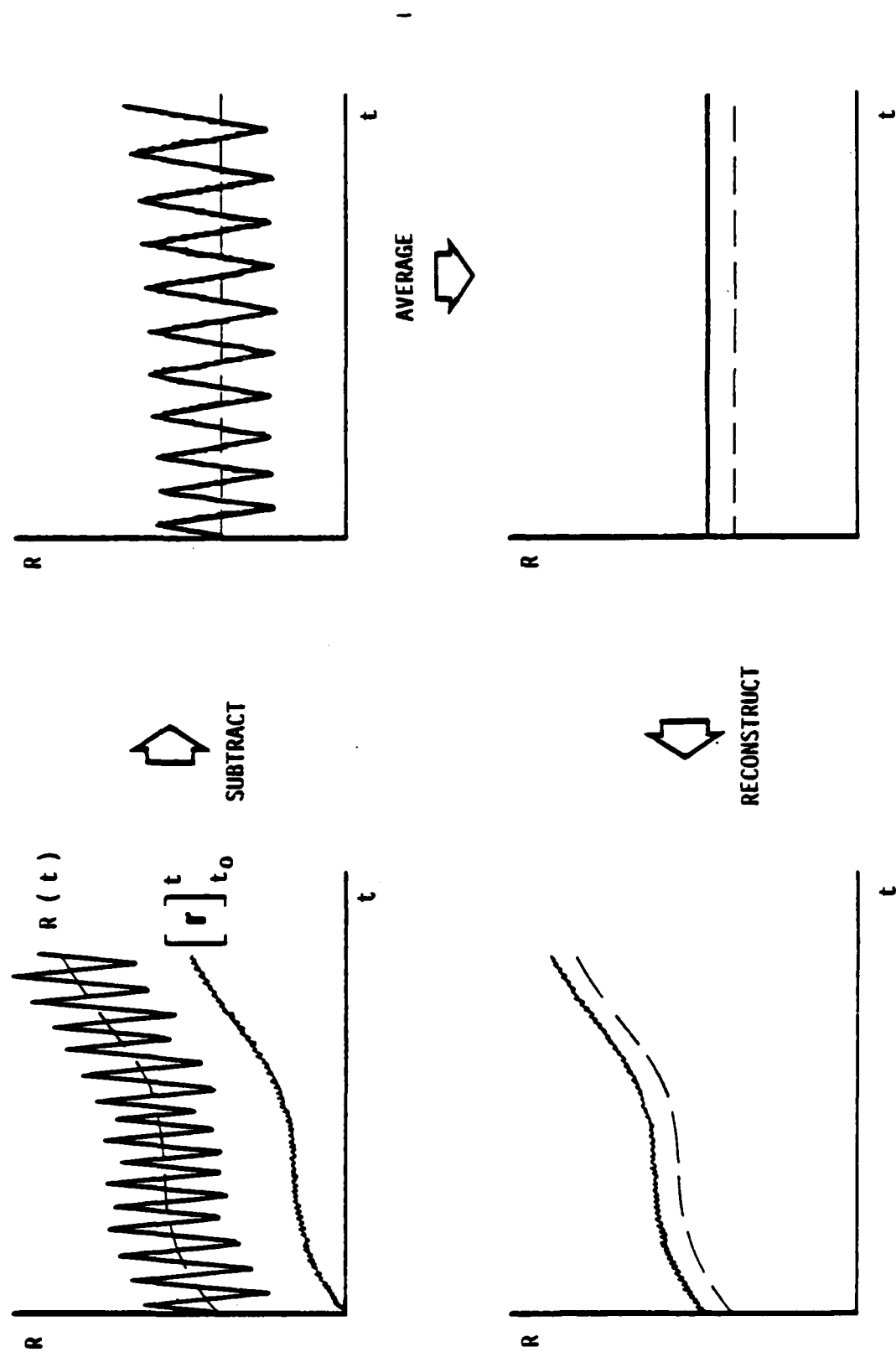


FIGURE 2.1 DOPPLER SMOOTHING TECHNIQUE

RSS value of all errors combined. In the range domain, the actual value of combined measurement error is called the User Equivalent Ranging Error (UERE), and the RSS value of all errors combined is called the one-Sigma UERE (1σ UERE).

The GPS system specifications document (Ref [4]) contains an error budget specification which is presented in Table 2.1. The errors have been placed in either Space, Control, or User Segment categories. Each error in the Space and Control categories is specified to have an RMS value less than the amount shown for each such error source for up to 24 hours after SV upload. The amounts shown for the User category error sources are based on use of the P-code for both navigation and dual frequency (L_1 , L_2) ionospheric delay compensation and on use of local measurements of temperature, pressure and relative humidity for tropospheric delay compensation. With no compensation, ionospheric and tropospheric delay errors can each vary approximately 2-20 meters, depending on elevation angle (SV relative to user) and atmospheric conditions.

The error budget specification is a useful guide for certain real-time applications of GPS. The specification does not, however, indicate the potential improvement in post-test applications utilizing better ephemeris and clock data in conjunction with better processing techniques. Neither does the error budget specification give an indication of the temporal variabilities of the constituent errors which significantly influence the performance of navigation algorithms which rely on filtering enhancements. Since the specification assumes use of the P-code, there is no indication of error magnitudes for C/A-code users. Finally, the specified error budget does not include noise terms for Doppler measurements, nor the variation of noise error levels with link margin.

In the remainder of this section, the issues which have been raised herein, and which are not addressed in the GPS error budget specification, will be explored further. Some of the details with respect to these issues, however, will be given in subsequent sections of the report. The culmination of this exploration will be the presentation of two basic error budgets. The first of these will apply nominally to various real-time GPS applications, while the second will be representative of post-test applications in which ideal conditions hold and special signal processing techniques are employed. Each of these budgets will be subject to some manipulation when specific applications

TABLE 2.1 GPS SYSTEM SPECIFICATION ERROR BUDGET

SEGMENT SOURCE	ERROR SOURCES	SYSTEM RESPONSIBILITY (METERS) 1σ
SPACE	CLOCK & NAVIGATION SUBSYSTEM SV PERTURBATIONS OTHER	2.7 1.0 0.5
CONTROL	EPOCHERIS PREDICTION AND MODEL IMPLEMENTATION OTHER	2.5 0.5
USER	IONOSPHERIC DELAY COMPENSATION TROPOSPHERIC DELAY COMPENSATION RECEIVER NOISE & RESOLUTION MULTIPATH OTHER	2.3 2.0 1.5 1.2 0.5
1σ SYSTEM UERE		5.3

are considered in later sections.

2.1 Pseudo-Range Noise Error

The GPS system specifications, ^{document} (Ref [4]) states that whenever the SV is above a 5° elevation angle, atmospheric losses are less than 2.0 dB, and the receiving antenna has gain equivalent to 0 DBI for a RH circular polarization (3 DBI for a linear polarization), the RF signal levels at the receiving antenna output shall not be less than the values shown in Table 2.2.

TABLE 2.2 RECEIVED SIGNAL LEVELS (SPECIFICATION)

CHANNEL	C/A-CODE	P-CODE
L ₁	-160 DBW	-163 DBW
L ₂	-166 DBW*	-166 DBW*

*P code only will normally be transmitted on L₂.

The available receiver noise power density, referred to the output of the receiver antenna, is expressed by

$$N_0 = k T_R$$

where $k = 1.38 \times 10^{-23}$ Joule / Kelvin is the Boltzmann constant and T_R is the effective receiver system noise temperature referred to the antenna output. With an assumed noise temperature of 580K, the available noise power density is equal to -201 DBW/Hz. Thus the estimated carrier power-to-noise power density ratio on each link is given by the following table.

TABLE 2.3 CARRIER-TO-NOISE DENSITY RATIOS

	C/A - CODE		P - CODE	
	L ₁	L ₂	L ₁	L ₂
C/N ₀ (DBHz)	41	35	38	35

The variance of the pseudo-ranging error due to receiver noise is expressed by

$$\sigma_R^2 = \frac{W^2 B_R}{C/N_0} ,$$

where W is the code chip width, B_R is the bandwidth of the code receiver/tracker, and C/N_0 is the carrier-to-noise density ratio. B_R is assumed to be 1 HZ, and

$$W = \begin{cases} 293.3 \text{ meters for C/A code,} \\ 29.33 \text{ meters for P code.} \end{cases}$$

Based on the above stated link assumptions, the RMS receiver noise errors for the four link and code combinations considered are given in the following table.

TABLE 2.4 PSEUDO-RANGING NOISE ERRORS (RMS)

	C/A-CODE		P-CODE	
	L ₁	L ₂	L ₁	L ₂
σ_R (METERS)	2.614	5.216	0.369	0.522

2.2 Pseudo-Range Ionospheric Delay Compensation

In order to perform dual frequency ionospheric delay compensation (Ref [18]) with pseudo-range measurements, the measurements on the two carrier links are first differenced. Thus

$$\Delta R = \bar{R}_2 - \bar{R}_1 ,$$

and if the correction is to be applied to link 1, the difference is multiplied by

$$K = \frac{f_2^2}{f_1^2 - f_2^2} ,$$

where f_1 and f_2 are the respective link carrier frequencies*, to obtain a measurement of ionospheric delay on link 1.

Since the receiver noise terms in L_1 and L_2 are uncorrelated, the variance of the noise in the measurement of ionospheric delay on L_1 is simply

$$\sigma_{D_1}^2 = K^2 (\sigma_{R_1}^2 + \sigma_{R_2}^2) .$$

After compensation for ionospheric delay on L_1 , the variance of the residual measurement noise is given by

$$\begin{aligned} \sigma_{R+D}^2 &= (1+K)^2 \sigma_{R_1}^2 + K^2 \sigma_{R_2}^2 \\ &= \frac{f_1^4 \sigma_{R_1}^2 + f_2^4 \sigma_{R_2}^2}{(f_1^2 - f_2^2)^2} . \end{aligned}$$

Note that

$$\sigma_{R+D}^2 \neq \sigma_{R_1}^2 + \sigma_{D_1}^2 ,$$

because of correlation of the noise terms in \tilde{R}_1 and $\Delta R = (\tilde{R}_2 - \tilde{R}_1)$. Also note that the residual noise variance has the same value whether L_1 or L_2 is selected for compensation.

Based on the assumed link margins, previously stated, the RMS noise errors before and after dual frequency ionospheric delay compensation are summarized in the following table.

* For L_1 and L_2 , $f_1 = 1575.42$ MHz and $f_2 = 1227.6$ MHz, respectively.

TABLE 2.5 RMS NOISE ERRORS BEFORE AND AFTER DUAL FREQUENCY IONOSPHERIC DELAY COMPENSATION

	C/A-CODE L_1	P-CODE L_1
σ_R (METERS)	2.614	0.369 (BEFORE)
σ_D (METERS)	9.018	0.988
σ_{R+D} (METERS)	10.454	1.238 (AFTER)

It should be noted that if variations in link margins occur which preserve the link ratios (such as variations due to receiver gain or losses and those due to atmospheric effects), the RMS noise errors in the above table can be compensated for these variations simply by scaling by the inverse of the square root of the carrier-to-noise density ratio.

2.3 Nominal Real-Time Error Budget

A nominal real-time error budget for GPS is now presented in Table 2.6. In this table, both C/A code and P code users have been considered, and slowly and rapidly fluctuating errors have been separately categorized.

Multipath errors have been arbitrarily estimated to have an RMS value equal to $W/25$, and have been assumed to be correlated (at least insofar as group or code delay) on L_1 and L_2 . The estimated value corresponds to the system specification (Table 2.1), but it is recognized that multipath error is heavily dependent on design and application factors. The correlation assumption on the two links explains why multipath error does not apply to dual frequency ionospheric delay compensation.

The nominal real-time error budget in Table 2.6 assumes dual frequency ionospheric delay compensation on whichever code is used for navigation. This assumption may not hold in all applications, however. First, in some differential navigation applications, it may be possible to ignore ionospheric delay by simply treating it as a common bias which cancels when measurement or navigation differences are formed. Second, and very significant

Table 2.6 GPS REAL-TIME ERROR BUDGET

SEGMENT SOURCE	ERROR SOURCES	1 σ ERRORS (METERS)	
		SLOW	FAST*
SPACE	CLOCK & NAVIGATION SUBSYSTEM	2.7	
	SV PERTURBATIONS	1.0	
	OTHER	0.5	
CONTROL	EPOCHERIS PREDICTION AND MODEL IMPLEMENTATION	2.5	
	OTHER	0.5	
USER	TROPOSPHERIC DELAY COMPENSATION	2.0	
	IONOSPHERIC DELAY COMPENSATION (L ₁ L ₂ Dual Frequency)		
	C/A / P		9.0 / 1.0
	RECEIVER NOISE*		2.6 / 0.4
	MULTIPATH C/A / P		12.0/1.2
	OTHER	0.5	
RSS		4.4	16.0 / 1.7
1 σ SYSTEM UERE		16.6/4.7	

* Data rate and noise bandwidth are each assumed to be 1 Hz.

to C/A code users, the C/A code on L_2 may be inhibited most or all of the time in the operational GPS. In this event, C/A code users must either forego ionospheric delay compensation or use alternatives such as modeled prediction or translocation for this purpose.

Thus a modified real-time error budget in which ionospheric delay compensation is considered independently is of interest in certain applications. This modification to the budget presented in Table 2.6 is accomplished by replacing the RSS value in the first column with 12.3/1.3 and by replacing the 1σ system UERE with 13.0/4.6. With this modification, ionospheric delay compensation errors, if applicable, must be separately taken into account.

2.4 Pseudo-Doppler Range Noise Error and Ionospheric Delay Compensation

When pseudo-range measurements are extracted from Doppler phase, the variance of error due to receiver noise is given by

$$\sigma_r^2 = \frac{\lambda^2}{(2\pi)^2} \frac{B_D}{C/N_0} ,$$

where λ is the carrier wavelength and B_D is the bandwidth of the carrier phaselock loop. B_D is assumed to be 10 Hz.

By analogy with code processing, the variance of the noise in dual frequency ionospheric delay compensation of the Doppler phase measurements on L_1 is given by

$$\sigma_{d_1}^2 = K^2 (\sigma_{r_1}^2 + \sigma_{r_2}^2) ,$$

where K has the same meaning as before. After compensation for ionospheric delay on L_1 , the variance of the residual noise in the pseudo-Doppler range measurement is given by

$$\begin{aligned} \sigma_{r+d}^2 &= (1+K)^2 \sigma_{r_1}^2 + K^2 \sigma_{r_2}^2 \\ &= \frac{f_1^4 \sigma_{r_1}^2 + f_2^4 \sigma_{r_2}^2}{(f_1^2 - f_2^2)^2} . \end{aligned}$$

Numerical values for the above quantities, based on the link margins in Table 2.3, are presented in the following table.

TABLE 2.7 PSEUDO-DOPPLER RANGE RMS NOISE ERRORS BEFORE AND AFTER IONOSPHERIC DELAY COMPENSATION

	C/A-CODE		P-CODE	
	L ₁	L ₂	L ₁	L ₂
σ_r (METERS)	0.00085	0.00219	0.00121	0.00219 (BEFORE)
σ_d (METERS)	0.00363		0.00387	
σ_{r+d} (METERS)	0.00402		0.00458	(AFTER)

From the values in the above table, estimated RMS noise errors for pseudo-Delta range, $\Delta r = [r]_t^{t+\Delta t}$, and pseudo-range rate, $\dot{r} = \Delta r / \Delta t$, can be obtained by means of

$$\sigma_r = \begin{cases} \sqrt{2} \sigma_r, & \text{before ionospheric delay compensation,} \\ \sqrt{2} \sigma_{r+d}, & \text{after ionospheric delay compensation,} \end{cases}$$

and

$$\sigma_{\dot{r}} = \begin{cases} \sqrt{2} \sigma_r B_D, & \text{before ionospheric delay compensation,} \\ \sqrt{2} \sigma_{r+d} B_D, & \text{after ionospheric delay compensation.} \end{cases}$$

Numerical values for the above quantities are presented in the following table for L₁ only.

TABLE 2.8 RMS NOISE ERRORS FOR PSEUDO-DELTA RANGE AND PSEUDO-RANGE RATE

	C/A (L ₁)	P (L ₁)	
$\sigma_{\Delta r}$ (METERS)	0.00121	0.00171	Before Ionospheric Delay Compensation
(METERS)	0.00569	0.00648	After Ionospheric Delay Compensation
$\sigma_{\dot{r}}$ (METERS/SECONDS)	0.0121	0.0171	Before Ionospheric Delay Compensation
(METERS/SECONDS)	0.0569	0.0648	After Ionospheric Delay Compensation

2.5 Ideal Post-Test Error Budget

In post-test applications, it is natural to expect some improvement in the error budget relative to that which applies in real-time. First, the clock and ephemeris errors should be reduced by post-test filtering and smoothing when compared to predicted values of these errors. Second, certain processing options are available post-test which may not be available in real-time. The most important of these involves processing Doppler phase measurements to obtain ultra low noise pseudo-range data at a relatively high rate (10 Hz). To achieve maximum utility from this Doppler processing technique, continuous measurements (with no dropouts or Doppler cycle slips) must be simultaneously available on both L₁ and L₂. Furthermore, prior to processing the pseudo-range measurements for navigation, one pass must be made through the data to obtain the ionospheric delay correction, and a second pass must be made to smooth the initial value of pseudo-range.

An error budget for post-test GPS applications is presented in Table 2.9. This budget is based on the ideal conditions outlined above in which the ephemeris and clock data have undergone post-test refinements by the control segment; and the user employs dual frequency ionospheric delay compensation and Doppler smoothing to reduce initialization error in pseudo-range measurements constructed from continuous Doppler data.

TABLE 2.9 GPS POST-TEST ERROR BUDGET

SEGMENT SOURCE	ERROR SOURCES	1 σ ERRORS (METERS)		
		SLOW	FAST*	
SPACE & CONTROL	CLOCK, NAVIGATION SUBSYSTEM, SV PERTURBATIONS, AND EPHEMERIS SMOOTHING	1.5		
USER	TROPOSPHERIC DELAY COMPENSATION (RAY TRACE)	0.2		
	IONOSPHERIC DELAY COMPENSATION (L ₁ L ₂ Dual Frequency) C/A / P	0.45/0.05	0.53/0.06	0.0036/0.0039
		0.13/0.02		0.0040/0.0046
	RECEIVER NOISE* C/A / P		0.00085/0.0012	
	MULTIPATH C/A / P	0.6/0.06	0.0076	
	OTHER	0.5		
	RSS	1.8 / 1.6		0.0086/0.0089
1 σ SYSTEM UERE		1.8/1.6		

* Data rate and noise bandwidth are each assumed to be 10 Hz.

It will be observed that ionospheric delay compensation, receiver noise, and multipath errors are indicated in both the slow and fast columns. Except for multi th, the numbers in the fast column are from Table 2.7. (The RMS multipath noise error (fast column) is assumed to be $\lambda_1/25$.) The values in the slow column are actually RMS bias errors induced by Doppler smoothing of the initial condition. These errors are due almost totally to noise in the code measurements of pseudo-range, and their magnitude depends on the length of the Doppler smoothing interval. Because the bandwidth of the code loop is taken to be 1 Hz, the RMS values of initialization errors induced by Doppler smoothing are obtained by dividing the respective values for noise given in Table 2.6 by \sqrt{T} , where T is the duration (expressed in seconds) of the Doppler smoothing. The values in Table 2.9 are based on a Doppler smoothing interval of 400 seconds duration.

In those applications where ionospheric delay compensation is either not performed, or is performed in some alternative fashion which is independent of receiver noise error, the post-test budget in Table 2.9 must be modified to delete terms due to dual frequency ionospheric delay compensation. The result of this modification is that the RSS values in the slow column become 1.7/1.6, the RSS values in the fast column become 0.0077/0.0077, and the 1σ system UEREs become 1.7/1.6. With this modification, ionospheric delay compensation errors, if applicable, must be separately taken into account.

The values of $\sigma_{\Delta r}$ and σ_f computed in connection with the real-time budget apply in the post-test budget without change.

2.6 Summary of Error Budget Properties

A top-level summary matrix is presented in Table 2.10. This matrix shows, in a qualitative manner, the extent to which various error sources enter different navigation modes for both real-time and post-test applications.

TABLE 2.10 ERROR EFFECTS FOR VARIOUS NAVIGATION MODES

ERROR SOURCES							
NAVIGATION MODE		SPACE	CONTROL	ATMOSPHERE	RECEIVER BIAS	MULTIPATH	RECEIVER NOISE
ABSOLUTE NAVIGATION	REAL TIME	■	■	■	■	■	■
	POST TEST	■	■	●	■	●	●
RELATIVE NAVIGATION	REAL TIME	○	○	○	■	■	■
	POST TEST	○	○	○	■	●	●
DELTA NAVIGATION	REAL TIME	○	○	○	○	●	●
	POST TEST	○	○	○	○	●	●

■ - Measurement error level corresponds to real-time budget.

■ - Error level is reducible by filter/smoothen prior to entering navigation solution.

● - Error level is reducible by Doppler processing.

○ - Error level is negligible over limited time and space.

The theoretical problem of assessing accuracy in any GPS application is solved whenever the joint probability distribution is known for the navigation errors of interest. In the cases where the UEREs from each SV are jointly Gaussian and the processing is essentially linear, the joint probability distribution of the navigation errors is Gaussian, and is therefore completely specified by its first and second moments (i.e., mean vector and covariance matrix). A simple example here will serve the purpose of illustrating the development of first and second moments of navigation errors, as well as providing a convenient vehicle to introduce the terminology of accuracy measures.

Consider that a user has made pseudo-range measurements to four suitable SVs and wishes to compute his position and clock error. The four pseudo-range measurements can be expressed as follows

$$R_i = \sqrt{(X-X_i)^2 + (Y-Y_i)^2 + (Z-Z_i)^2} + Ct + \epsilon_i, \quad i = 1, 2, 3, 4.$$

In this expression, i denotes the SV, R_i is measured pseudo-range, ϵ_i is UERE, (X, Y, Z) are user coordinates, (X_i, Y_i, Z_i) are indicated SV coordinates, t is user clock offset, and C is the speed of light.

The user solution for (X, Y, Z, t) , denoted by (X', Y', Z', t') is given by

$$R_i = \sqrt{(X'-X_i)^2 + (Y'-Y_i)^2 + (Z'-Z_i)^2} + Ct', \quad i = 1, 2, 3, 4.$$

Eliminating R_i from the two sets of equations and expanding to first order in $\delta X = X' - X$, $\delta Y = Y' - Y$, $\delta Z = Z' - Z$, and $\delta t = t' - t$ leads to

$$\frac{(X'-X_i)\delta X + (Y'-Y_i)\delta Y + (Z'-Z_i)\delta Z}{\sqrt{(X'-X_i)^2 + (Y'-Y_i)^2 + (Z'-Z_i)^2}} + C\delta t = \epsilon_i, \quad i = 1, 2, 3, 4.$$

The latter four equations can be written in matrix form as

$$H\bar{\beta} = \bar{\epsilon},$$

where

$$H = \begin{bmatrix} e_1^T & 1 \\ e_2^T & 1 \\ e_3^T & 1 \\ e_4^T & 1 \end{bmatrix}, \quad \bar{B} = \begin{bmatrix} \delta X \\ \delta Y \\ \delta Z \\ C\delta t \end{bmatrix}, \quad \bar{\epsilon} = \begin{bmatrix} \epsilon_1 \\ \epsilon_2 \\ \epsilon_3 \\ \epsilon_4 \end{bmatrix},$$

and

$$e_i^T = \frac{[(X' - X_i), (Y' - Y_i), (Z' - Z_i)]}{\sqrt{(X' - X_i)^2 + (Y' - Y_i)^2 + (Z' - Z_i)^2}}$$

is the unit vector from the i -th SV to the user, consistent with the solution.

It follows that

$$\bar{B} = H^{-1} \bar{\epsilon},$$

and the first and second moments of \bar{B} are given by

$$E\{\bar{B}\} = H^{-1} E\{\bar{\epsilon}\} = \bar{0},$$

$$C\{\bar{B}\} = E\{\bar{B}\bar{B}^T\} = (H^T H)^{-1} \sigma_R^2,$$

where σ_R is the RSS UERE common to all 4 measurements, and the 4 UEREs are assumed to be statistically independent.

Now

$$C\{\bar{B}\} = \begin{bmatrix} \sigma_X^2 & \sigma_{XY} & \sigma_{XZ} & C\sigma_{Xt} \\ \sigma_{YX} & \sigma_Y^2 & \sigma_{YZ} & C\sigma_{Yt} \\ \sigma_{ZX} & \sigma_{ZY} & \sigma_Z^2 & C\sigma_{Zt} \\ C\sigma_{tX} & C\sigma_{tY} & C\sigma_{tZ} & C^2\sigma_t^2 \end{bmatrix}$$

is the symmetric covariance matrix of the error vector $[\delta X, \delta Y, \delta Z, C\delta t]^T$. In more general applications, the processing may be more involved, and the error vector may contain additional terms such as velocities, frequency, etc. In such cases the error covariance matrix is extended to contain the variances and cross covariances of each error term.

In terms of the covariance matrix for the simple problem considered above, several accuracy measures can be defined immediately. The trace of the covariance matrix is given by

$$\sigma_G^2 = \sigma_X^2 + \sigma_Y^2 + \sigma_Z^2 + C^2\sigma_t^2 ,$$

and σ_G is the Figure Of Merit (FOM) for the solution. The FOM combines UERE statistics and geometry to assess accuracy. The RSS Position Solution Error is given by

$$\sigma_P = \sqrt{\sigma_X^2 + \sigma_Y^2 + \sigma_Z^2} .$$

It is important to realize that by the properties of orthogonal matrices, both σ_G and σ_P are invariant with respect to orthogonal transformations. Hence σ_G and σ_P are independent of the Cartesian coordinate system in which the solution is expressed.

If a particular coordinate frame is selected in which the X-Y plane is horizontal and the Z-axis is vertical, then the RSS Horizontal Position Solution Error is given by

$$\sigma_H = \sqrt{\sigma_X^2 + \sigma_Y^2} ,$$

and the RMS Vertical Position Solution Error is given by

$$\sigma_V = \sigma_Z .$$

Each of the quantities σ_G , σ_P , σ_H , σ_V , $C\sigma_t$ is termed an accuracy measure. When an accuracy measure is normalized by σ_R , the "Dilution Of Precision" (or DOP) resulting from geometry and processing is obtained. For the above accuracy measures, DOPs are defined as follows:

$$\text{GDOP} = \sigma_G / \sigma_R ,$$

$$\text{PDOP} = \sigma_P / \sigma_R ,$$

$$\text{HDOP} = \sigma_H / \sigma_R ,$$

$$\text{VDOP} = \sigma_V / \sigma_R , \quad \text{and}$$

$$\text{TDOP} = C\sigma_t / \sigma_R .$$

Other measures of accuracy are often defined, such as Spherical Error Probable (SEP), Circular Error Probable (CEP), Spherical Standard Error (σ_S), and Circular Standard Error (σ_C). However use of these accuracy measures is generally restricted to applications in which the error components are jointly Gaussian. These accuracy measures will be defined in the sequel, and for the Gaussian case, relationships between the various accuracy measures will be explored.

3.1 Three Dimensional Error Probability Distribution

Let X , Y , Z be zero mean jointly Gaussian random variables with covariance matrix

$$C = \begin{bmatrix} \sigma_X^2 & \sigma_{XY} & \sigma_{XZ} \\ \sigma_{XY} & \sigma_Y^2 & \sigma_{YZ} \\ \sigma_{XZ} & \sigma_{YZ} & \sigma_Z^2 \end{bmatrix}$$

which is assumed to be nonsingular. It can be shown that there exists an orthogonal matrix L such that

$$L^T C L = \Lambda ,$$

where Λ is a diagonal matrix, and moreover, $\text{tr} C = \text{tr} \Lambda$.

Defining, ξ, η, ζ by

$$\begin{bmatrix} \xi \\ \eta \\ \zeta \end{bmatrix} = L^T \begin{bmatrix} X \\ Y \\ Z \end{bmatrix} ,$$

it follows that ξ, η, ζ are zero mean independent Gaussian random variables with covariance matrix

$$\Lambda = \begin{bmatrix} \sigma_\xi^2 & 0 & 0 \\ 0 & \sigma_\eta^2 & 0 \\ 0 & 0 & \sigma_\zeta^2 \end{bmatrix} .$$

Now

$$\frac{\xi^2}{\sigma_\xi^2} + \frac{\eta^2}{\sigma_\eta^2} + \frac{\zeta^2}{\sigma_\zeta^2} = K^2$$

is the equation of an ellipsoid. With $K \geq 0$, the probability that the point (X, Y, Z) lies within the ellipsoid is denoted by $P_E(K;3)$ and is given by

$$P_E(K;3) = \int \int \int_{\frac{\xi^2}{\sigma_\xi^2} + \frac{\eta^2}{\sigma_\eta^2} + \frac{\zeta^2}{\sigma_\zeta^2} \leq K^2} \frac{\exp \left\{ -\frac{1}{2} \left(\frac{\xi^2}{\sigma_\xi^2} + \frac{\eta^2}{\sigma_\eta^2} + \frac{\zeta^2}{\sigma_\zeta^2} \right) \right\}}{(2\pi)^{3/2} \sigma_\xi \sigma_\eta \sigma_\zeta} d\xi d\eta d\zeta .$$

$P_E(K;3)$ is called an Elliptical Error Probability in 3 dimensions, and it is a simple matter to show that

$$P_E(K;3) = P_r[x_3^2 \leq K^2] ,$$

where x_3^2 is a "chi-squared" random variable with 3 degrees of freedom. Thus elliptical error probabilities can be obtained from readily available tables of χ^2 -probabilities.

In contrast, the probability that the point (X, Y, Z) lies within a sphere of radius R, denoted by $P_S(R)$, is given by

$$P_S(R) = \int \int \int_{\xi^2 + \eta^2 + \zeta^2 \leq R^2} \frac{\exp\{-\frac{1}{2}(\frac{\xi^2}{\sigma_\xi^2} + \frac{\eta^2}{\sigma_\eta^2} + \frac{\zeta^2}{\sigma_\zeta^2})\}}{(2\pi)^{3/2} \sigma_\xi \sigma_\eta \sigma_\zeta} d\xi d\eta d\zeta .$$

$P_S(R)$ is called a Spherical Error Probability, and in general bears no simple relationship to probabilities associated with χ^2 or other commonly tabulated random variables. The value of R which results in $P_S = 0.5$ is called the Spherical Error Probable and is denoted by SEP. Thus

$$P_S(SEP) = 0.5 .$$

By reference to χ^2 tables it is seen that $P_E(1;3) = 0.198748 \dots$. That is, the probability that (X, Y, Z) is within the "1 σ -ellipsoid" is 0.198748 ..., and this is the basis for the definition of the spherical standard error. The value of R which results in $P_S = 0.198748 \dots$ is called the Spherical Standard Error and is denoted by σ_S . Thus

$$P_S(\sigma_S) = 0.198748 \dots = P_E(1;3) .$$

A special case of particular interest occurs when $\sigma_\xi = \sigma_\eta = \sigma_\zeta$ and the "1 σ -ellipsoid" is actually a sphere. In this case the Gaussian random variables X, Y, Z are said to be Spherically Distributed, and $\sigma_S = \sigma_\xi = \sigma_\eta = \sigma_\zeta$.

3.2 Two-Dimensional Error Probability Distribution

By analogy with the above development, if X and Y are zero mean jointly Gaussian random variables with covariance matrix

$$C = \begin{bmatrix} \sigma_X^2 & \sigma_{XY} \\ \sigma_{XY} & \sigma_Y^2 \end{bmatrix},$$

there exists an orthogonal matrix L such that

$$L^T C L = \Lambda,$$

where Λ is diagonal and $\text{tr} C = \text{tr} \Lambda$. With (ξ, η) defined by

$$\begin{bmatrix} \xi \\ \eta \end{bmatrix} = L^T \begin{bmatrix} X \\ Y \end{bmatrix},$$

it follows that ξ, η are zero mean independent Gaussian random variables with covariance matrix

$$\Lambda = \begin{bmatrix} \sigma_\xi^2 & 0 \\ 0 & \sigma_\eta^2 \end{bmatrix}.$$

Assuming C is nonsingular, it follows that

$$\frac{\xi^2}{\sigma_\xi^2} + \frac{\eta^2}{\sigma_\eta^2} = K^2$$

is the equation of an ellipse. With $K \geq 0$, the probability that the point (X, Y) lies within the ellipse, denoted by $P_E(K; 2)$, is given by

$$P_E(K;2) = \int \int_{\frac{\xi^2}{\sigma_\xi^2} + \frac{\eta^2}{\sigma_\eta^2} \leq K^2} \frac{\exp\{-\frac{1}{2}(\frac{\xi^2}{\sigma_\xi^2} + \frac{\eta^2}{\sigma_\eta^2})\}}{2\pi\sigma_\xi\sigma_\eta} d\xi d\eta .$$

$P_E(K;2)$ is called an Elliptical Error Probability in 2 dimensions, and

$$P_E(K;2) = P_r[x_2^2 \leq K^2] = 1 - e^{-K^2/2} ,$$

where x_2 is a "chi-squared" random variable with 2 degrees of freedom.

The probability that the point (X, Y) lies within a circle of radius R , denoted by $P_C(R)$ and given by

$$P_C(R) = \int \int_{\xi^2 + \eta^2 \leq R^2} \frac{\exp\{-\frac{1}{2}(\frac{\xi^2}{\sigma_\xi^2} + \frac{\eta^2}{\sigma_\eta^2})\}}{2\pi\sigma_\xi\sigma_\eta} d\xi d\eta ,$$

is called a Circular Error Probability. The value of R which results in $P_C = 0.5$ is called the Circular Error Probable and is denoted by CEP. Thus

$$P_C(\text{CEP}) = 0.5 .$$

Now the probability that (X, Y) is within the " 1σ -ellipse" is $P_E(1;2) = 0.393469 \dots$, and this is the basis for the Circular Standard Error, denoted by σ_C and defined implicitly by

$$P_C(\sigma_C) = 0.393469 \dots = P_E(1;2) .$$

Thus σ_C is the radius of the circle which contains (X, Y) with probability 0.393469

In the special case when $\sigma_\xi = \sigma_\eta$, the " 1σ -ellipse" is a circle and $\sigma_C = \sigma_\xi = \sigma_\eta$. In this case the Gaussian random variables X, Y are said to be Circularly Distributed.

3.3 One-Dimensional Error Probability Distribution

In analogy with the above developments for 2 and 3 dimensional cases, if x is zero mean Gaussian random variable with variance σ_x^2 , define

$$P_E(K;1) = \int_{\frac{x^2}{\sigma_x^2} \leq K^2} \frac{1}{\sqrt{2\pi}\sigma_x} e^{-x^2/2\sigma_x^2} dx$$

and

$$P_L(R) = \int_{x^2 \leq R^2} \frac{1}{\sqrt{2\pi}\sigma_x} e^{-x^2/2\sigma_x^2} dx .$$

$P_E(K;1)$ is an Elliptical Error Probability in 1 dimension and $P_L(R)$ is called a Linear Error Probability. But it is easily seen that

$$P_E(K;1) = P_L(K\sigma_x) = P_r[x_1^2 \leq K^2] ,$$

where x_1 is a "chi-squared" random variable with 1 degree of freedom.

The Linear Error Probable (LEP) is defined by

$$P_L(\text{LEP}) = 0.5 ,$$

and it follows that

$$\text{LEP} \approx (0.675)\sigma_L ,$$

where $\sigma_L = \sigma_x$ is the Linear Standard Error.

3.4 Dilution of Precision

The "Dilution Of Precision" or DOP for each of the spherical, circular, and linear accuracy measures can be defined in analogy with the DOPs which were defined earlier for the RSS accuracy measures σ_G , σ_P , σ_H , and σ_V . Thus for GPS applications, where σ_R denotes 1σ UERE,

$$\text{SEPDOP} = \text{SEP}/\sigma_R ,$$

$$\text{SDOP} = \sigma_S/\sigma_R ,$$

$$\text{CEPDOP} = \text{CEP}/\sigma_R ,$$

$$\text{CDOP} = \sigma_C/\sigma_R ,$$

$$\text{LEPDOP} = \text{LEP}/\sigma_R ,$$

$$\text{LDOP} = \sigma_L/\sigma_R .$$

It is clear now that a plethora of accuracy measures can be defined. Furthermore, there are no general algebraic relationships between the relatively few accuracy measures defined above. One thing is certain however. All accuracy measures defined above are implicitly contained in the error covariance matrix. In fact, the error covariance matrix is itself the ultimate accuracy measure of the types defined above. Moreover, when the errors are jointly Gaussian, the mean vector and covariance matrix provide a complete statistical characterization of the errors. Since the RSS quantities σ_G , σ_p , σ_H , σ_V can be obtained virtually by inspection from the covariance matrix, RSS errors are particularly convenient accuracy measures.

3.5 Accuracy Measure Relationships

In certain special cases, it is possible to determine numerical relationships between variously defined accuracy measures. These relationships will be examined first for the 3 dimensional case and then for the 2 dimensional case. For both cases it is assumed that the errors are jointly Gaussian.

Consider first the case in which the 1 σ ellipsoid is a sphere, i.e., $\sigma_\xi = \sigma_\eta = \sigma_\zeta = \sigma > 0$ and the errors are spherically distributed. In this case, $\sigma_S = \sigma$, $\sigma_p = \sqrt{3} \sigma_S$, and for $K \geq 0$,

$$P_S(K\sigma_S) = P_r[x_3^2 \leq K^2] .$$

For the 50th percentile of a χ_3^2 random variable, it follows that $SEP = \sqrt{\chi_3^2} \sigma_S = (1.538 \dots) \sigma_S$.

When $\sigma_\xi = \sigma_\eta = \sigma > 0$ and $\sigma_3 = 0$, the 3-dimensional distribution is said to be Circularly Degenerate. In this case $\sigma_p = \sqrt{2} \sigma$, and for $K \leq 0$,

$$P_S(K\sigma) = P_r[\chi_2^2 \leq K^2].$$

From this relation and the χ_2^2 tables, it follows that $\sigma_S = (0.6657 \dots) \sigma$ and $SEP = (1.1774 \dots) \sigma$, respectively.

Finally when $\sigma_\xi = \sigma > 0$ and $\sigma_\eta = \sigma_3 = 0$, the 3-dimensional distribution is said to be Linearly Degenerate. In this case $\sigma_p = \sigma$, and for $K \geq 0$, $P_S(K\sigma) = P_r[\chi_1^2 \leq K^2]$. From this relation it follows that $\sigma_S = (0.2517 \dots) \sigma$ and $SEP = (0.67448 \dots) \sigma$.

For the 2 dimensional case, consider first the case in which the errors are circularly distributed, i.e., the 1σ ellipse is a circle with $\sigma_\xi = \sigma_\eta = \sigma > 0$. In this case, $\sigma_C = \sigma$, $\sigma_H = \sqrt{2} \sigma_C$, and for $K \geq 0$,

$$P_C(K\sigma_C) = P_r[\chi_2^2 \leq K^2].$$

From this expression and the χ_2^2 tables, it follows that $CEP = (1.1774 \dots) \sigma_C$.

In the 2 dimensional case where $\sigma_\xi = \sigma > 0$ and $\sigma_\eta = 0$, the distribution is Linearly Degenerate. In this case $\sigma_H = \sigma$, and for $K \geq 0$,

$$P_C(K\sigma) = P_r[\chi_1^2 \leq K^2].$$

From this relation it follows that $\sigma_C = (0.515 \dots) \sigma$ and $CEP = (0.67448 \dots) \sigma$.

The accuracy measure relationships for the above special cases are summarized in Tables 3.1 and 3.2.

As can be seen immediately from these tables, the selected accuracy measure relationships vary significantly with the shape (i.e., eccentricity and/or degeneracy) of the 1σ ellipsoid (or ellipse). This is indicative that none

TABLE 3.1 3 DIMENSIONAL ACCURACY RELATIONS

CASE	$\frac{\sigma_P}{\sigma_S}$	$\frac{\sigma_P}{SEP}$	$\frac{SEP}{\sigma_S}$
SPHERICAL DISTRIBUTION	1.732	1.126	1.538
CIRCULAR DEGENERACY	2.124	1.201	1.769
LINEAR DEGENERACY	3.973	1.483	2.680

TABLE 3.2 2 DIMENSIONAL ACCURACY RELATIONS

CASE	$\frac{\sigma_H}{\sigma_C}$	$\frac{\sigma_H}{CEP}$	$\frac{CEP}{\sigma_C}$
CIRCULAR DISTRIBUTION	1.414	1.201	1.177
LINEAR DEGENERACY	1.942	1.483	1.310

of the accuracy measures discussed above (except the covariance matrix itself) can give a complete assessment of all aspects of accuracy. Consequently, in order to gain clearer insight into the meaning and utility of each scalar accuracy measure, it is necessary to relate each individually to an appropriate probability distribution. The most useful distributions for this purpose are the spherical and circular error probability distributions defined earlier. (Note that $P_S(R)$ is the probability distribution of radial error in 3 dimensions, and $P_C(R)$ is the probability distribution of radial error in 2 dimensions.)

3.6 Error Probability Relationships to Accuracy Measures

In Figures 3.1 - 3.3, plots of P_S versus R are given, where R has been normalized by σ_S , SEP, and σ_p , respectively. In each figure, graphs of the special cases of spherical distribution of errors, circular degeneracy, and linear degeneracy have been included. In Figures 3.4 - 3.6, plots of P_C versus R are given, where R has been normalized by σ_C , CEP, and σ_H , respectively. In each figure, graphs of the special cases of circular distribution of errors and linear degeneracy have been included.

Observe in Figure 3.1 that the three graphs pass through the point $P_S \approx 0.19875$, $R = \sigma_S$ (as they must, by definition) but as R increases the three graphs diverge. Consequently, σ_S is not a very good indicator of the value of R at, say, $P = 0.5$ or higher. In Figure 3.2 the three graphs pass through $P_S = 0.5$, $R = \text{SEP}$ (as required) but diverge considerably at $P = 0.75$ or higher. In Figure 3.3, there is no single point (other than the origin) through which the three graphs all pass. However, the three graphs are very near each other in the vicinity of $P_S = 0.77$, $R = 1.2\sigma_p$; and for higher values of P_S , the graphs do not diverge as severely as those in Figures 3.1 and 3.2.

An obvious conclusion to be drawn from Figures 3.1 - 3.3 is that while σ_S is a "perfect" indicator of R for $P_S \approx 0.19875$ and SEP is a "perfect" indicator of R for $P_S = 0.5$, $1.2\sigma_p$ is a "good" indicator of R for $P_S \approx 0.77$; and furthermore, σ_p is a more "robust" indicator (i.e., less sensitive to the shape of the 1σ ellipsoid) of the value of R for $P_S = 0.75$, or higher, than either SEP or σ_S . This conclusion, coupled with the fact that σ_p is easily computed from the covariance matrix, makes σ_p a useful choice of accuracy measure whenever spherical error probabilities of .75 or greater are of interest.

Examination of Figures 3.4 - 3.6 leads to conclusions for 2 dimensions which are analogous to those for 3 dimensions. In particular, σ_H is a useful choice of accuracy measure whenever circular error probabilities of 0.75 or greater are of interest.

There are occasions when elliptical error probabilities are of interest. These probabilities have the property of being independent of the shape of the 1σ ellipsoid (or ellipse) as long as the distribution is non-degenerate. Elliptical error probabilities can be read directly from tables for χ^2 random variables. (The number of degrees of freedom of the χ^2 random variable equals the effective number of dimensions of the error vector including any reduction due to degeneracy.) Plots of elliptical error probabilities for cases where the effective dimension of the error vector is three, two, or one, respectively, are presented in Figures 3.7 - 3.9.

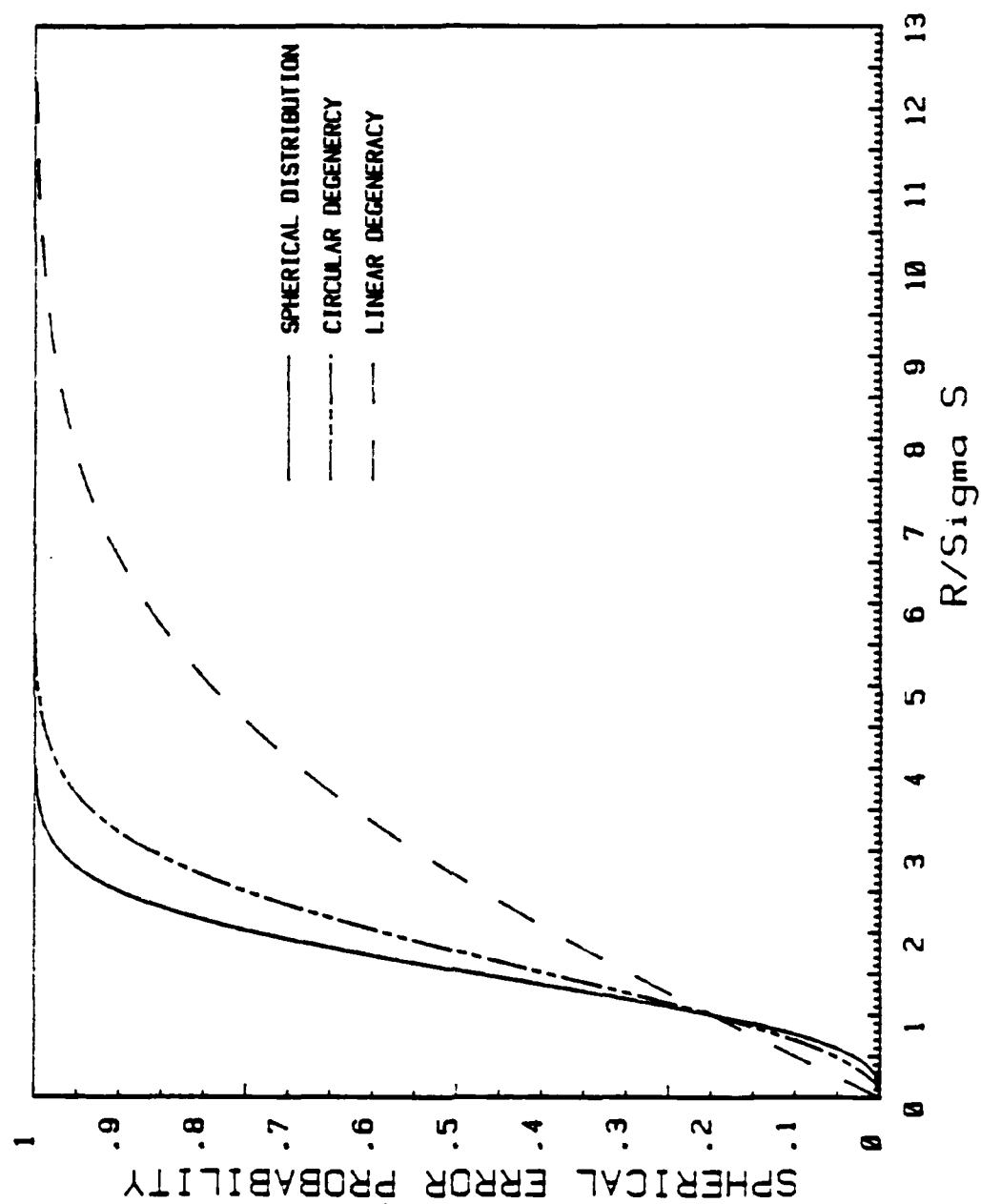


FIGURE 3.1 DISTRIBUTION OF 3 DIMENSIONAL RADIAL ERROR NORMALIZED BY SIGMA S

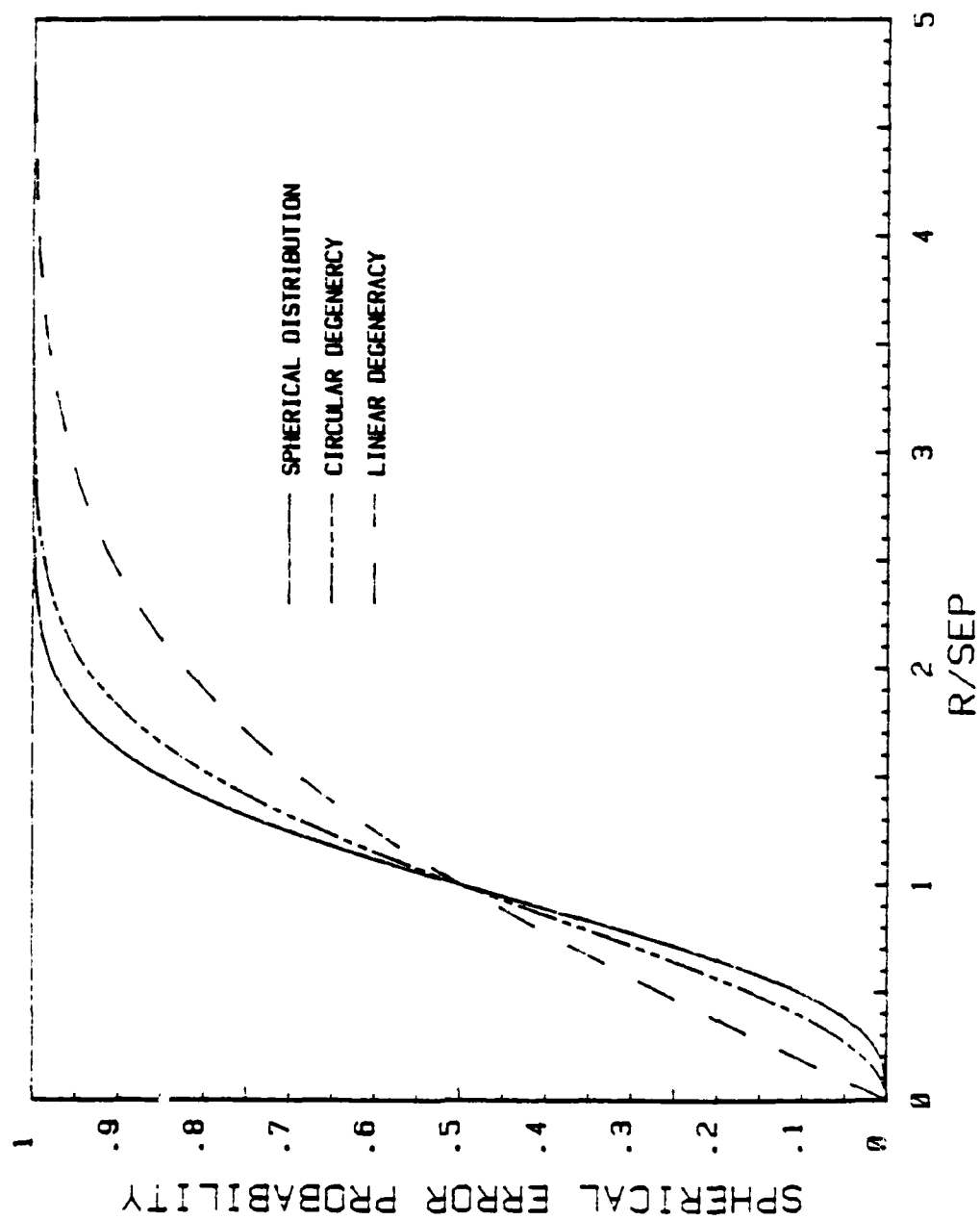


FIGURE 3.2 DISTRIBUTION OF 3 DIMENSIONAL RADIAL ERROR NORMALIZED BY SEP

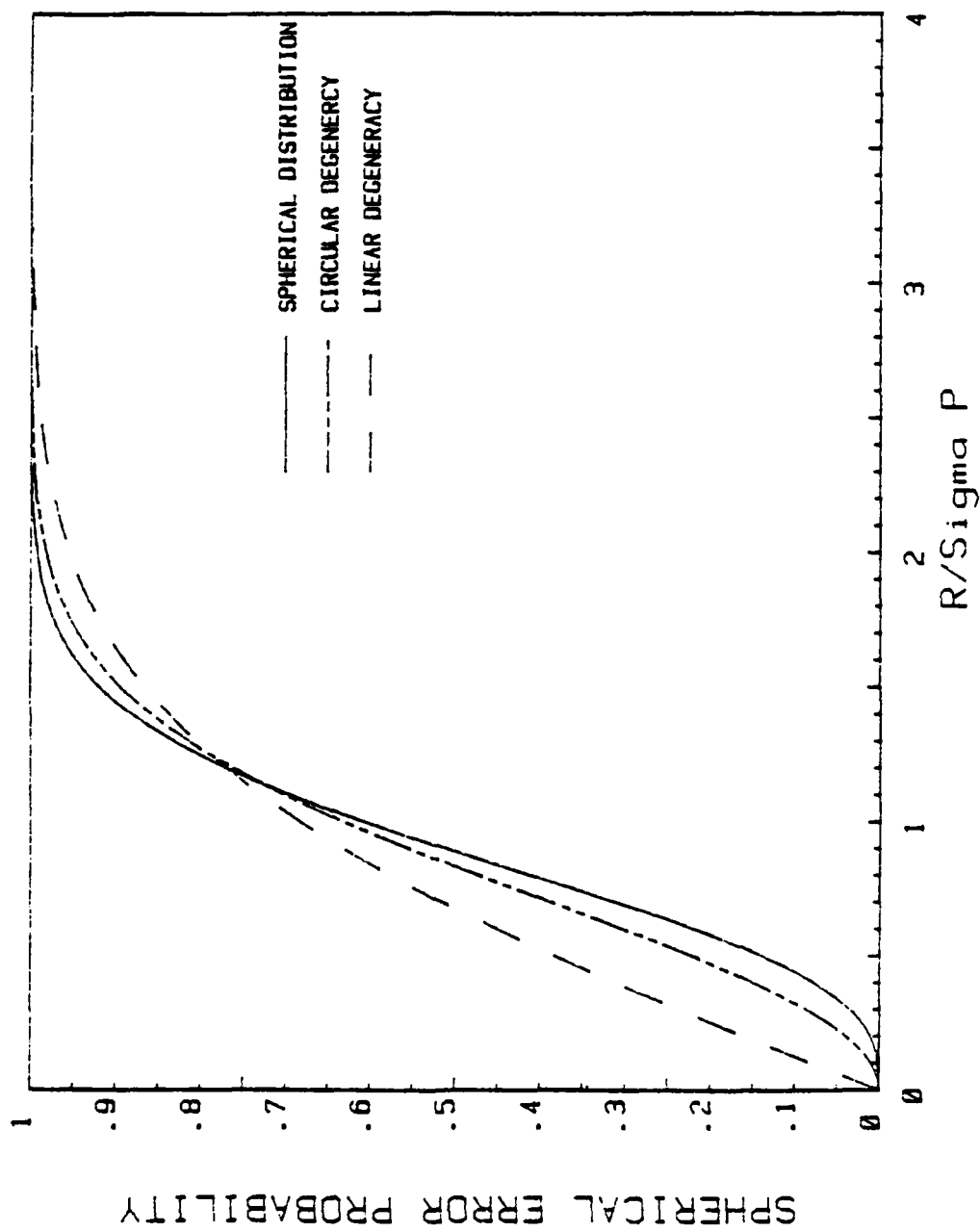


FIGURE 3.3 DISTRIBUTION OF 3 DIMENSIONAL RADIAL ERROR NORMALIZED BY SIGMA P

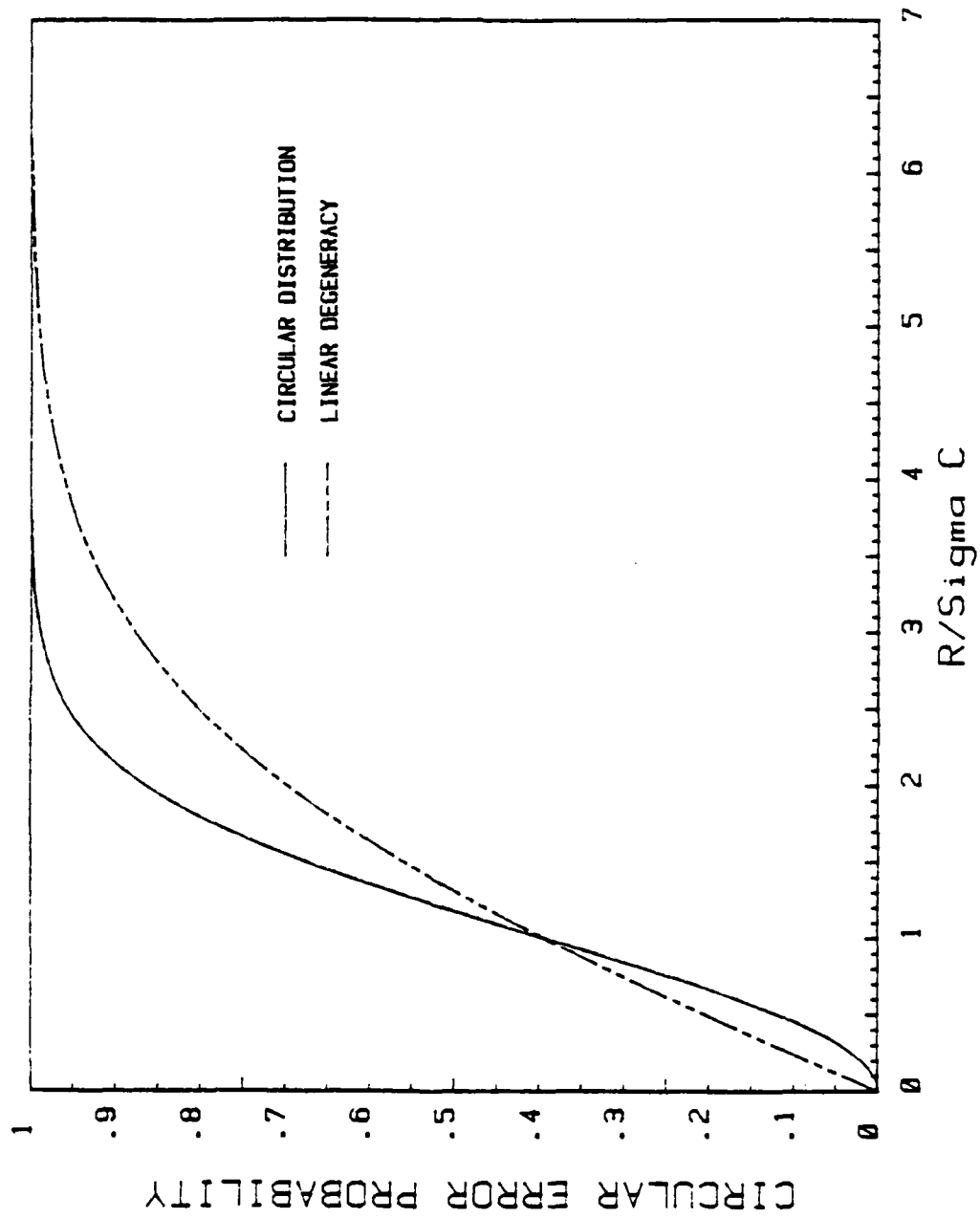


FIGURE 3.4 DISTRIBUTION OF 2 DIMENSIONAL RADIAL ERROR NORMALIZED BY SIGMA C

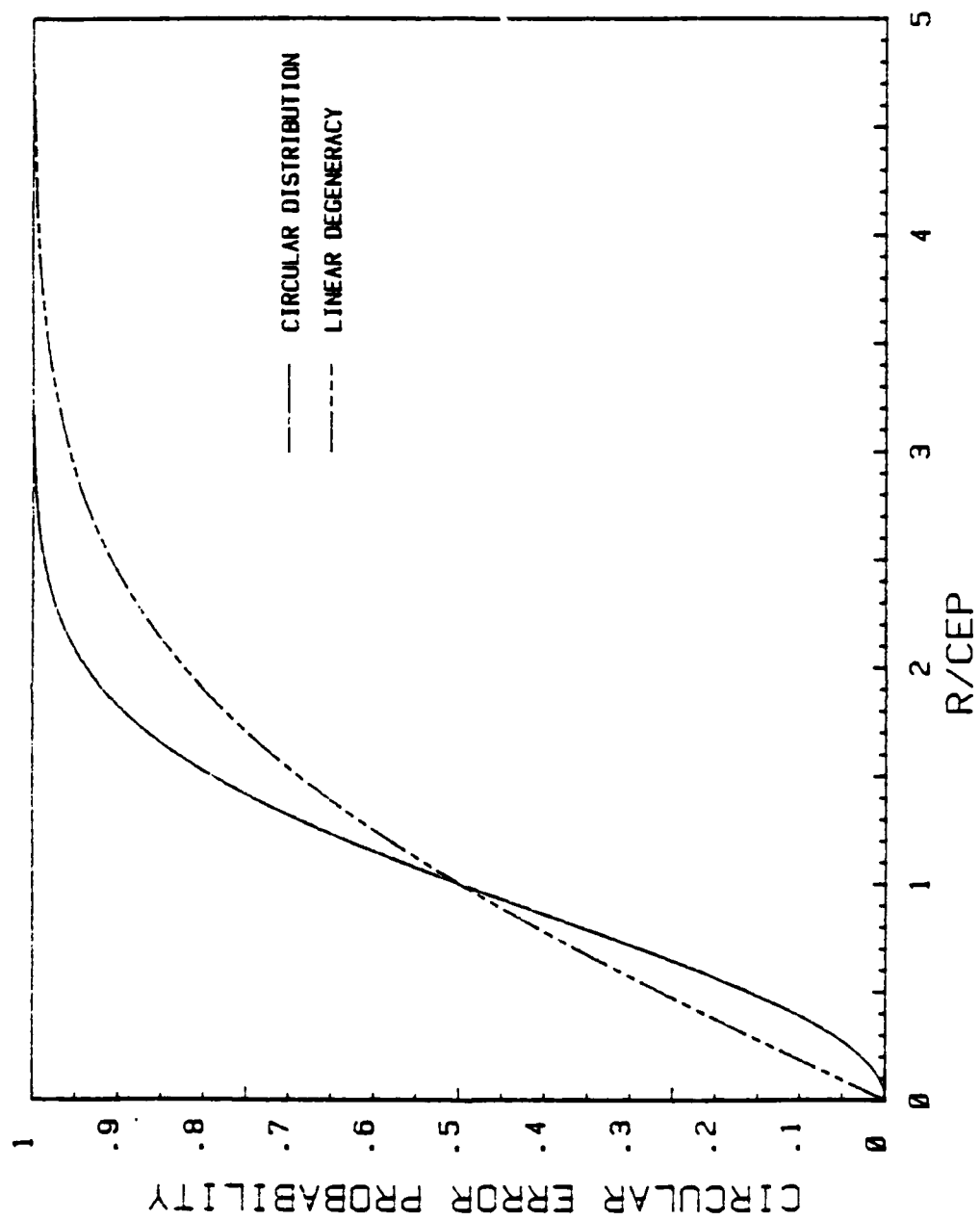


FIGURE 3.5 DISTRIBUTION OF 2 DIMENSIONAL RADIAL ERROR NORMALIZED BY CEP

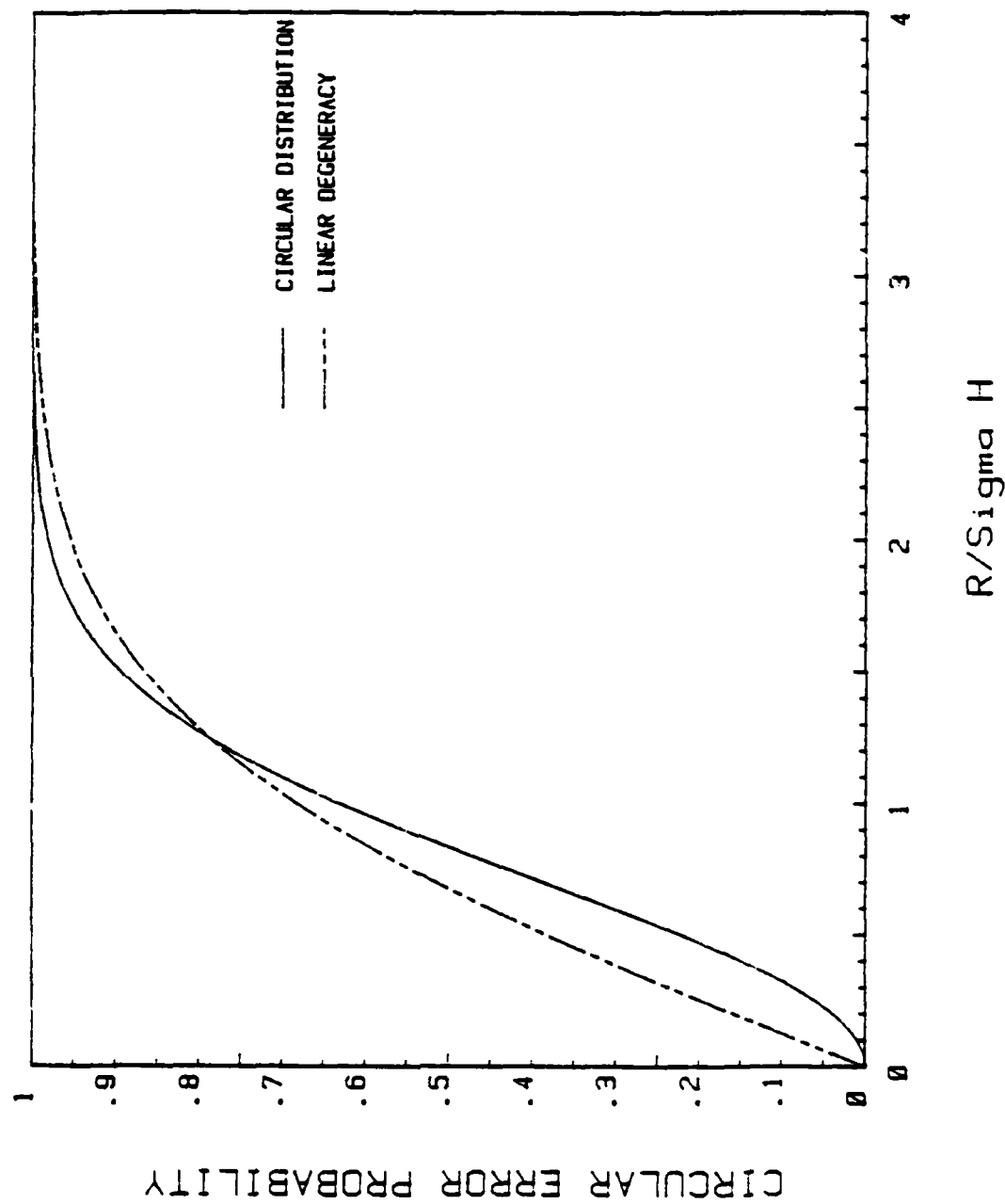


FIGURE 3.6 DISTRIBUTION OF 2 DIMENSIONAL RADIAL ERROR NORMALIZED BY SIGMA H

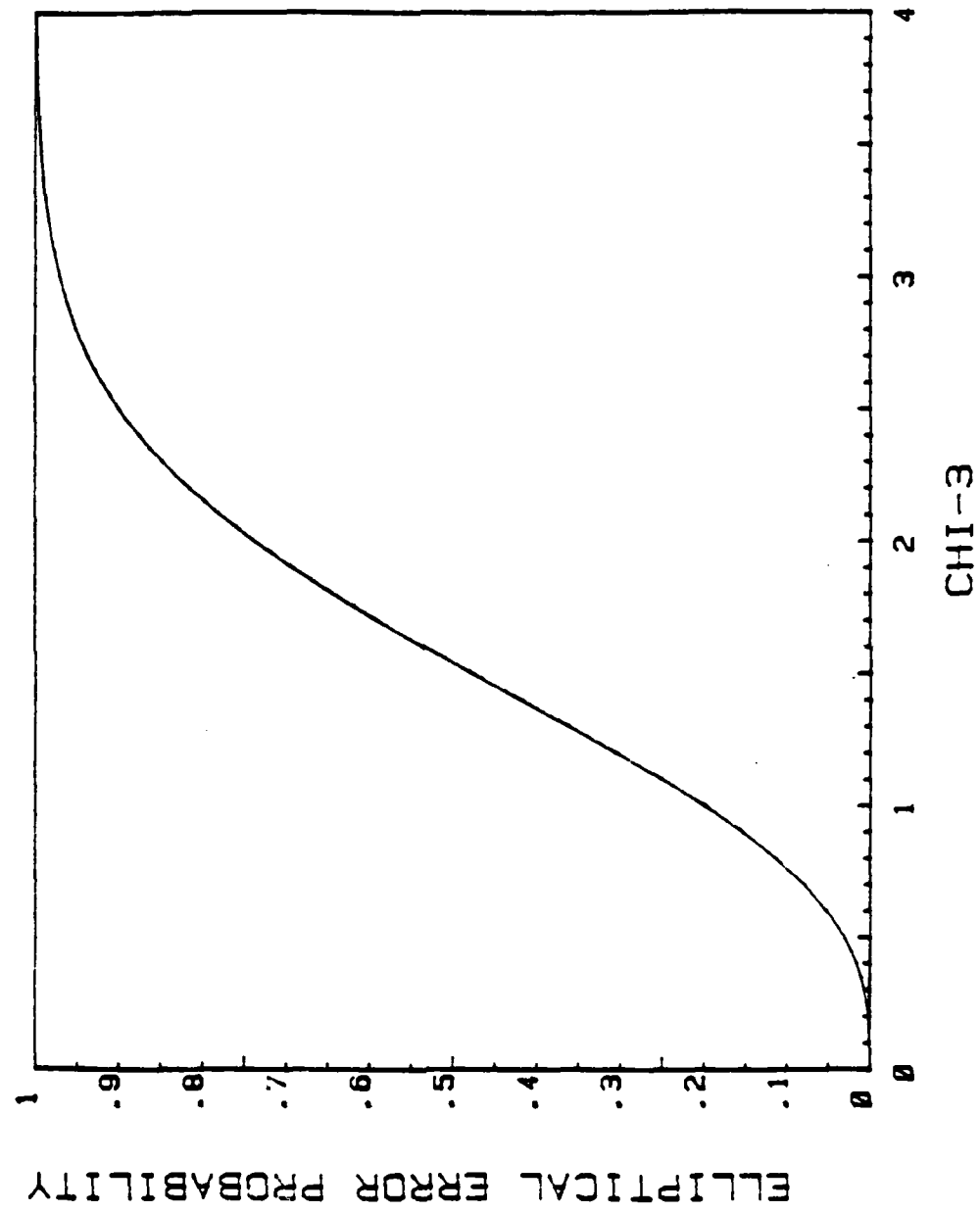


FIGURE 3.7 EEP FOR 3 DIMENSIONS (EFFECTIVE)

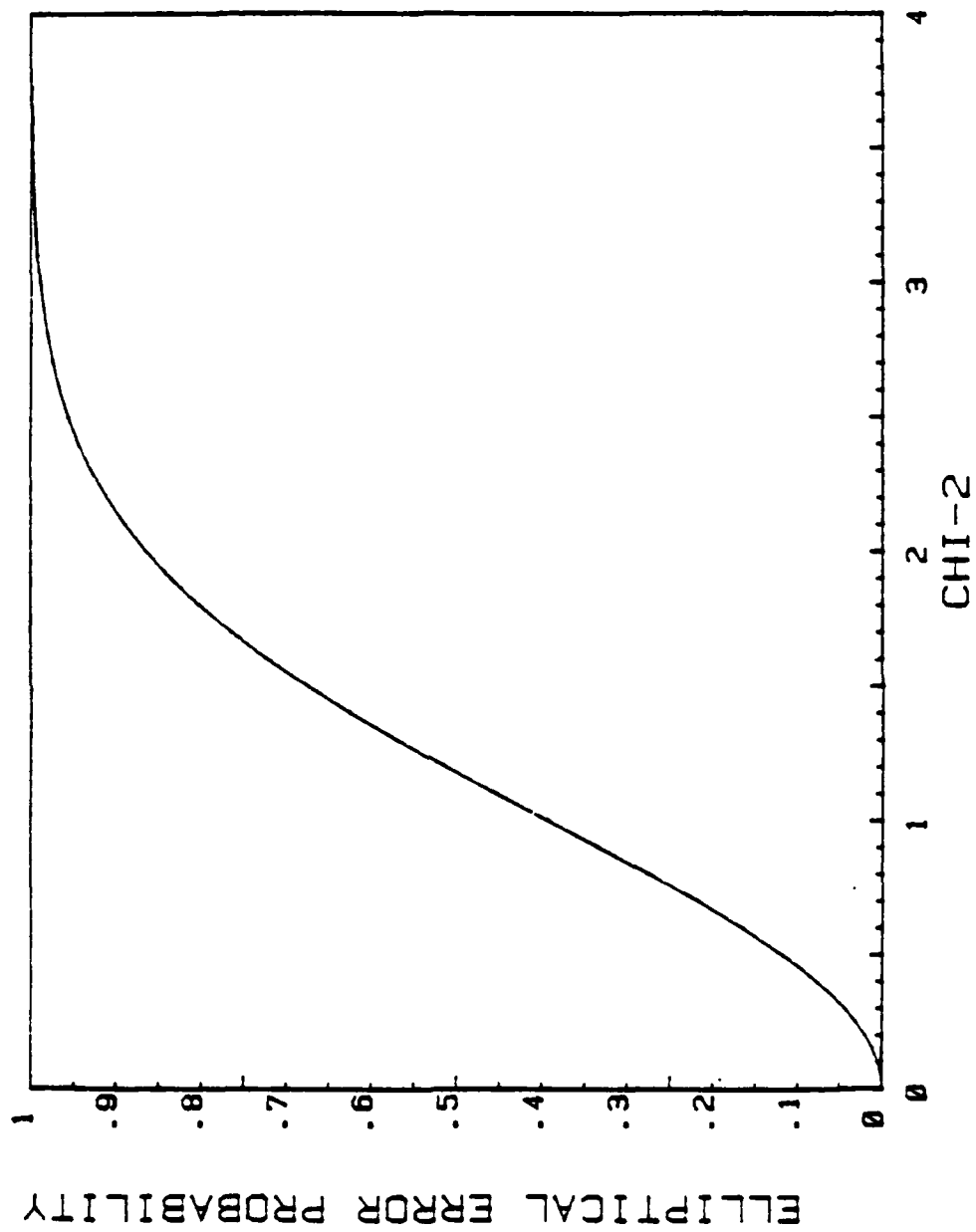


FIGURE 3.8 EEP FOR 2 DIMENSIONS (EFFECTIVE)

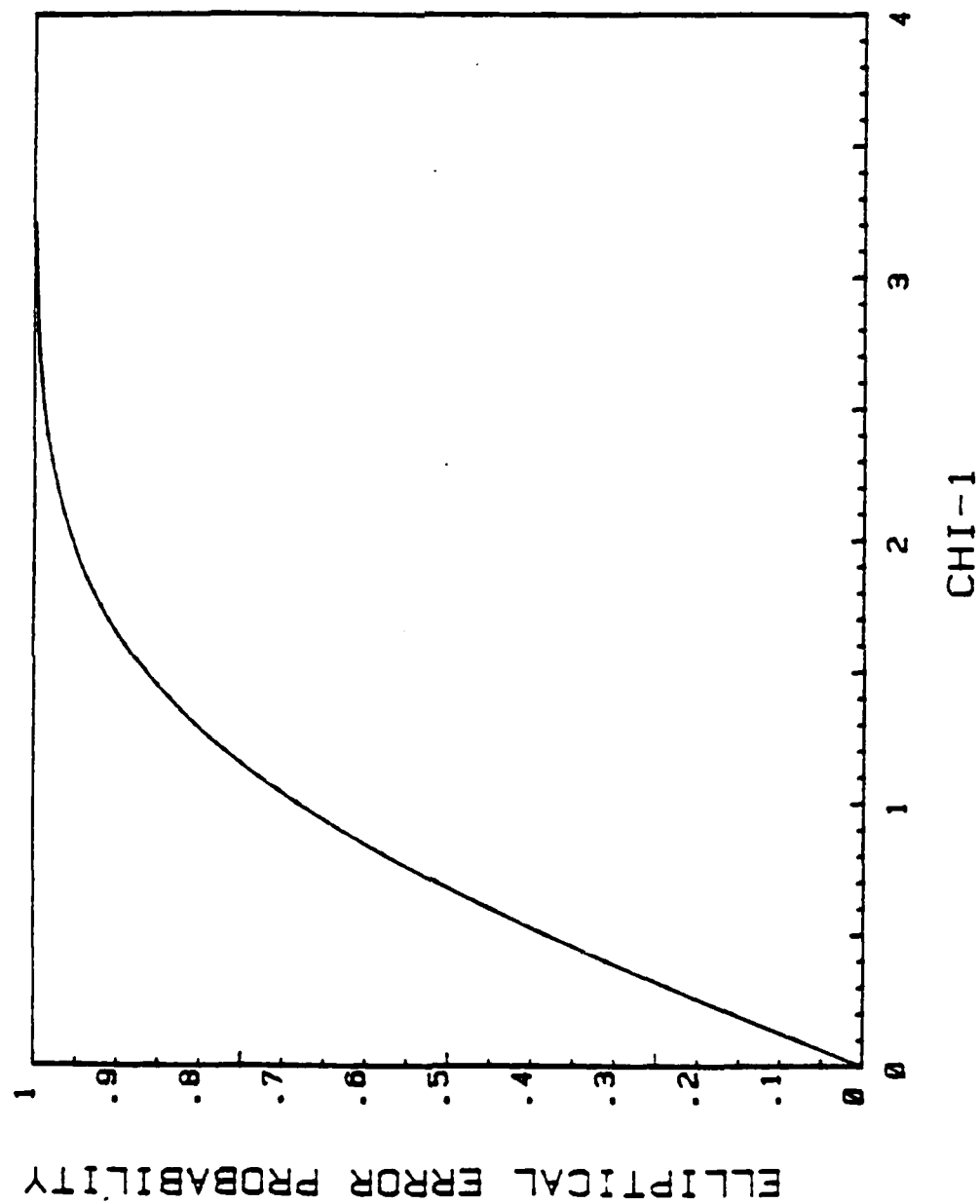


FIGURE 3.9 EEP FOR 1 DIMENSION (EFFECTIVE)

4.0⁻ APPLICATION CONSIDERATIONS

The purpose of this section is to provide the range analyst information for developing GPS compatible range instrumentation and data processing systems. Range requirements vary from simple coarse position data to sophisticated Post-test data processing estimates and cannot be adequately covered in this document. Subjects discussed in this section are major concerns that became apparent during the initial phase of a Triservice GPS Range Applications Study currently in progress. The data processing subjects are refinements developed during GPS projects at the Western Space and Missile Center, Vandenberg AFB, California. These subjects were researched and developed by several members of the Systems Performance Analysis Department; consequently, individualistic styles are apparent. Recommendations for further work are provided in some sections.

4.1 Real-Time versus Post-Test

As in virtually all test and training range applications there are decidedly different methods and uses of processing data in real-time and post-test and the same is true for GPS data. As already discussed in Section 2, the accuracies one can expect from GPS differ from real-time to post-test. Several other sections in this report address various aspects of this issue (particularly Sections 4.10 and 4.11); the purpose of this section is to give a general discussion of the overall real-time versus post-test considerations. The slowly varying errors referred to in Section 2 are, for simplicity, loosely called biases and the rapidly varying errors we refer to as noise.

Many of the Triservices GPS test and training applications will be recognized as real-time scenarios. Typical examples are:

1. Ballistic missile tracking for flight safety.
2. Fleet, unit and formation relative positioning.
3. Aircraft or missile absolute positioning using a GPS aided navigation solution.
4. Ship, vehicle, or troop absolute positioning and deployment.
5. Targeted small missiles control and tracking.

Post-test processing might serve to merely improve upon real time results, but post-test scenarios also form a separate class requiring higher accuracy and larger data sets than real-time scenarios. Thus post-test reexamination and analysis of GPS data can apply to the above real-time list.

Typical applications more strictly classified as post-test include:

1. Trajectory reconstruction.
2. Instrumentation accuracy analysis.
3. Surveying.
4. Point positioning such as certain impact scoring scenarios which have no real time processing requirements.

In addition, test scenarios might specify a "quick look" GPS data processing capability which may generally be classified as post-test. This category may allow data processing at sites conveniently removed from the test location and test conditions.

This section discusses real-time versus post-test accuracies. The analysis examines the individual terms of the error budgets presented in Section 2. Estimated measurement uncertainties propagate directly into expected user state uncertainties. Two factors explain the increased accuracies attainable post-test: (1) improved removal of bias from the GPS pseudo-range measurements, and (2) optimal processing over larger data sets. These factors depend on the quality of the data and the nature of its use, as discussed below.

4.1.1 Bias Removal

Many Triservices GPS scenarios will not be affected by Space Segment or atmospheric delay biases. User state solutions for participants in small arena differential navigation (discussed in Section 4.2) will be offset by a common bias. Therefore, they are not included in either the real-time or post-test processing error budgets for these scenarios. Thus the following discussion does not fully pertain to relative positioning or differential navigation scenarios.

The real-time versus post-test biases of chief concern appear in (1) satellite ephemerides, (2) satellite clock predictions, and (3) atmospheric delay corrections. The first two errors are closely related and difficult to distinguish in practice (Ref [16], p 9). They are the values of satellite state which are used in functional equations relating user to satellite slant ranges. The atmospheric refraction correction is an estimated bias which is subtracted from pseudo-range measurements to give corrected values.

The GPS Control segment tracks GPS satellites over extended periods of time. The error model of the Control segment determination of satellite ephemerides includes both bias and noise terms. Optimal processing techniques provide "best available" estimates of the true satellite ephemerides which are in turn periodically uploaded to the satellites and placed into satellite data formats. Thus the GPS ephemeris data contains residual offsets or biases.

The Aerospace Corporation can provide corrected ephemeris estimates having smaller bias errors approximately thirty days after the fact. The improved

reduction of bias results in higher post-test user accuracies. In GPS Phase III, the real-time ephemerides will eventually be known as precisely as Phase II post-test ephemerides available now. Furthermore, late Phase III gains in post-test processing due to the removal of ephemeride biases will not be as dramatic as in current Phase II except for replacement satellites (due to inexact knowledge of their ephemerides for some time).

Satellite clock and timing information is extracted from the GPS data format in the form of clock drift prediction model error coefficients and satellite clock offset estimates previously uploaded by the Control Segment. Thus, satellite timing uncertainties increase with the length of time since the last update and can cause significant errors in real-time. Accuracy gains in post-test data processing can be important in this area. Satellite clock errors do affect state estimates, but errors correlated between satellites can result in a compensating value of user clock offset such that a common Control Segment uploaded clock error may not degrade user coordinate estimates noticeably (although users of GPS time would be affected).

Errors introduced by refraction corrections are due to errors in (1) the estimated tropospheric delay and (2) the estimated ionospheric delay. These corrections may be determined by (1) a priori constant correction and/or (2) a priori atmospheric modeling with/without actual parametric data. The latter method is generally more accurate. Dual frequency P code users have the advantage of improved ionospheric corrections in real-time if the L_1 - L_2 ionospheric correction is used. Furthermore, pooled data concerning atmospheric conditions can increase both real-time and post-test results. Extensive off line modeling using available atmospheric data and dual frequency ionospheric delay measurements can improve the final atmospheric corrections for ionospheric and tropospheric delay for post-test.

4.1.2 Processing Considerations

Other than the removal of bias from pseudo-range measurements, the major real-time versus post-test consideration is the method of processing GPS and other measurements. The categories of concern are (1) the available GPS measurement history as compared to the processed data span, (2) computer algorithms, and (3) the use of supporting non GPS data. In this section GPS measurements are

considered to be simultaneous, that is, pseudo-range and delta pseudo-range measurements are taken from each of four satellites at the same time instant (thus assuming a four or more channel receiver):

There are several different methods of processing the measurements, two of which are (1) compute a single point estimate of user state using only the measurements taken at a single time instant, or (2) compute a point estimate of user state using a subset of GPS measurement history and known equations of motion. Both methods model the measurement process and include both the slowly and rapidly varying terms in the error model.

The first method can provide better post-test accuracy (than real-time) because some of the GPS error budget terms are smaller. Here the emphasis is on the better satellite state information provided post-test as explained above. When GPS measurements are corrected for "known" biases, the UERE terms from Section 2 are lower, and these smaller expected measurement errors lead directly to smaller expected user state errors.

The second method can provide more accurate results post-test than real-time because of both the above reason and the constraints of the equations of motion, assuming these are adequately specified. Here the emphasis is on the rejection of random noise in the GPS measurements by user software processing. The effect of user receiver noise can be reduced, and receiver biases can possibly be identified.

A full error analysis is required to analytically bound the noise terms of the GPS error budget on an individual basis for multi sample processing. Simplified methods exist which should suffice to indicate a reasonable final UERE. First, an empirical approach is to find test accuracy results for scenarios similar to that of the user. If the PDOP terms are specified the apparent UERE may be readily factored from the position coordinate residuals. Here the user knows a correct single sample UERE (as from Section 2), and previous tests indicate a noise reduction scale factor for projected scenarios. A second method is to classify expected user dynamics as high, medium or low in terms of user velocity, acceleration and jerk. This simplified error analysis was described in Ref [2] which lists expected user coordinate uncertainties. Again the PDOP term must be specified in order to factor the

apparent UERE, and the UERE is needed because PDOP is widely variable (albeit calculable) for GPS Phase II and will be somewhat variable for Phase III.

Stationary users and those with smooth dynamics will achieve satisfactory noise reduction in real-time and post-test. For stationary users Doppler smoothing of the pseudo-range data can be accomplished because of the complementing nature of delta pseudo-range measurements. An important application is accurate surveying in a matter of minutes (Ref [3]). The reduction of noise is necessarily limited by unmodeled errors and multipath effects, but in some cases noise terms in the applicable error budget can be reduced by \sqrt{n} , n being the number of independent samples. Doppler smoothing over reasonable intervals of continuous simultaneous tracking has been claimed to achieve this reduction, both for receiver and atmospheric correction random noise. For these reasons, insofar as real-time vs post-test processing is concerned, it can generally be stated that post-test accuracies will be better than real-time accuracies.

The data rate at which these measurements can be taken and stored or relayed to recording equipment may exceed the real-time processing capabilities of on-board navigation computers and real-time test support computers on ships, aircraft, mobile stations or even permanent land based sites. Similarly, updated navigation solutions would probably not be available after every GPS type measurement. Thus post-test processing will probably involve a larger data set, and, additionally, optimal batch least squares or Kalman filter/smoothers will operate over the entire data set, while real-time processing will be basically sequential with no or limited smoothing. These considerations involve both the processed data span and computer algorithms.

Some scenarios might include non GPS data such as vehicle state estimates from radar and telemetry data, measurements from inertial devices, altimeter readings, tide tables, or survey coordinates of participants. These additional data sets improve both real-time and post-test user state estimates, or conversely, GPS data augments traditional tracking and user state estimation schemes.

4.2 Relative versus Absolute and Small Arena versus Global Navigation Issues

4.2.1 Relative vs Absolute Accuracies

The most direct method of GPS navigation is to utilize four or more pseudo-range measurements (from suitable SVs) and solve for user position and the user time offset relative to GPS time. The user position is solved in an earth centered coordinate system. This method is called absolute or global navigation. The non absolute navigation means either that one user set is navigating relative to another user set via a data link, or that the user has been at a given point at some prior time and is navigating relative to coordinates measured at that point. Both of these methods are referred to as differential navigation but for the purpose of this section we will refer to the former as relative and the latter as delta.

The GPS system errors have been presented in Table 2.1. These system errors will affect the accuracy of the absolute navigation. When the determination of only the coordinate differences between two locations is the main concern, the differential navigation techniques can provide increased accuracy. Since the bias errors caused by transmitter imperfections, ephemeris and clock prediction, and ionospheric delay are similar at both the user location and the destination, they approximately cancel. These errors are usually the largest component of the total error. The receiver bias, which is user dependent, is another component of the total error. The receiver bias is cancelled out in the delta navigation, but not in the relative navigation. The gains (one sigma) that can be made in accuracy in relative navigation versus absolute navigation are summarized in Table 4.2.1.

An illustration of the effect produced by the differential navigation techniques is shown in Figure 4.2.1, (Ref [9]). It is a segment of the 11 January 1980 mission data, using Texas Instrument's High Dynamic User Equipment (HDUE). When operating in the normal (absolute navigation) mode, the HDUE provided position estimates that had root mean square errors about 20 meters horizontally and near 40 meters vertically. When HDUE was placed in the differential mode, these errors were immediately reduced to the neighborhood of 5 meters in this example.

TABLE 4.2.1 GPS ERROR BUDGET (ABSOLUTE AND RELATIVE NAVIGATION)

ERROR SOURCE	ABSOLUTE (meters)	RELATIVE (meters)
Clock and Navigation Subsystem Stability	2.7	0
Predictability of Satellite Perturbation	1.0	0
Other	0.866	0
Ephemeris and Clock Prediction	2.5	0
Ionospheric Delay Compensation	2.3	0
Tropospheric Delay Compensation	2.0	0
Receiver Bias	0.5	$0.5\sqrt{2}$
Receiver Noise and Resolution	1.5	$1.5\sqrt{2}$
Multipath	1.2	$1.2\sqrt{2}$
1 σ UERE	5.3	2.8

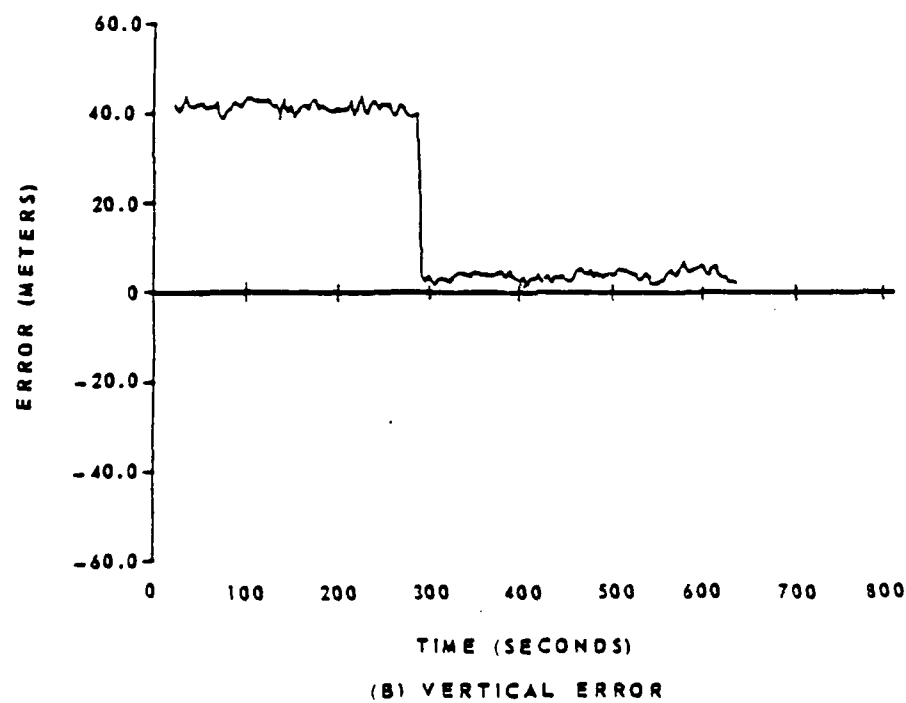
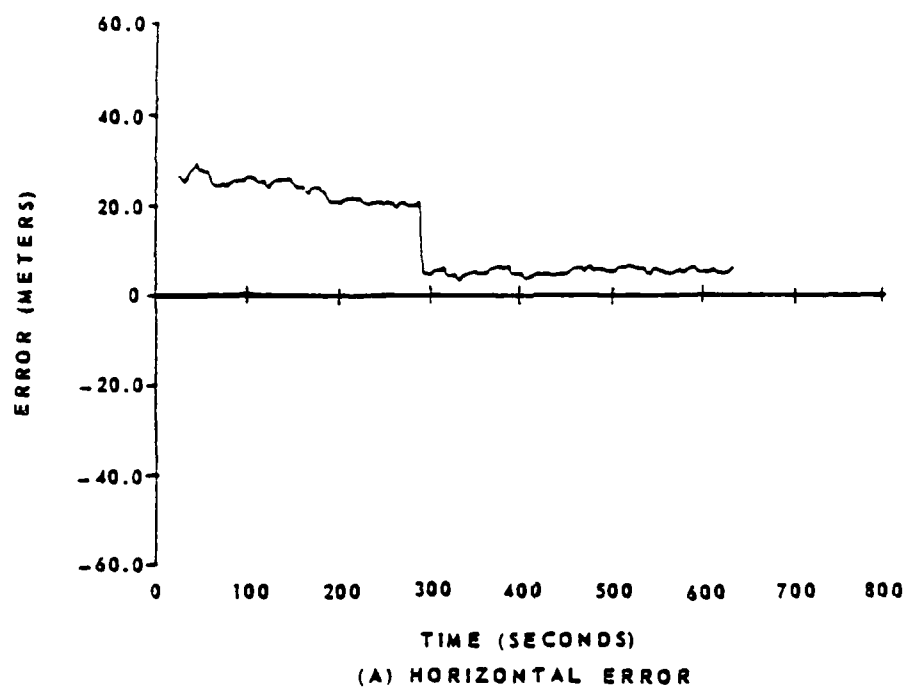


FIGURE 4.2.1 HORIZONTAL AND VERTICAL ERRORS (ONE SIGMA)

Ionospheric refraction generates range errors which can be approximately cancelled out in the relative navigation if the two receivers are relatively near one another. The cancellation will, however, be gracefully degraded over space and time due to the translocation of ionospheric correction.

The ionospheric error is dependent on both the characteristics of the ionosphere at zenith (at a given time) and the elevation angle to the satellite from the user. The ionospheric delay at a given elevation is increased, relative to the delay for a ray to a satellite at zenith, by the obliquity factor. The obliquity factor's dependence on elevation is illustrated in Figure 4.2.2 (Ref [16], p 34), and Figure 4.2.3 (Ref [16], p 34) shows typical measurements of ionospheric delay for an L-band signal received at vertical incidence. The mean ionospheric delay (vertical incidence) is about ten nsec at nighttime, while it can be as large as 50 nsec during daytime. The delays can be significantly larger in regions near the geomagnetic equator or near the poles, particularly during the magnetic storm periods. As shown in Figure 4.2.2, the ionospheric delay can be three times the values given above, at low elevation angle. Thus the degradation of the cancellation of ionospheric correction errors over space and time must be considered in relative navigation applications.

The degradation due to translocation of Space and Control Segment errors can be bounded in a rather straightforward fashion for both relative and delta navigation. The case for relative navigation between two points A and B is illustrated in Figure 4.2.4. Here it is assumed that the pseudo-range errors are monitored at a known location A and applied to correct the pseudo-ranges measured at B. The relative navigation solution is degraded only by the difference in pseudo-range error at A and B. Thus, SV clock error has no effect on the solution, and only the SV ephemeris error which is orthogonal to the bisector of angle ASVB and in the plane ASVB contributes to pseudo-range error differences at A and B.

The case for delta navigation is illustrated in Figure 4.2.5. Here it is assumed that the pseudo-range errors are monitored at a known initial location and applied to correct the pseudo-ranges measured subsequently as a single vehicle moves away from the initial location. The pseudo-range error bound shown in the figure is based on the first harmonic of a slowly varying

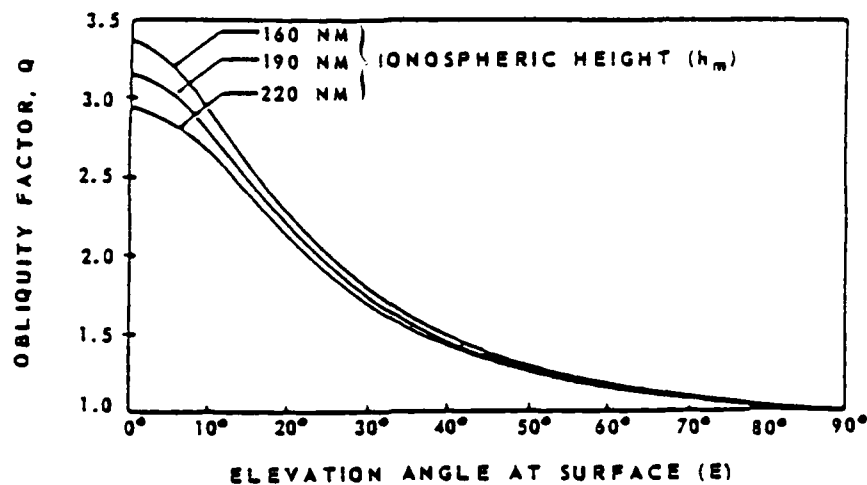


FIGURE 4.2.2 RELATIONSHIP OF OBLIQUITY FACTOR TO SURFACE ELEVATION ANGLE

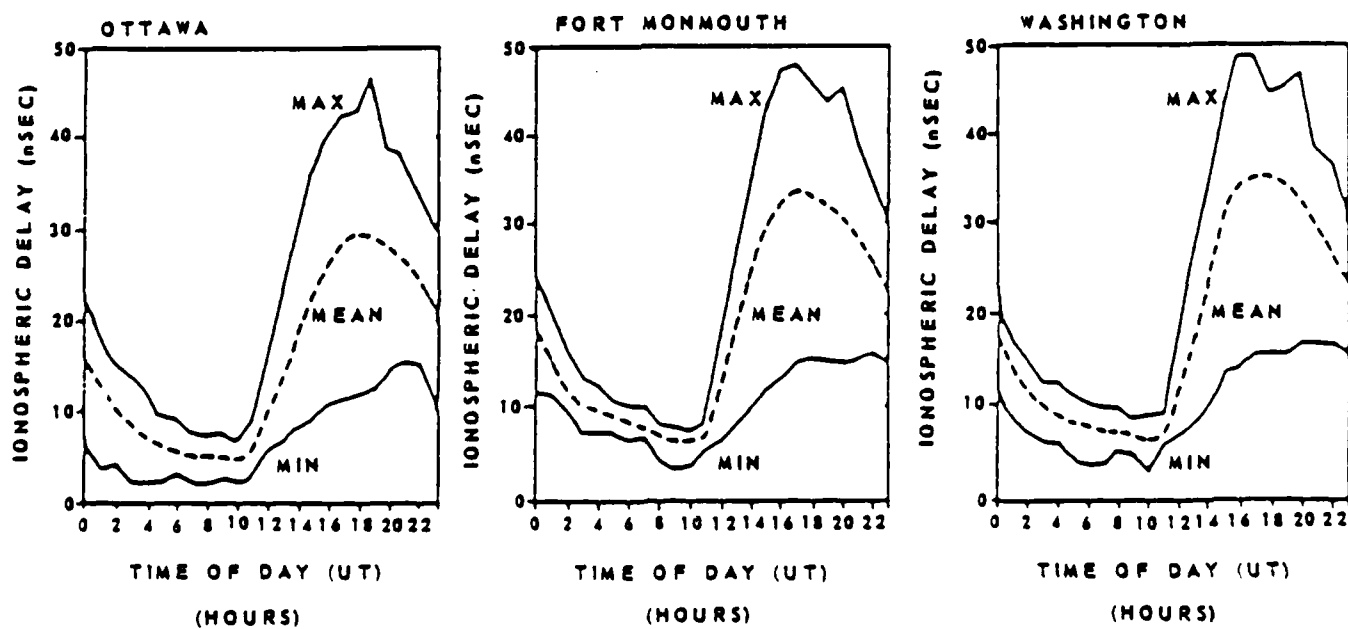


FIGURE 4.2.3 MEAN IONOSPHERIC DELAY AND ENVELOPE OF DELAY VARIATION vs TIME OF DAY
DURING MARCH, 1958 - SATELLITE AT ZENITH, $f = 1.6$ GHz

0 ONLY SV POSITION ERRORS IN THE PLANE COMMON TO A, B AND SV AND \perp TO THE BISECTOR CONTRIBUTE TO PSEUDO-RANGING ERROR DIFFERENCES @ A AND B.

0 FOR A AND B NEAR EARTH SURFACE, WORST CASE ERROR IS APPROXIMATELY BOUNDED BY

$$|\Delta R| \approx |\Delta R_A - \Delta R_B| \leq \frac{d\delta}{H}$$

$$\therefore \frac{|\Delta R|}{d\delta} \leq 5 \times 10^{-8} \text{ M/M}^2$$

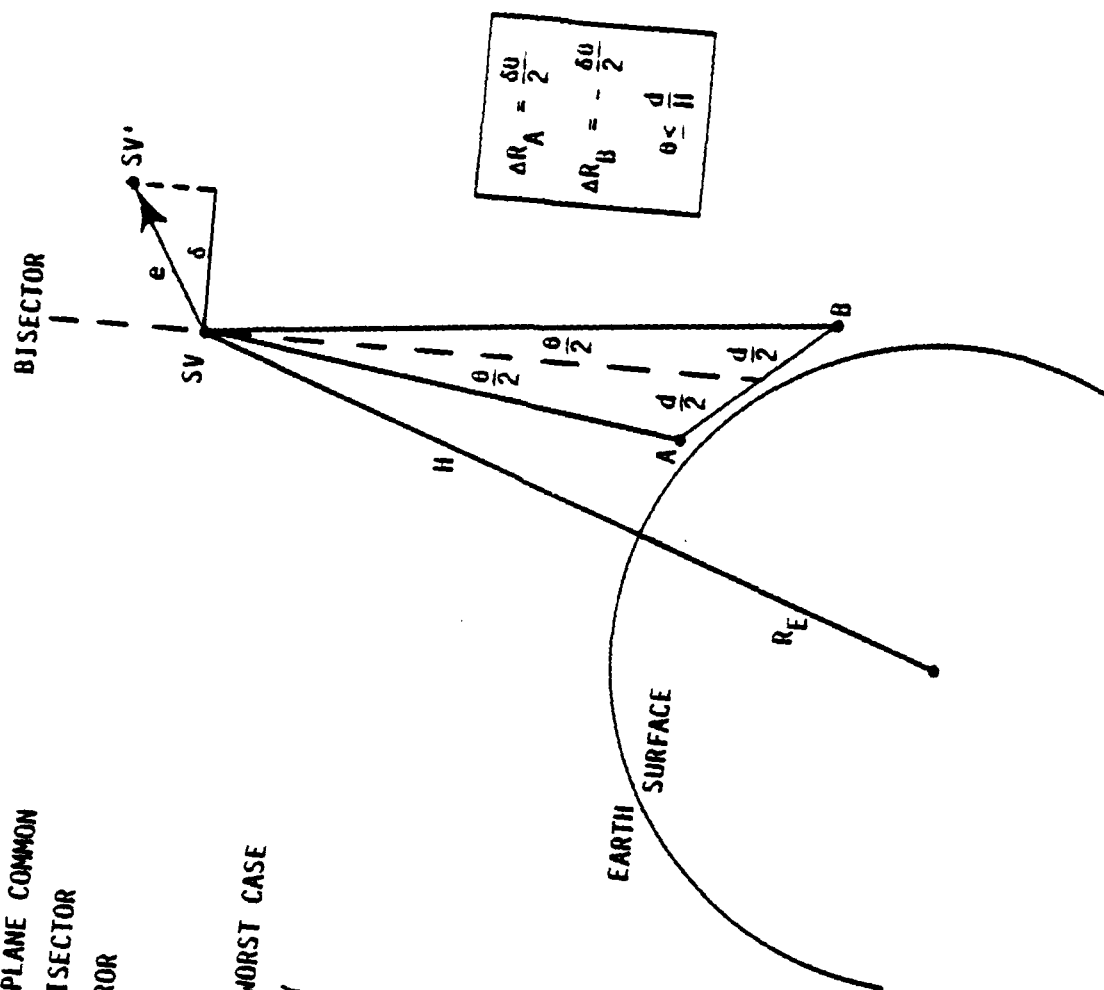


FIGURE 4.2.4 SPATIAL VARIATION OF PSEUDO-RANGE ERROR DUE TO SPACE AND CONTROL SEGMENTS

$$\Delta R = \delta \cdot \bar{e}_R$$

$$\dot{\Delta R} = \dot{\delta} \cdot \bar{e}_R + \delta \cdot \dot{\bar{e}}_R$$

$$\leq 4\pi \frac{|\delta_{\max}|}{T} + \left| \frac{2\pi(R_E + H)}{HT} + \Omega_E \right| |\delta|$$

$$\approx 4\pi \frac{|\delta_{\max}|}{T} + \left| \frac{8\pi}{3} + \pi \right| \frac{|\delta|}{T}$$

$$\leq \left| 4\pi + \frac{8\pi}{3} + \pi \right| \frac{|\delta_{\max}|}{T} \approx 2.0 \text{ M/HR/M} |\delta_{\max}|$$

$$\therefore \frac{|\dot{\Delta R}|}{|\delta_{\max}|} \leq 2.0 \text{ M/HR/M}$$

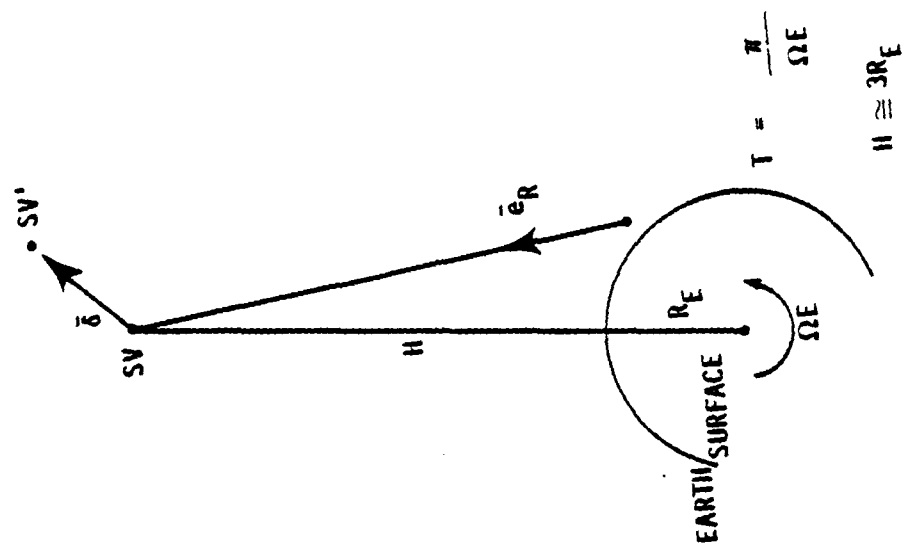


FIGURE 4.2.5 TEMPORAL VARIATION OF PSEUDO-RANGE ERROR DUE TO SPACE AND CONTROL SEGMENTS

ephemeris error. The period of the harmonic is $\frac{T}{2}$, where T is the SV period. To this bound on $|\Delta\dot{R}|$ must be added the term $C \Delta f/f_0$, where f_0 is the nominal value of SV clock frequency, Δf is the magnitude of the SV clock frequency from nominal, and C is the speed of light. Assuming the values

$$|\delta_{\max}| = 10 \text{ meters}$$

and

$$\frac{\Delta f}{f_0} = 5 \times 10^{-12},$$

which are larger than implied by the GPS error budget, it follows that

$$|\Delta\dot{R}| \leq 0.007 \text{ meters/sec.}$$

4.2.2 Small Arena vs Global Navigation Issues

Small Arena applications generally relate relative positions to a known position. These may involve the use of a large network of receivers or translators for multiple objects of interest. Global Navigation applications generally involve the use of receivers and the availability of virtually a complete NAVSTAR constellation to determine absolute position. Both Small Arena and Global Navigation applications may use post-test processing, pseudo satellites, and other methods to improve the solution's accuracy.

4.2.2.1 Small Arena Issues

Most Small Arena applications involve the use of test ranges where controlled conditions and some post-test processing can be employed. The main issue for Small Arena applications using translators or transdigitizers (discussed in Section 4.7) is spectral bandwidth. With the C/A code signal this involves the use of ≈ 2 MHz per object of interest (with dual frequency P code translators this increases to ≈ 40 MHz). It is obvious that extreme care must be used to avoid jamming and intermodulation problems.

If only relative position is desired ionospheric refraction is less of a problem for the Small Arena as all receivers can observe the same NAVSTAR satellites with similar viewing angles thus allowing the atmospheric delay

error to virtually cancel. It should be noted that many Small Arena applications, while involving the relative position, require that a control point "absolute" position be known. The absolute position of a fixed central point may be determined from geodetic survey references with a root mean square accuracy of ≤ 1 meter. This level of absolute accuracy may also be achieved with a GPS receiver with good PDOP and post-test refinement. If a mobile control point is required (such as for GPS-SMILS) then the need to determine the absolute location of this moving point virtually dictates the use of a dual frequency P code GPS receiver with post-test refinement. Pseudo satellites can be used to augment the current limited NAVSTAR constellation whenever practical. Pseudo satellites should improve the PDOP, interval of coverage, and reduce the level of post-test processing.

4.2.2.2 Global Navigation Issues

The use of GPS receivers for Global Navigation generally augment other sources of navigation data such as inertial systems, LORAN, and other navigation data to provide absolute position. An example of this is the location of a SLBM submarine for launch coordinates. The nature of these applications limit the amount of practical post-test processing and thus limits the potential accuracy to ≈ 10 meters (one sigma). Most Global Navigation applications are in remote locations where the availability of absolute geodetic fixes (terrestrial benchmarks) are limited.

4.3 Satellite Constellations Current and Planned

With the reduction of the number of GPS satellites from 24 to 18, various alternative 18-satellite arrangements were studied. The objective of these studies was to maximize the availability of the system to users despite the reduction in the number of satellites. Of the many alternatives considered, the current baseline Phase III, orbital configuration for the operational phase employs 18 satellites in 55-deg inclined, circular, 12 hour orbits to transmit navigation signals. It will provide continuous three dimensional global coverage by placing three satellites equally spaced (120 degrees apart) in each of six orbit planes. These six orbit planes are 60 degrees apart in inertial space, as depicted in Figure 4.3.1. This arrangement of 18 satellites has been found to be best as far as accuracy (good GDOP) and uniform global coverage is concerned. An alternate constellation employs six satellites in each of three orbital planes.

With only four, five or six satellites in the current development phase, GPS provides potential users a few hours of service each day. Navigation intervals for 42 cities around the world are tabulated as follows. Table 4.3.1 shows the interval for four satellites. As the fifth and sixth satellites are added, the periods of navigation get considerably longer, as shown in Tables 4.3.2 and 4.3.3 (Ref [7]). The total GPS daily coverage based on the criterion: $PDOP < 6$, is shown for several locations of interest in Table 4.3.4 as the number of satellites varies from 6 to 18.

The primary location for GPS testing with the current constellation is the Army Proving Grounds in Yuma, Arizona. The accuracy of 3 Dimensional navigation at Yuma with four Space Vehicles (SV) is indicated by the solid line on Figure 4.3.2 (Ref [7]). The SEP (Spherical Error Probable), defined in Section 3, during the two-hour period is shown. Near the middle of the navigation interval when the satellite geometry is more favorable, the SEP is about 10 m. With the addition of a fifth satellite, the available test time is extended about 90 minutes, as shown by the dotted line in Figure 4.3.2. The accuracy during this additional time period, however, is degraded, because of the poor satellite geometry at Yuma. Similar figures for Grand Bahama Island and Cold Lake, Canada are shown in Figures 4.3.3 and 4.3.4.

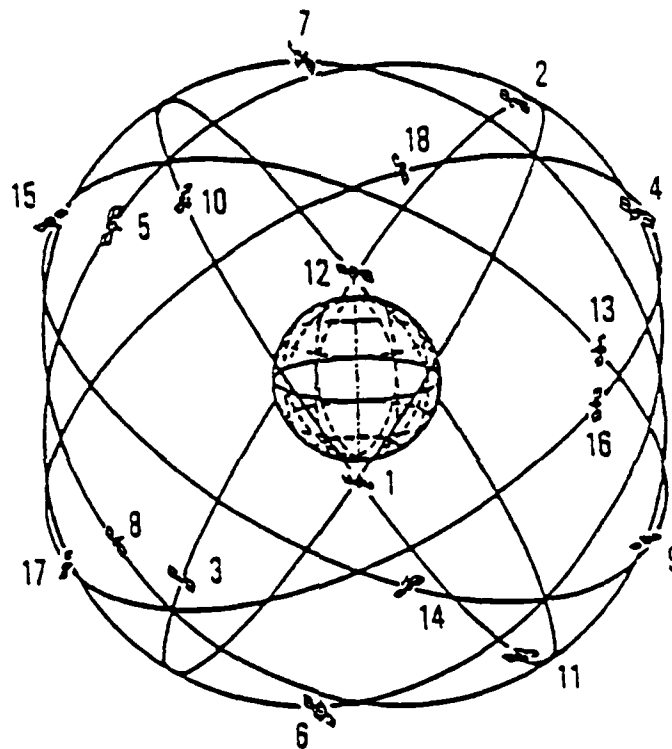


FIGURE 4.3.1 NAVSTAR/GPS 6-PLANE, 18-SATELLITE CONFIGURATION

TABLE 4.3.1 NAVIGATION AVAILABILITY WITH FOUR SATELLITES

User Location	GMT Start	GMT End	HRS Duration	GMT Start	GMT End	HRS Duration	Total Duration (HRS)
Acapulco, Mexico	14.5	15.5	1.0				1.0
Anchorage, Alaska	14.5	16.0	1.5				1.5
Ankara, Turkey	1.17	3.3	1.5				1.5
Brussels, Belgium	2.5	3.5	1.0				1.0
Buenos Aires, Argentina	19.5	21.0	1.5				1.5
Camp Parks, California	13.5	15.8	2.3				2.3
Calcutta, India	2.5	4.0	1.5				1.5
Cape Kennedy, Florida	14.5	16.2	1.7				1.7
Cape Town, South Africa	20.5	22.2	1.7				1.7
Caracas, Venezuela	15.5	16.1	0.6				0.6
Charleston, South Carolina	14.2	16.2	2.0				2.0
Christchurch, New Zealand	8.0	10.3	2.3				2.3
Cold Lake, Canada	14.2	16.3	2.0				2.0
Diego Garcia	Not available						
Eglin Air Force Base	14.2	16.2	2.0				2.0
Farnborough, United Kingdom	2.5	3.5	1.0				1.0
Fort Monmouth, New Jersey	14.5	16.2	1.7				1.7
Fortuna, North Dakota	14.2	16.3	2.0				2.0
Galveston, Texas	14.2	16.2	2.0				2.0
Grand Bahama Island	14.5	16.2	1.7				1.7
Guam	Not available						
Honolulu, Hawaii	13.2	14.3	1.1				1.1
Hormuz	1.2	3.3	2.0				2.0
Las Palmas, Canary Islands	Not available						
Lima, Peru	Not available						
New Hampshire (SCF)	14.7	16.2	1.5				1.5
New London, Connecticut	14.7	16.2	1.5				1.5
Pago Pago, American Samoa	9.0	10.2	1.2				1.2
Panama Canal	15.2	15.8	0.5				0.5
Riyadh, Saudi Arabia	1.2	3.0	1.8				1.8
Rome, Italy	2.0	3.0	1.0				1.0
Seychelles Island	Not available						
Sidney, Australia	7.5	9.5	2.0				2.0
Stockholm, Sweden	2.5	4.0	1.5				1.5
Taipei, Formosa	3.5	4.2	0.7				0.7
Tananarive, Malagasy Republic	Not available						
Tel Aviv, Israel	1.2	3.0	1.8				1.8
Thule, Greenland	Not available						
Tokyo, Japan	Not available						
Tromsø, Norway	2.7	3.8	1.0				1.0
Vandenberg Air Force Base	13.5	15.5	2.0				2.0
Yuma, Arizona	13.5	15.8	2.3				2.3

Notes: Navigation intervals of less than 0.5 hr were not included because they are not considered useful.

TABLE 4.3.2 NAVIGATION AVAILABILITY WITH FIVE SATELLITE CONSTELLATION

User Location	GMT Start	GMT End	HRS Duration	GMT Start	GMT End	HRS Duration	Total Duration (HRS)
Acapulco, Mexico	13.0	15.3	2.3				2.3
Anchorage, Alaska	13.2	16.0	2.8				2.8
Ankara, Turkey	0.5	3.3	2.8				2.8
Brussels, Belgium	1.5	3.6	2.1				2.1
Buenos Aires, Argentina	18.2	21.1	2.8				2.8
Camp Parks, California	13.0	15.9	2.9				2.9
Calcutta, India	1.5	4.2	2.7				2.7
Cape Kennedy, Florida	14.0	17.2	3.2				3.2
Cape Town, South Africa	20.5	23.5	3.0				3.0
Caracas, Venezuela	14.9	18.8	3.8				3.8
Charleston, South Carolina	14.2	17.2	2.9				2.9
Christchurch, New Zealand	7.5	10.7	3.2				3.2
Cold Lake, Canada	13.0	16.7	3.7				3.7
Diego Garcia	1.7	2.3	0.5				0.5
Eglin Air Force Base	14.0	16.7	2.7				2.7
Farnborough, United Kingdom	1.7	3.5	1.8				3.5
Fort Monmouth, New Jersey	14.2	17.5	3.3				3.3
Fortuna, North Dakota	13.2	16.7	3.5				3.5
Galveston, Texas	13.7	16.5	2.7				2.7
Grand Bahama Island	14.0	17.2	3.2				3.2
Guam	Not available						
Honolulu, Hawaii	12.0	14.4	2.4				2.4
Hormuz	1.0	3.3	2.3				2.3
Las Palmas, Canary Islands	Not available						
Lima, Peru	18.6	19.1	0.5				0.5
New Hampshire (SCF)	14.6	17.5	2.9				2.9
New London, Connecticut	14.6	17.5	2.9				2.9
Pago Pago, American Samoa	7.5	8.3	0.8	8.8	10.4	1.6	2.4
Panama Canal	13.5	14.3	0.8	14.9	15.9	1.0	1.8
Riyadh, Saudi Arabia	0.5	3.1	2.6				2.6
Rome, Italy	1.0	3.1	2.1				2.1
Seychelles Island	1.2	2.0	0.8				0.8
Sidney, Australia	7.2	9.6	2.3				2.3
Stockholm, Sweden	1.5	4.0	2.5				2.5
Taipei, Formosa	3.2	6.3	3.0				3.0
Tananarive, Malagasy Republic	22.0	23.3	1.3				1.3
Tel Aviv, Israel	0.2	3.1	2.8				2.8
Thule, Greenland	13.7	14.4	0.6	15.2	17.3	2.0	2.6
Tokyo, Japan	3.2	5.0	1.8				1.8
Tromsø, Norway	1.5	2.4	0.9	2.6	3.8	1.2	2.1
Vandenberg Air Force Base	13.0	15.6	2.6				2.6
Yuma, Arizona	13.5	15.9	2.4				2.4

NOTE: Navigation intervals of less than 0.5 hr were not included because they are not considered useful.

TABLE 4.3.3 NAVIGATION AVAILABILITY WITH SIX SATELLITE CONSTELLATION

User Location	GMT Start	GMT End	HRS Duration	GMT Start	GMT End	HRS Duration	Total Duration (HRS)
Acapulco, Mexico	13.0	15.6	2.6	16.1	18.3	2.2	4.7
Anchorage, Alaska	0.2	3.2	1.0	4.5	5.0	0.5	
	13.2	16.0	2.8	16.6	17.8	1.2	5.4
Ankara, Turkey	0.5	5.0	4.5				4.5
Brussels, Belgium	1.4	3.9	2.5				2.5
Buenos Aires, Argentina	18.2	23.0	4.8				4.8
Camp Parks, California	13.0	17.5	4.5				4.5
Calcutta, India	1.5	7.3	5.8				5.3
Cape Kennedy, Florida	14.0	18.8	4.8				4.8
Cape Town, South Africa	20.5	0.5	4.0				4.0
Caracas, Venezuela	14.9	18.8	3.8				3.8
Charleston, South Carolina	14.2	18.8	4.5				4.5
Christchurch, New Zealand	7.5	12.5	5.0				5.0
Cold Lake, Canada	13.0	18.3	5.3				5.3
Diego Garcia	1.7	2.3	0.5	5.0	5.5	0.5	1.0
Eglin Air Force Base	14.0	18.8	4.8				4.8
Farnborough, United Kingdom	1.7	3.8	2.1				2.1
Fort Monmouth, New Jersey	14.2	18.3	4.0				4.0
Fortuna, North Dakota	13.2	18.3	5.0				5.0
Galveston, Texas	13.7	19.0	5.3				5.3
Grand Bahama Island	14.0	18.8	4.8				4.8
Guam	Not available						
Honolulu, Hawaii	12.0	16.3	4.3				4.3
Hormuz	1.0	5.8	4.8				4.8
Las Palmas, Canary Islands	27.5	3.5	1.0				1.0
Lima, Peru	18.5	22.1	3.6				3.6
New Hampshire (SCF)	14.6	18.0	3.4				3.4
New London, Connecticut	14.6	18.0	3.4				3.4
Pago Pago, American Samoa	7.5	8.3	0.8	8.9	10.4	1.6	
	10.8	13.8	3.0				5.3
Panama Canal	13.5	14.3	0.8	14.9	15.9	1.0	
	17.1	20.3	3.2				5.0
Riyadh, Saudi Arabia	0.5	5.8	5.3				5.3
Rome, Italy	1.0	4.0	3.0				3.0
Seychelles Island	1.2	2.0	0.8	4.7	5.5	1.8	1.5
Sidney, Australia	7.2	11.5	4.3				4.3
Stockholm, Sweden	1.5	4.0	2.5	4.6	5.5	0.9	
	14.5	15.2	0.7				4.1
Taipei, Formosa	3.2	6.3	3.0				3.0
Tananarive, Malagasy Republic	22.0	23.3	1.3				1.3
Tel Aviv, Israel	0.2	5.0	4.8				4.8
Thule, Greenland	2.0	3.3	1.3	3.7	4.8	1.0	
	13.7	17.3	3.5				5.8
Tokyo, Japan	3.2	5.0	1.8				1.8
Tromsø, Norway	1.5	4.4	2.9	4.6	5.5	0.9	
	14.2	15.2	1.0	15.7	17.0	1.3	6.1
Vandenberg Air Force Base	13.0	17.5	4.5				4.5
Yuma, Arizona	13.5	17.8	4.3				4.3

NOTE: Navigation intervals of less than 0.5 hr were not included because they are not considered useful.

NUMBER OF SATELLITES

	6	8	10	12	14	16	18
VAFB	4.4	5.3	8.3	12.3	17.2	22.2	23.5
YUMA	4.7	5.3	3.3	11.4	18.2	22.4	23.2
EGLIN	3.5	5.0	6.9	11.2	17.0	23.4	24.0
FT. MONMOUTH	5.0	5.3	8.7	11.5	17.3	21.8	22.8
HAWAII	1.5	5.2	6.5	12.6	18.1	21.8	24.0
GALVESTON	4.3	5.6	7.8	11.0	17.0	22.5	23.6

LOCATIONS

(UNITS ARE HOURS, CRITERIA IS PDOP < 6)

TABLE 4.3.4 TOTAL GPS DAILY COVERAGE

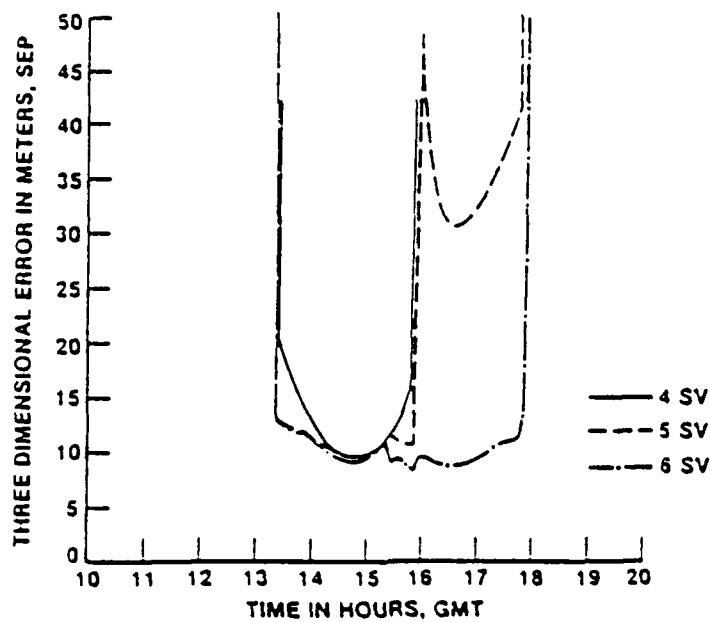


FIGURE 4.3.2 THREE-DIMENSIONAL NAVIGATION AT YUMA

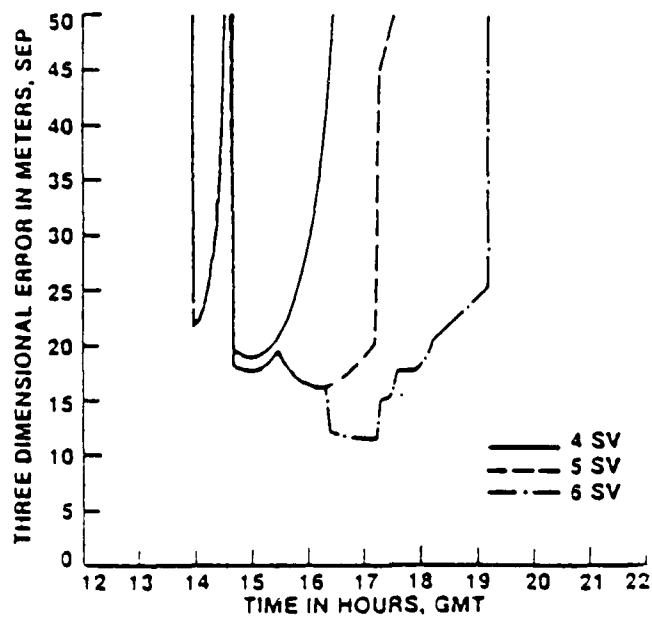


FIGURE 4.3.3 THREE-DIMENSIONAL NAVIGATION AT GRAND BAHAMA

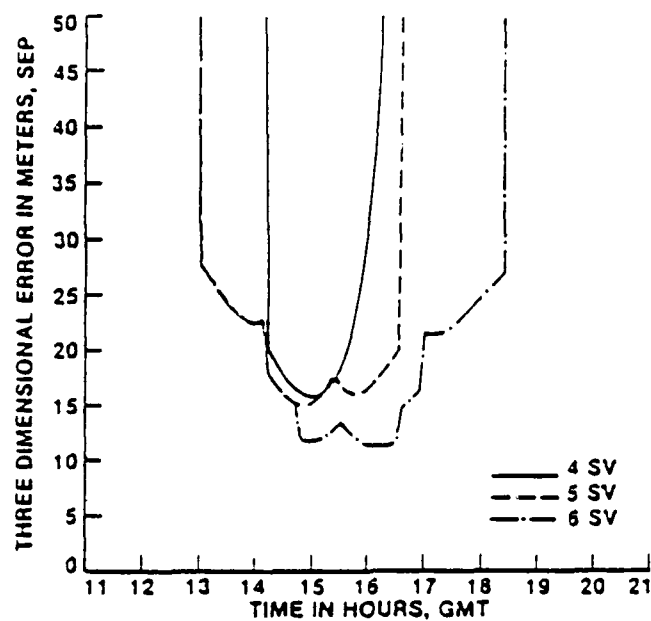


FIGURE 4.3.4 THREE-DIMENSIONAL NAVIGATION AT COLD LAKE

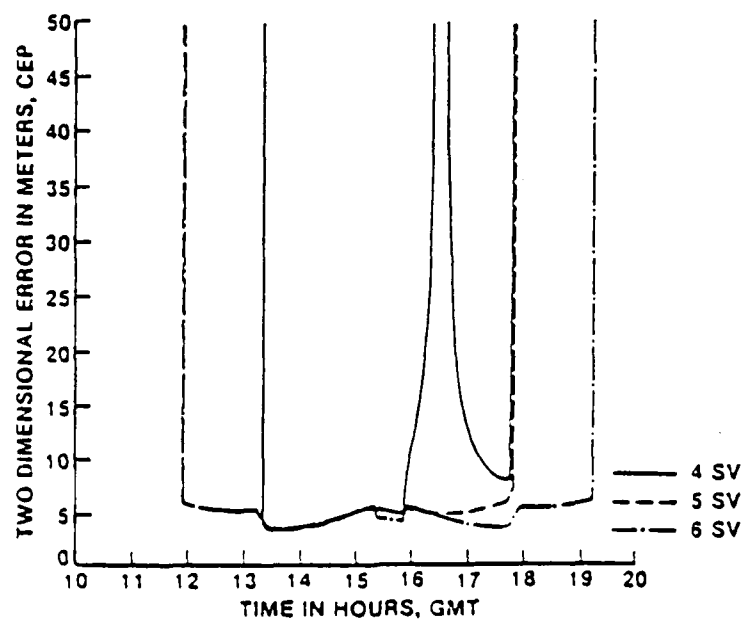


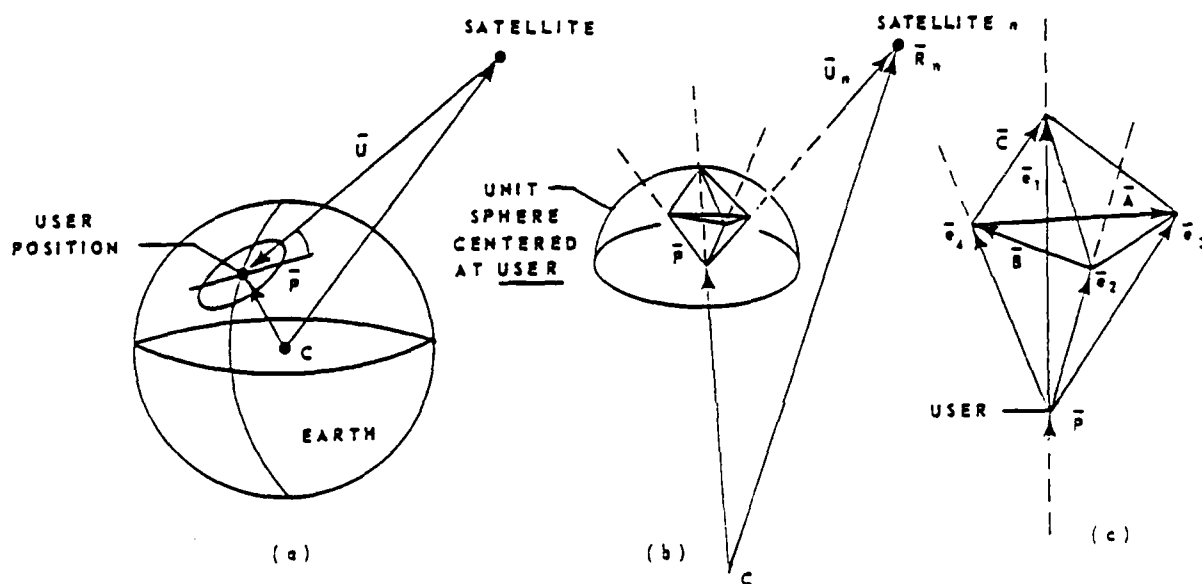
FIGURE 4.3.5 TWO-DIMENSIONAL NAVIGATION AT YUMA

When the altitude at the user location is known, 2 Dimensional (horizontal) navigation can be performed (see Section 4.4 for an analysis of this method). It is noticed that the time period available for testing 2 Dimensional navigation at Yuma is extended considerably as shown in Figure 4.3.5. This is due to the fact that this mode of navigation makes use of some geodetic height information thus necessitating the use of only three satellites (see Section 4.4).

The user position errors in GPS navigation are determined by two factors: the magnitude of the ranging errors and the geometry relative to the selected satellites. The ranging errors are statistically described by 1σ UERE, while the effect of the geometry is expressed by geometric dilution of precision (GDOP) parameters. These parameters include PDOP, HDOP, VDOP and TDOP, as discussed in Section 3.

Small values of PDOP and HDOP indicate good geometry of the selected satellites and, correspondingly, small errors in user position estimation. Geometrical dilution can be visualized by the volume of a special tetrahedron as shown in Figure 4.3.6. Let \bar{P} denote the user position and let S be a unit sphere centered at \bar{P} . The vectors from the user position to each satellite will intersect the unit sphere at four points. The tetrahedron, formed by connecting these points has a volume V . As the volume of the tetrahedron becomes larger, the geometric strength of the solution improves accordingly. It is noted that the volume is maximized when one satellite is at the user's zenith, and the other three are separated by 120° and are as low on the horizon as permitted by the user's antenna elevation angle.

GDOP parameters depend only on the orientation of the selected satellites relative to the user. They are functions of the user location on earth, and change during the course of a day, due to earth rotation and satellite motion. There is no analytical method to determine the statistical behavior of GDOP parameters. The GDOP parameters are generally given in terms of percentiles, such as the fiftieth and ninetieth percentile by conducting a Monte Carlo simulation covering all latitude, longitude and time. The lack of a mathematical expression for the geographical distribution of GDOP parameters has prevented the establishment of a mathematical relationship between percentile of GDOP and that of user navigation errors.



V = VOLUME OF THE TETRAHEDRON FORMED BY CONNECTING THE ENDS OF THE FOUR UNIT VECTORS TO EACH SATELLITE.

FIGURE 4.3.6 GEOMETRIC METHOD TO SELECT OPTIMUM SATELLITE CONSTELLATION

A computer program to perform Monte Carlo simulation has been developed (Ref [13], [23]). It divides the earth into regions bounded by increments of latitude and longitude and computes the GDOP parameters for a user at the center of these regions. Since the GDOP value varies during the course of a day, the computations are repeated at successive time increments for each region. The results are given in Table 4.3.5 (Ref [16], p 1) together with corresponding values of the user error based on 1 σ UERE (11.8 to 20.7 feet). Note that the results are based on the original 24 satellite constellations. Corresponding results based on 4, 12 or 18 satellites are not available at this time.

TABLE 4.3.5 ANTICIPATED WORLDWIDE USER POSITION ERROR DISTRIBUTION

	Horizontal				Vertical				Time		
	HDOP	User Error Parameter	User Error (Meters)	User Error (Feet)	VDOP	User Error Parameter	User Error (Meters)	User Error (Feet)	TDOP	User Error Parameter	User Error (Nanoseconds)
50th percentile	1.39	1.15	4.1-7.2	14-24	1.99	1.39	5.0-8.8	16-29	1.05	0.73	8-15
rms	1.44	1.45	5.2-9.1	17-30	2.16	2.21	8.0-13.9	26-46	1.21	1.22	14-25
90th percentile	1.71	2.19	7.9-13.8	26-45	2.80	3.57	12.9-22.5	42-74	1.76	1.96	23-40

Based on Range Error Budget 11.8-20.7 feet; 24-Satellite Baseline Constellation; 5-degree Satellite Elevation Mask Angle.

4.4 2 versus 3 Dimensional Navigation

The NAVSTAR/GPS system is designed to provide accurate 3 dimensional position to a user anywhere on or near the earth. When the entire eighteen satellite constellation is complete this 3 dimensional navigation will be possible at almost all times. However, until the constellation is complete many areas will have only a fraction of each day when the requisite four satellites (necessary for the 3 dimensional navigation) are suitably located for use. When adequate altitude information is available a user can use only three satellites to perform a 2 dimensional (horizontal) navigation. The uncertainty in the altitude information, of course, directly influences the accuracy of this 2 dimensional navigation. In this section, 3D navigation means that a priori altitude information is optimally combined with GPS measurements to construct a 3D solution. On the other hand, 2D navigation means that a priori altitude information is assumed perfect and combined with GPS measurements to construct only the 2D (horizontal) part of the solution.

The general GPS 3 dimensional navigation has been discussed in Section 3, where no a priori estimate uncertainties are considered. The purpose of this subsection is to analyze accuracy measures for both 2 and 3 dimensional navigation when a priori altitude estimates are available. When an a priori estimate of the geodetic height is known, with a given variance, both HDOP and PDOP can be improved if the a priori estimate is properly weighted using the a priori variance.

Let an orthogonal coordinate system be selected such that the x-y plane is horizontal and the z-axis is vertical. The basic equations for GPS navigation systems are

$$\sqrt{(x-x_i)^2 + (y-y_i)^2 + (z-z_i)^2} + ct = R_i, \quad i = 1, 2, 3, 4, \quad (4.4.1)$$

where x , y , z and t are user position and unknown clock bias; c is the speed of light; x_i , y_i , z_i are the i th SV position, and R_i is the pseudo-range measurement to the i th SV.

Since equation (4.4.1) is nonlinear, a linearization using first-order Taylor expansion is applied. Let \bar{x} , \bar{y} , \bar{z} and \bar{t} be the nominal values of x , y , z and t , and let δx , δy , δz and δt be the corrections to these nominal values, i.e., $\delta x = x - \bar{x}$, $\delta y = y - \bar{y}$, $\delta z = z - \bar{z}$ and $\delta t = t - \bar{t}$. The nominal value of the pseudo-range measurement from the i th SV to user is given by

$$\bar{R}_i = \sqrt{(\bar{x} - x_i)^2 + (\bar{y} - y_i)^2 + (\bar{z} - z_i)^2} + c\bar{t} \quad (4.4.2)$$

The offset of the pseudo-range measurement from its nominal value is

$$\Delta R_i = R_i - \bar{R}_i$$

Expansion of (4.4.1) to first order about the nominal leads to

$$\frac{(\bar{x} - x_i)\delta x + (\bar{y} - y_i)\delta y + (\bar{z} - z_i)\delta z}{\bar{R}_i - c\bar{t}} + c\delta t = \Delta R_i, \quad i = 1, 2, 3, 4. \quad (4.4.3)$$

These four equations can be written in a matrix form as

$$H\mathbf{B} = \Delta\mathbf{R}$$

where

$$H = \begin{bmatrix} e_1^T & 1 \\ e_2^T & 1 \\ e_3^T & 1 \\ e_4^T & 1 \end{bmatrix}, \quad \mathbf{B} = \begin{bmatrix} \delta x \\ \delta y \\ \delta z \\ c\delta t \end{bmatrix}, \quad \Delta\mathbf{R} = \begin{bmatrix} \Delta R_1 \\ \Delta R_2 \\ \Delta R_3 \\ \Delta R_4 \end{bmatrix},$$

and

$$e_i^T = [(\bar{x} - x_i) \quad (\bar{y} - y_i) \quad (\bar{z} - z_i)] / (\bar{R}_i - c\bar{t})$$

is the unit vector from i th SV to user.

Let P_0 denote the covariance matrix of the nominal values of x , y , z and t . Since the geodetic height of the user position is known, it is assumed that

\tilde{z} is Gaussian distributed with mean z and variance σ_z^2 . The variances of \tilde{x} , \tilde{y} and \tilde{t} are assumed infinity. Thus

$$P_0 = \begin{bmatrix} \infty & 0 & 0 & 0 \\ 0 & \infty & 0 & 0 \\ 0 & 0 & \sigma_z^2 & 0 \\ 0 & 0 & 0 & \infty \end{bmatrix}$$

where zero correlation is assumed.

The minimum-variance estimates of δx , δy , δz and $c\delta t$ are given by

$$\hat{\beta} = [P_0^{-1} + H^T M^{-1} H]^{-1} H^T M^{-1} \Delta R$$

where M is the covariance matrix of the pseudo-range measurements. It is assumed that the four UEREs are statistically independent and σ_R is the RSS UERE common to all four measurements. Thus $M = \sigma_R^2 I_4$, where I_m is a $m \times m$ identity matrix. The covariance matrix of $\hat{\beta}$ is given by

$$P = [P_0^{-1} + H^T M^{-1} H]^{-1}$$

$$= \begin{bmatrix} \sigma_x^2 & \sigma_{xy} & \sigma_{xz} & c\sigma_{xt} \\ \sigma_{yx} & \sigma_y^2 & \sigma_{yz} & c\sigma_{yt} \\ \sigma_{zx} & \sigma_{zy} & \sigma_z^2 & c\sigma_{zt} \\ c\sigma_{tx} & c\sigma_{ty} & c\sigma_{tz} & c^2\sigma_t^2 \end{bmatrix}.$$

In Section 3, PDOP is defined by $(\sigma_x^2 + \sigma_y^2 + \sigma_z^2)^{1/2}/\sigma_R$ and HDOP is defined by $(\sigma_x^2 + \sigma_y^2)^{1/2}/\sigma_R$. Both PDOP and HDOP are functions of H , M and P_0 .

Figures 4.4.1, (a)-(d), show the relationship of PDOP, HDOP and (σ_z/σ_R) with various SV arrangements. The geometry of the SVs is arbitrary, and is selected for demonstration only.

In the 2 dimensional navigation case, the a priori altitude estimate is assumed perfect and only the horizontal coordinates of the user position are estimated. Hence, it is of interest to investigate the accuracy of the 2 dimensional solution as a function of the unmodeled altitude variance.

It follows from (4.4.3) that:

$$\frac{(\bar{x}-x_i) \delta x + (\bar{y}-y_i) \delta y}{\bar{R}_i - c\bar{t}} + c\delta t = \epsilon_i, \quad i = 1, 2, 3, 4, \quad (4.4.4)$$

where $\epsilon_i = \Delta R_i - (\bar{z}-z_i)(z-\bar{z})/(\bar{R}_i - c\bar{t})$.

The four equations in (4.4.4) can be written in a matrix form as

$$H\beta = \epsilon,$$

where

$$H = \begin{bmatrix} e_1^T & 1 \\ e_2^T & 1 \\ e_3^T & 1 \\ e_4^T & 1 \end{bmatrix}, \quad \beta = \begin{bmatrix} \delta x \\ \delta y \\ c\delta t \end{bmatrix}, \quad \epsilon = \begin{bmatrix} \epsilon_1 \\ \epsilon_2 \\ \epsilon_3 \\ \epsilon_4 \end{bmatrix}$$

and

$$e_i^T = [(\bar{x}-x_i), (\bar{y}-y_i)] / (\bar{R}_i - c\bar{t}).$$

Note that $E(\epsilon) = 0$, and $E(\epsilon\epsilon^T) = \sigma_R^2 I + \sigma_z^2 f f^T$ where $f = [f_1, f_2, f_3, f_4]^T$ with $f_i = (\bar{z} - z_i)/(\bar{R}_i - c\bar{t})$.

The least-square estimate of β is $\hat{\beta} = (H^T H)^{-1} H^T e$, and the covariance matrix of $\hat{\beta}$ is given by

$$c(\hat{\beta}) = [H^T H]^{-1} H^T (\sigma_R^2 I + \sigma_Z^2 f f^T) H [H^T H]^{-1}$$

or

$$c(\hat{\beta}) = \sigma_R^2 [H^T H]^{-1} + \sigma_Z^2 [H^T H]^{-1} H^T f f^T H [H^T H]^{-1}.$$

Here, the HDOP is a function of H , f , σ_R^2 and σ_Z^2 . Figures 4.4.2, (a)-(d), show the relationship of HDOP and (σ_Z/σ_R) with various SVs geometry. It should be noted that three SVs are sufficient to perform 2 dimensional navigation, for only x , y , and t are to be estimated. The relationship of HDOP and (σ_Z/σ_R) for 3 SVs is also included in Figures 4.4.2, (a)-(d).

As an aid in quantifying the ideas and results of this section, it is useful to introduce the notion of Constellation Value (CV). For a given navigation accuracy criterion and a given SV constellation, CV is defined as the probability of satisfying the criterion, as determined by the fraction of each day for which the criterion is satisfied averaged over the entire globe.

It is of interest to examine the behaviour of CV during the GPS constellation buildup, and this is illustrated for three cases of interest in Figure 4.4.3. The three cases are:

1. 3D navigation with PDOP < 6
2. 2D navigation with HDOP < 4
3. 2D navigation with HDOP < 4 assuming perfect altitude.

In the first two cases, no a priori altitude information is available, while in the third case the a priori (or independent) measure of altitude is assumed perfect.

The figure shows that the CV is not much improved by specifying only a 2D navigation criterion unless an independent measure of altitude is available, in which event, the CV improves considerably. For example, at the time when the constellation contains 12 satellites, with no independent altitude information the CV for 3D navigation (PDOP < 6) is $\approx 60\%$ and the CV for 2D navi-

gation ($\text{HDOP} < 4$) is $\approx 70\%$, but with perfect altitude, the CV for 2D navigation ($\text{HDOP} < 4$) is $\approx 90\%$.

Thus, during constellation buildup, augmentation of GPS navigation solutions with independent altitude measurements can significantly extend the daily window of operability with GPS.

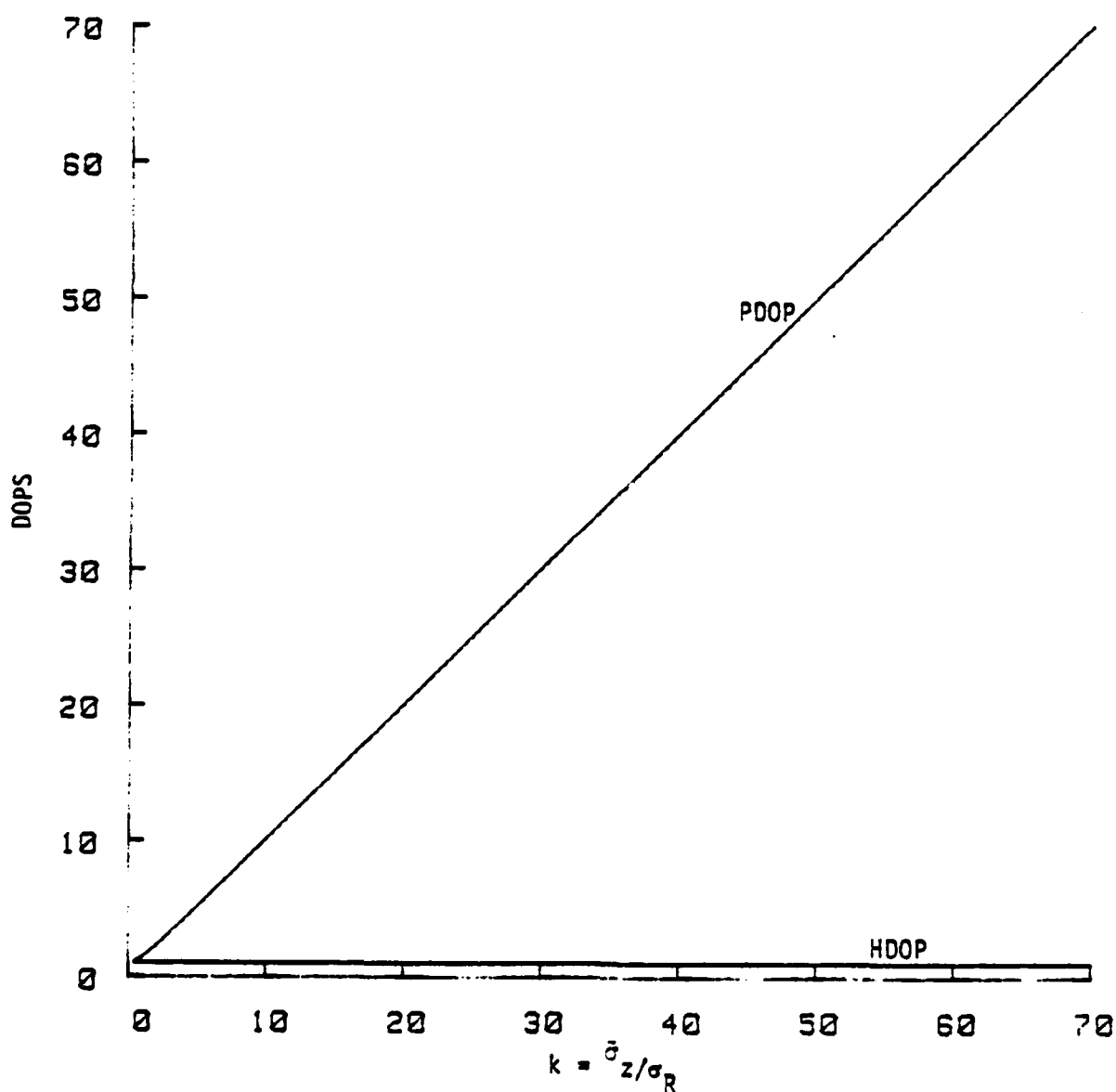


FIGURE 4.4.1(a) RELATIONSHIP OF PDOP AND HDOP WITH A PRIORI ALTITUDE UNCERTAINTY IN 3 DIMENSIONAL NAVIGATION.

Satellite configuration (AZ,EL), (0°,10°), (90°,10°), (180°,10°), (270°,10°)

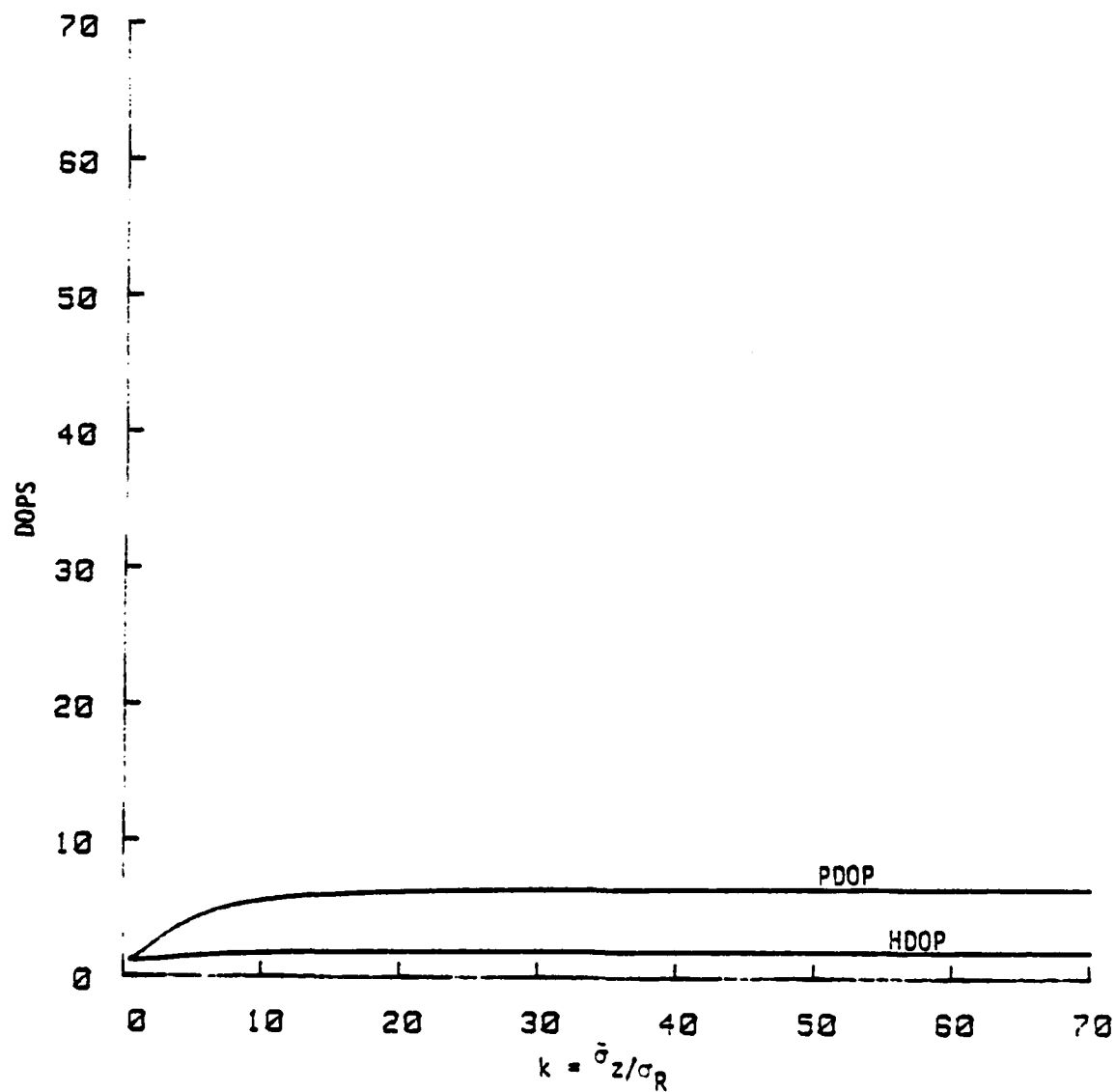


FIGURE 4.4.1(b) RELATIONSHIP OF PDOP AND HDOP WITH A PRIORI ALTITUDE UNCERTAINTY IN 3 DIMENSIONAL NAVIGATION.

Satellite configuration (AZ,EL), (0°,10°), (90°,20°), (180°,30°), (270°,40°)

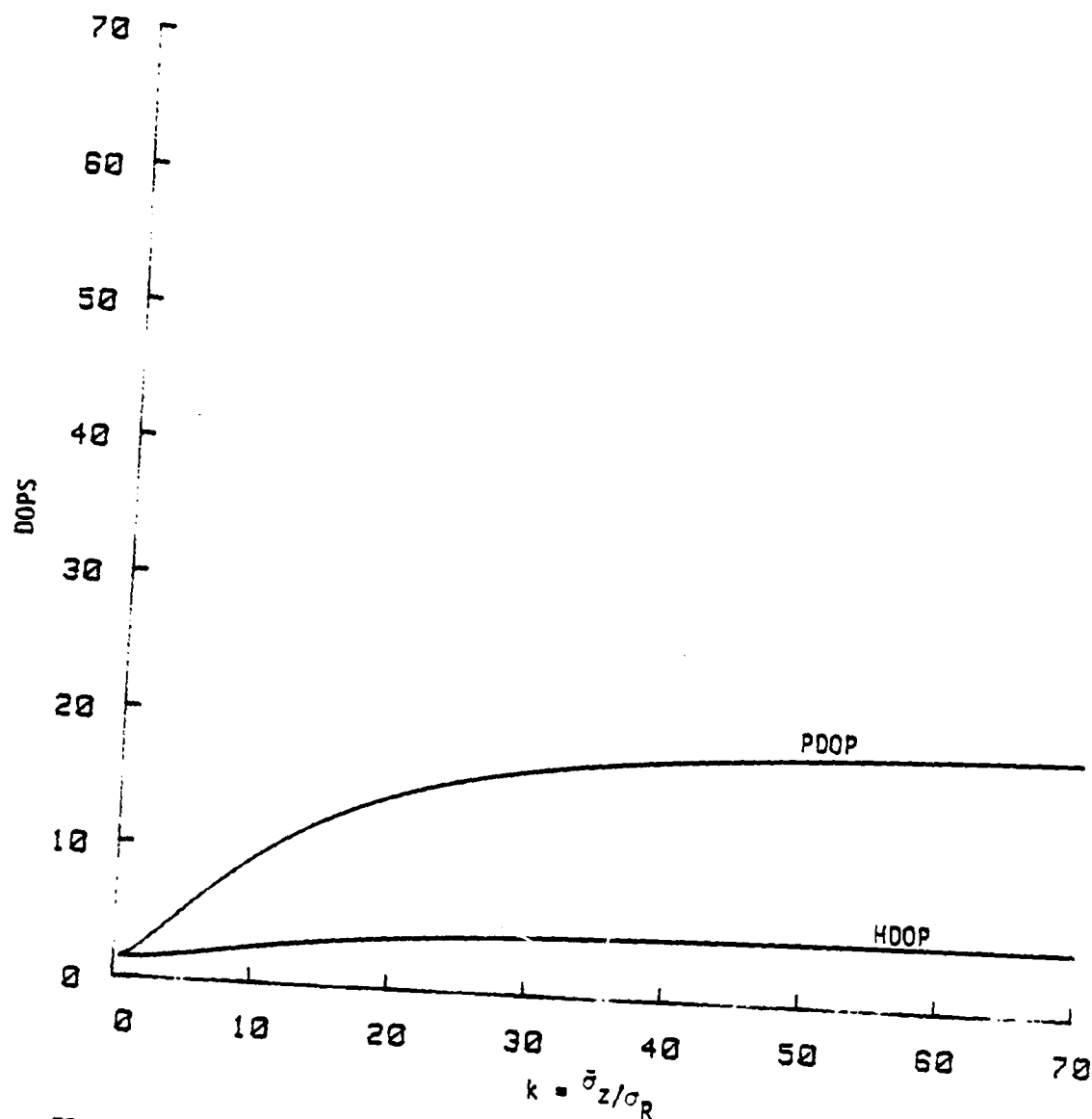


FIGURE 4.4.1(c) RELATIONSHIP OF PDOP AND HDOP WITH A PRIORI ALTITUDE UNCERTAINTY IN 3 DIMENSIONAL NAVIGATION.

Satellite configuration (AZ,EL), (0°,10°), (60°,20°), (120°,30°), (180°,40°)

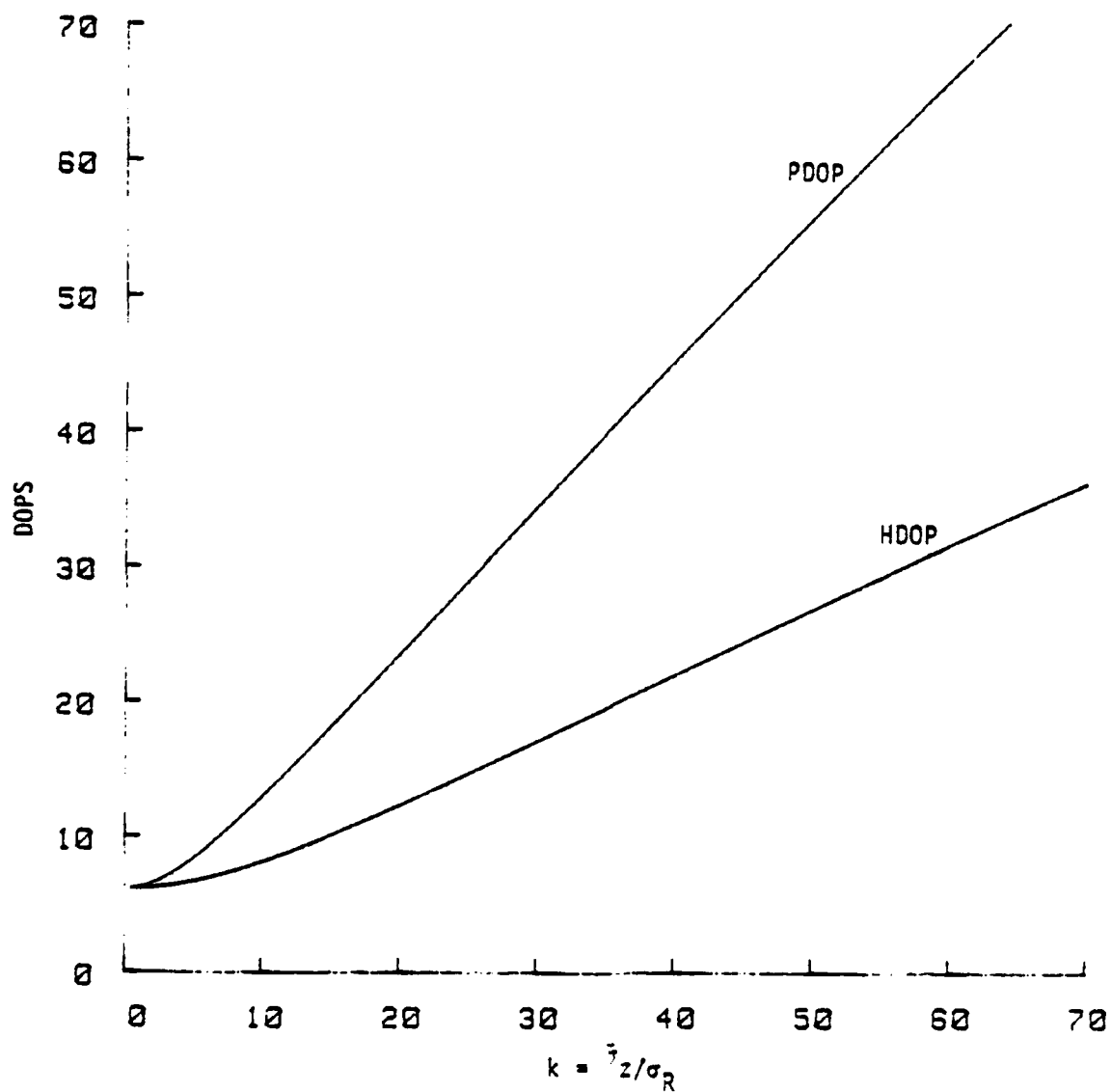


FIGURE 4.4.1(d) RELATIONSHIP OF PDOP AND HDOP WITH A PRIORI ALTITUDE UNCERTAINTY IN 3 DIMENSIONAL NAVIGATION.

Satellite configuration (AZ,EL), (0°,30°), (30°,40°), (45°,50°), (60°,60°)

AD-A128 955

GPS (GLOBAL POSITIONING SYSTEM) ERROR BUDGETS ACCURACY 2/2
AND APPLICATIONS C. (U) FEDERAL ELECTRIC CORP
VANDENBERG AFB CA SYSTEMS PERFORMANCE A.

UNCLASSIFIED

R A BROOKS ET AL. DEC 82 A5300-T-82-33

F/G 17/7

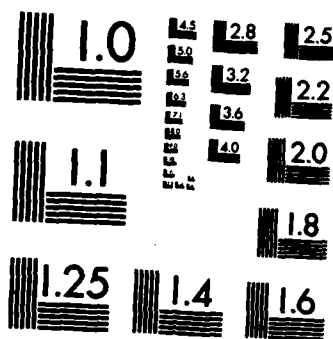
NL

END

FILED

IN

DTIC



MICROCOPY RESOLUTION TEST CHART
NATIONAL BUREAU OF STANDARDS-1963-A

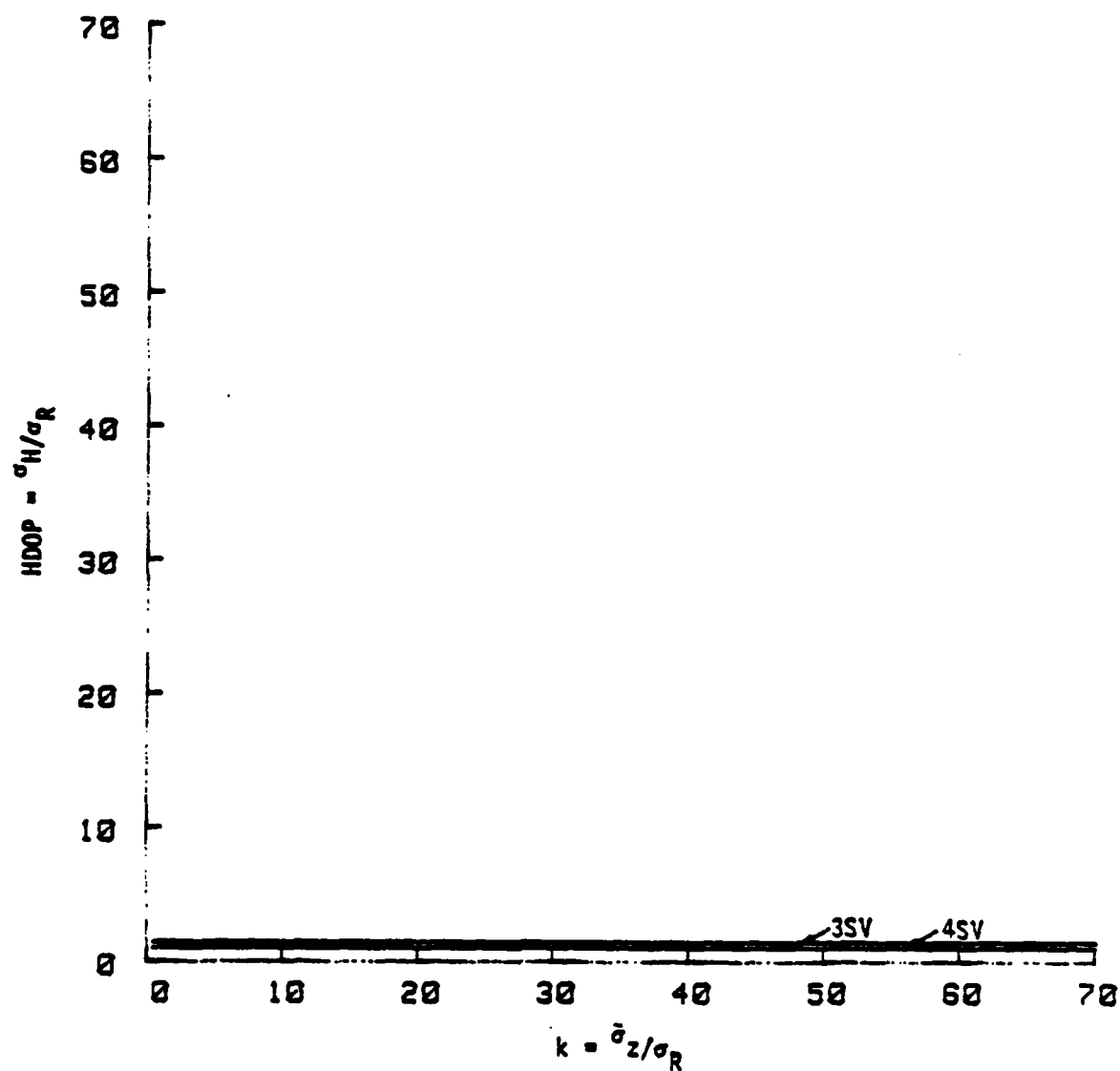


FIGURE 4.4.2(a) RELATIONSHIP OF HDOP WITH A PRIORI ALTITUDE UNCERTAINTY
IN 2 DIMENSIONAL NAVIGATION.

Satellite configuration (AZ,EL), (0°,10°), (90°,10°), (180°,10°), (270°,10°)

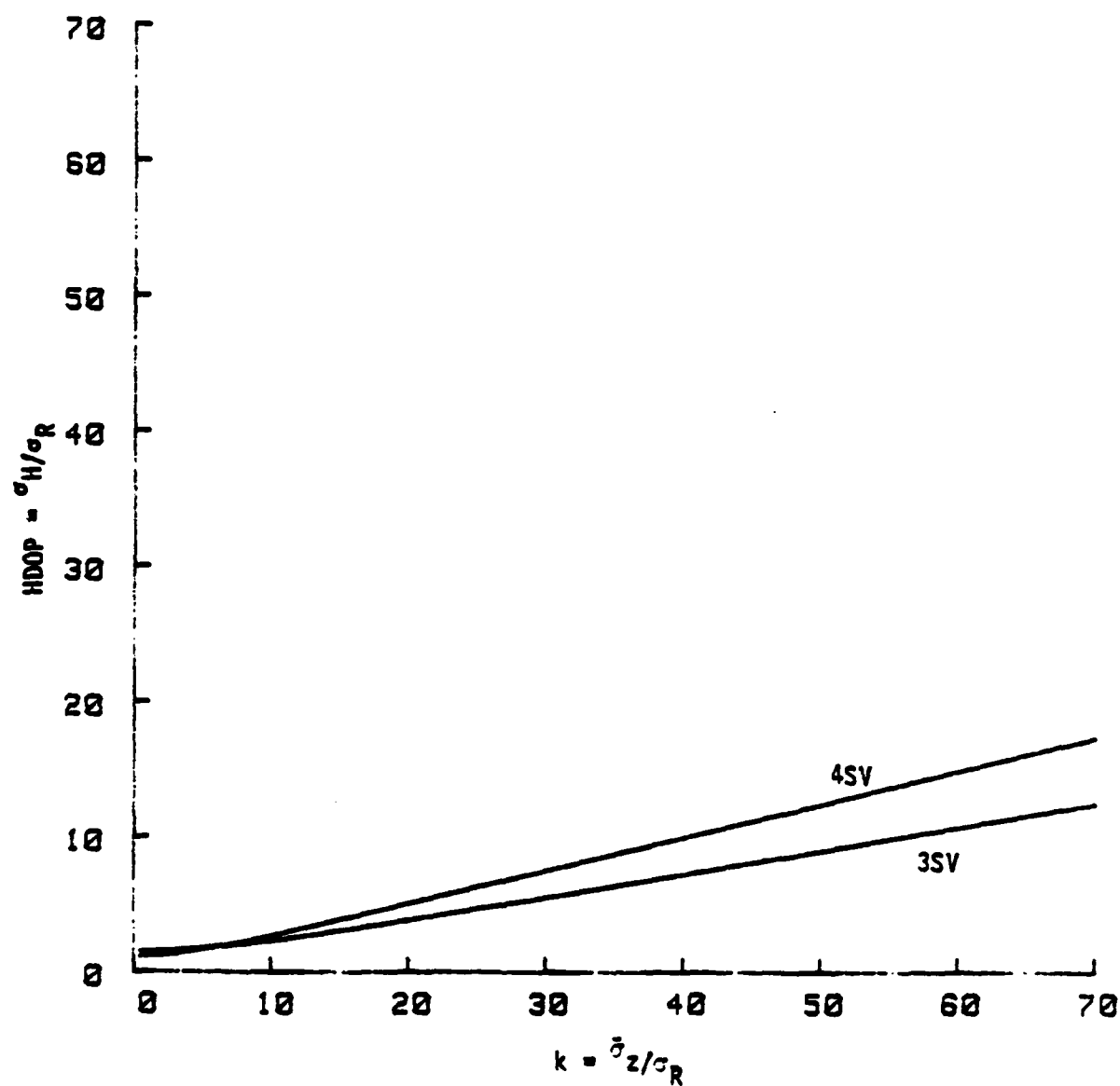


FIGURE 4.4.2(b) RELATIONSHIP OF HDOP WITH A PRIORI ALTITUDE UNCERTAINTY IN 2 DIMENSIONAL NAVIGATION.

Satellite configuration (AZ,EL), (0°,10°), (90°,20°), (180°,30°), (270°,40°)

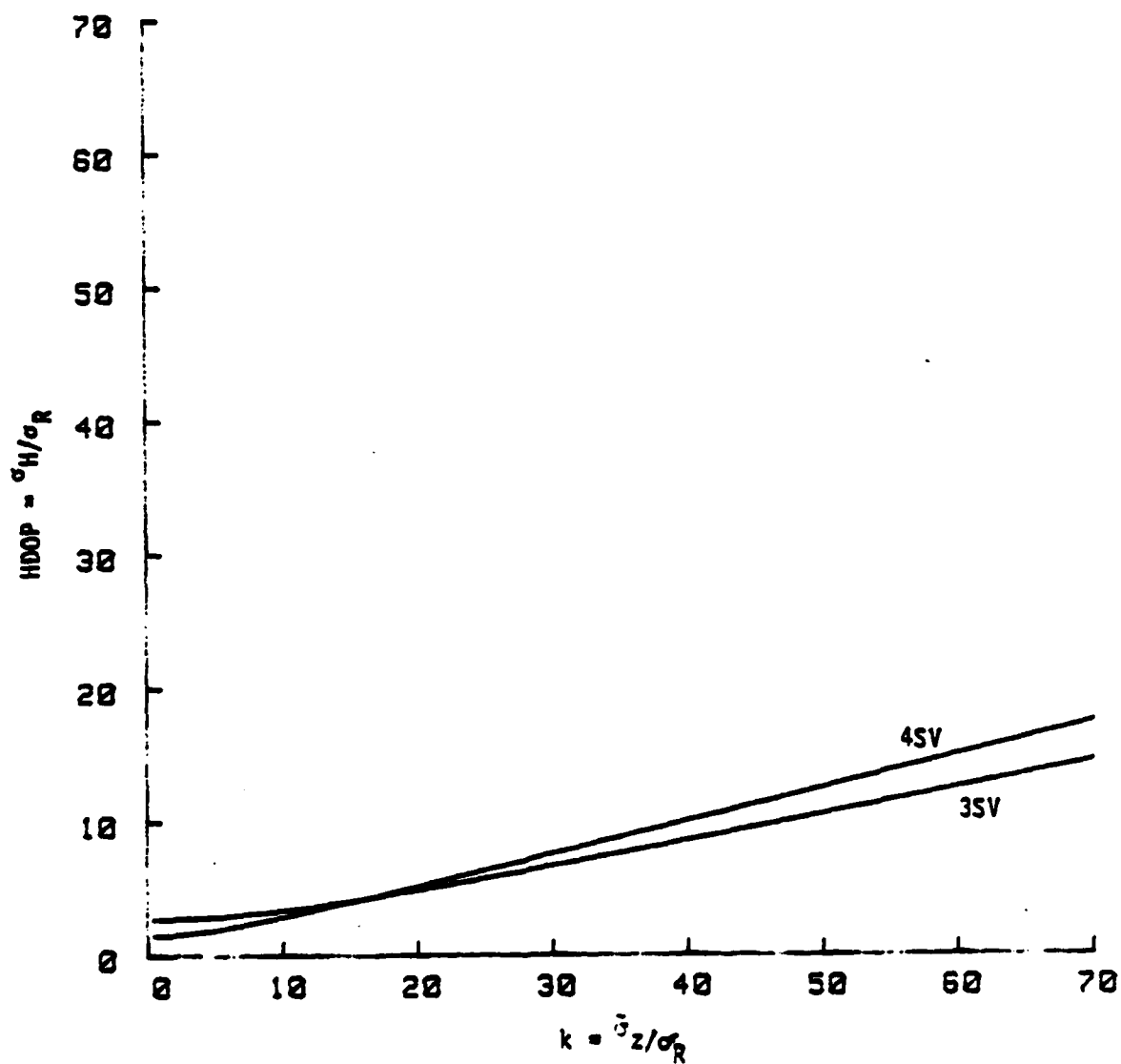


FIGURE 4.4.2(c) RELATIONSHIP OF HDOP WITH A PRIORI ALTITUDE UNCERTAINTY IN 2 DIMENSIONAL NAVIGATION.

Satellite configuration (AZ,EL), (0°,10°), (60°,20°), (120°,30°), (180°,40°)

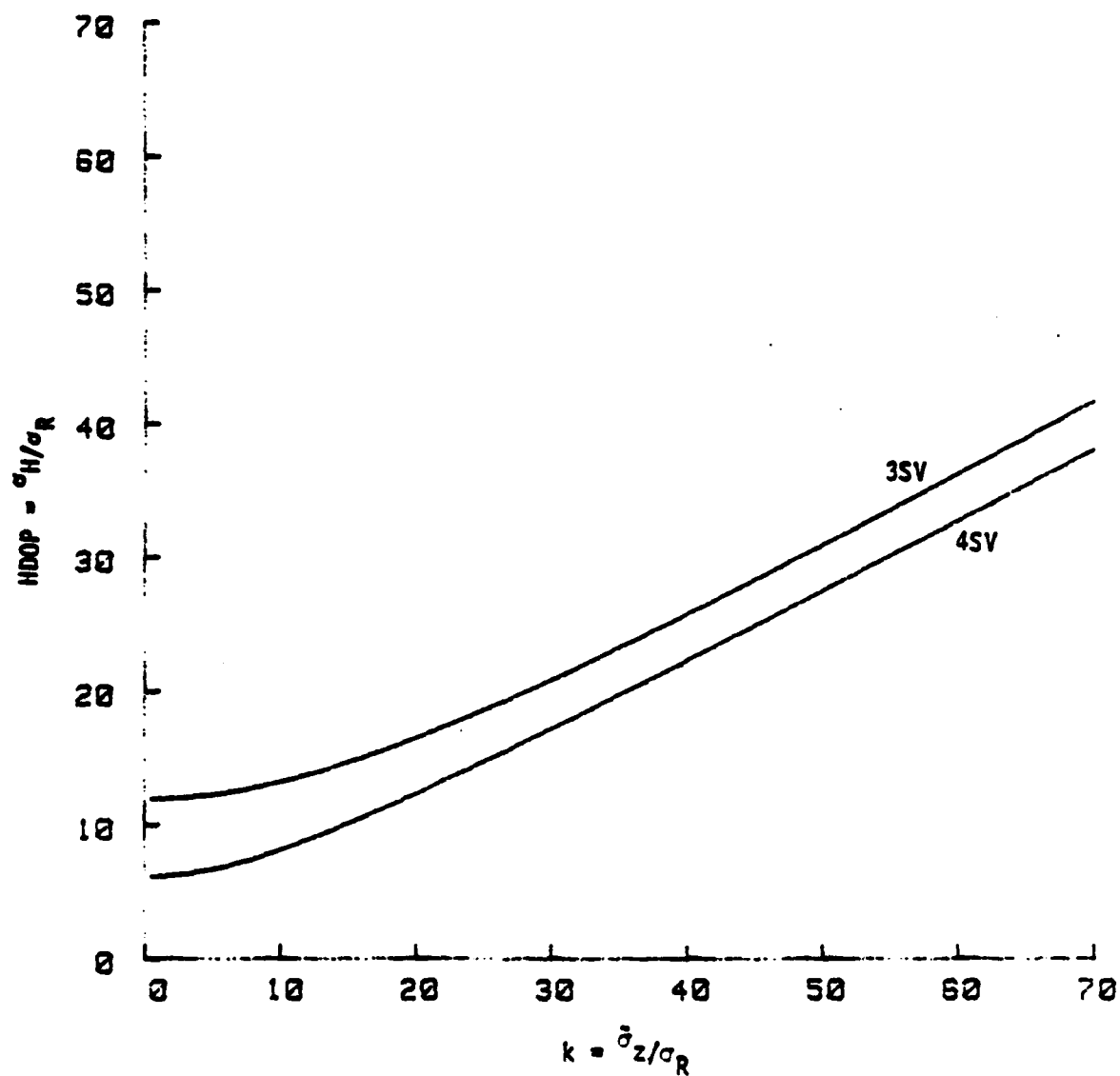


FIGURE 4.4.2(d) RELATIONSHIP OF HDOP WITH A PRIORI ALTITUDE UNCERTAINTY
IN 2 DIMENSIONAL NAVIGATION.

Satellite configuration (AZ,EL), (0°,30°), (30°,40°), (45°,50°), (60°,60°)

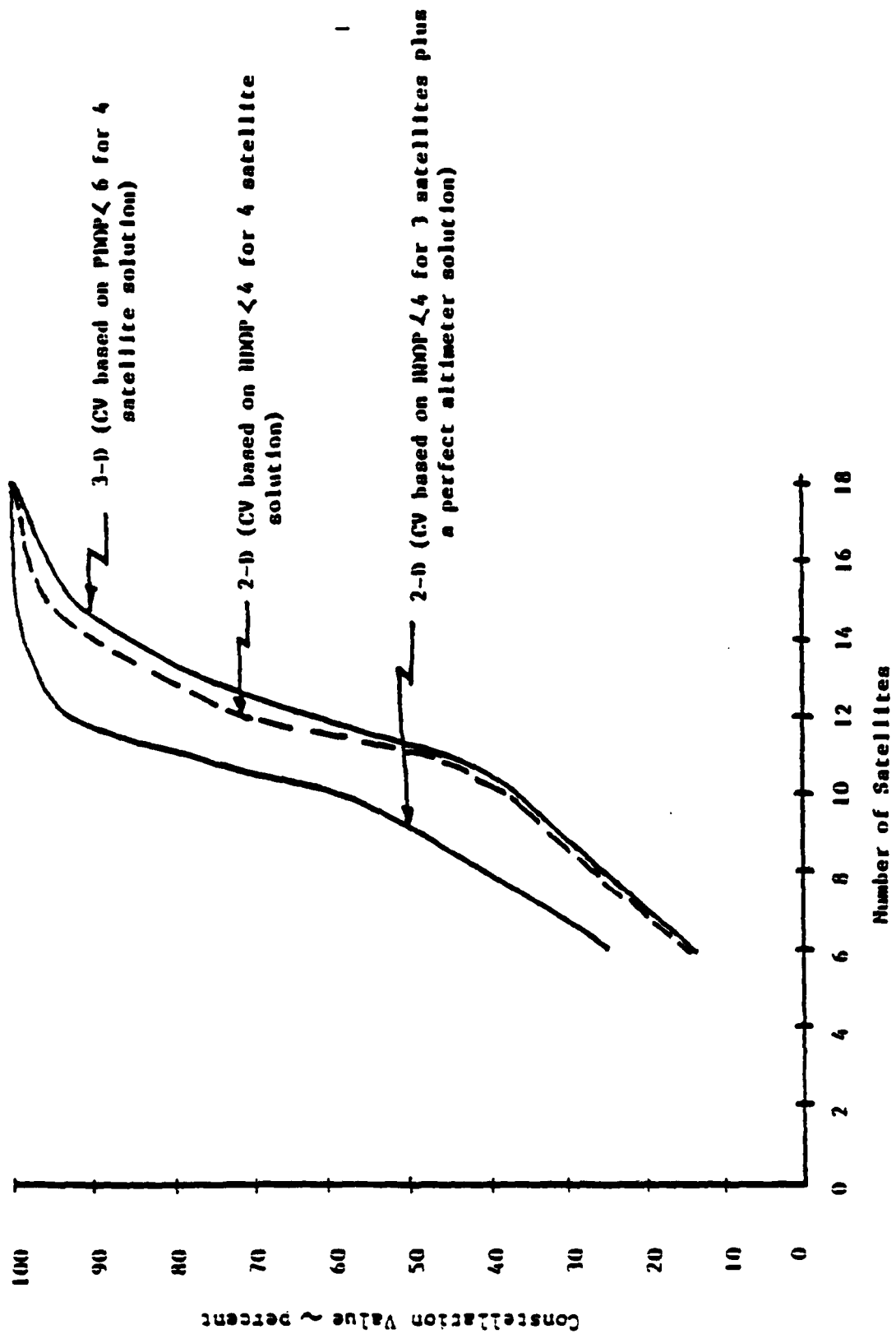


FIGURE 4.4.3 2D AND 3D CONSTELLATION VALUE (CV) DURING BUILDUP

Courtesy of JPO and Aerospace Corporation

4.5 Pseudo-Satellites

Ground stations that transmit signals compatible with GPS satellite signals are referred to as pseudo-satellites. An example of their use is at the Yuma Proving Grounds using a configuration called Inverted GPS (Ref [64]). Their purpose is to supplement or replace the need for GPS satellite signals during demonstration tests of GPS concepts and User Equipment. Their use in Range instrumentation systems would have two major advantages. First, test scheduling would be independent of satellite coverage and, second, they could provide improvements in data results due to geometrical considerations and/or satellite signal reception problems. Command, control and communications (C³) functions can be combined with the pseudo-satellite uplink. For some ranges, it might be necessary to operate pseudo-satellites even after GPS is operational with the full 18 satellite array.

Two problems must be considered for use of pseudo-satellites. The first problem concerns situations when test vehicles would operate very near the pseudo-satellite and its signal level would be sufficiently higher than the satellites or other pseudo-satellites to prevent their acquisition or track. If there is only one test vehicle, this might be overcome by adjusting the transmitter power using various control schemes. If all participants are sufficiently far from the pseudo-satellite, one power level might be found that would be acceptable. Conversely, the test vehicle could control the received signal level with a directional antenna array.

In practice, the near-far problem has not been a serious constraint at the Yuma Proving Grounds Inverted GPS Range. An acceptable transmitter power is selected and GPS receivers on test vehicles operate satisfactorily except for acquisition of a low level signal when near a pseudo-satellite. Better definition of the constraints for various receiver and translator configurations and signal level control techniques must be developed before evaluating use of GPS technology in Range instrumentation. The range of signal levels acceptable during various receiver and translator configurations operation must be determined analytically and verified with experiments for representative cases. Then pseudo-satellite signal level control requirements can be defined and suitable configurations developed for particular

range situations. Figure 4.5-1 shows a missile tracking configuration being considered at WSMC in which the pseudo-satellite transmitter power level could be controlled in an open loop manner using a priori trajectory data or in a closed loop manner using telemetered GPS receiver signal level data or it may not be necessary to vary the level.

For some situations, use of a different frequency might be advantageous. For instance, if the test vehicle receives L_1 signals from the GPS satellites, the pseudo-satellite could be operated on L_2 , L_3 or another frequency. The advantage is that the pseudo-satellite signal level problem is greatly simplified. The disadvantage is that the receiver has to be able to receive on two frequencies. The downlink bandwidth problem can be minimized by overlaying the received signals if the levels are compatible. Obviously, the test vehicle receiver becomes more complicated.

Use of C/A code would be adequate and even preferable for many Range applications. The pseudo-satellite uplink bandwidth requirements using C/A code are one tenth those for P Code. The L_1 C/A code signal level is 3 dB higher than the P Code level transmitted by the GPS satellites.

The second problem that must be considered with pseudo-satellites is that their data is not used in a solution the same way that normal GPS satellite data is used. Since the pseudo-satellites are ground stations, ephemerides are not applicable and their position is provided in static earth-fixed coordinates. For situations using algorithms developed for the range application, this can be taken into account. For situations using User Equipment developed for operations with satellites, there are potential incompatibilities. Other considerations for pseudo-satellites are that the range of Doppler effects is lower than satellites, the station location is accurately known in an earth fixed coordinate system (not GPS), and a reference receiver operated with the pseudo-satellite would provide data for relating these coordinate systems.

Pseudo-satellites could be operated on moving platforms such as aircraft and ships. Positions of the pseudo-satellites could be determined from GPS signals if sufficient satellites or other pseudo-satellites and an acceptable combination of codes and frequencies are available. Dynamic pseudo-

SIGNALS:

(1) L1 C/A

(2) L1 C/A & P. L2 P

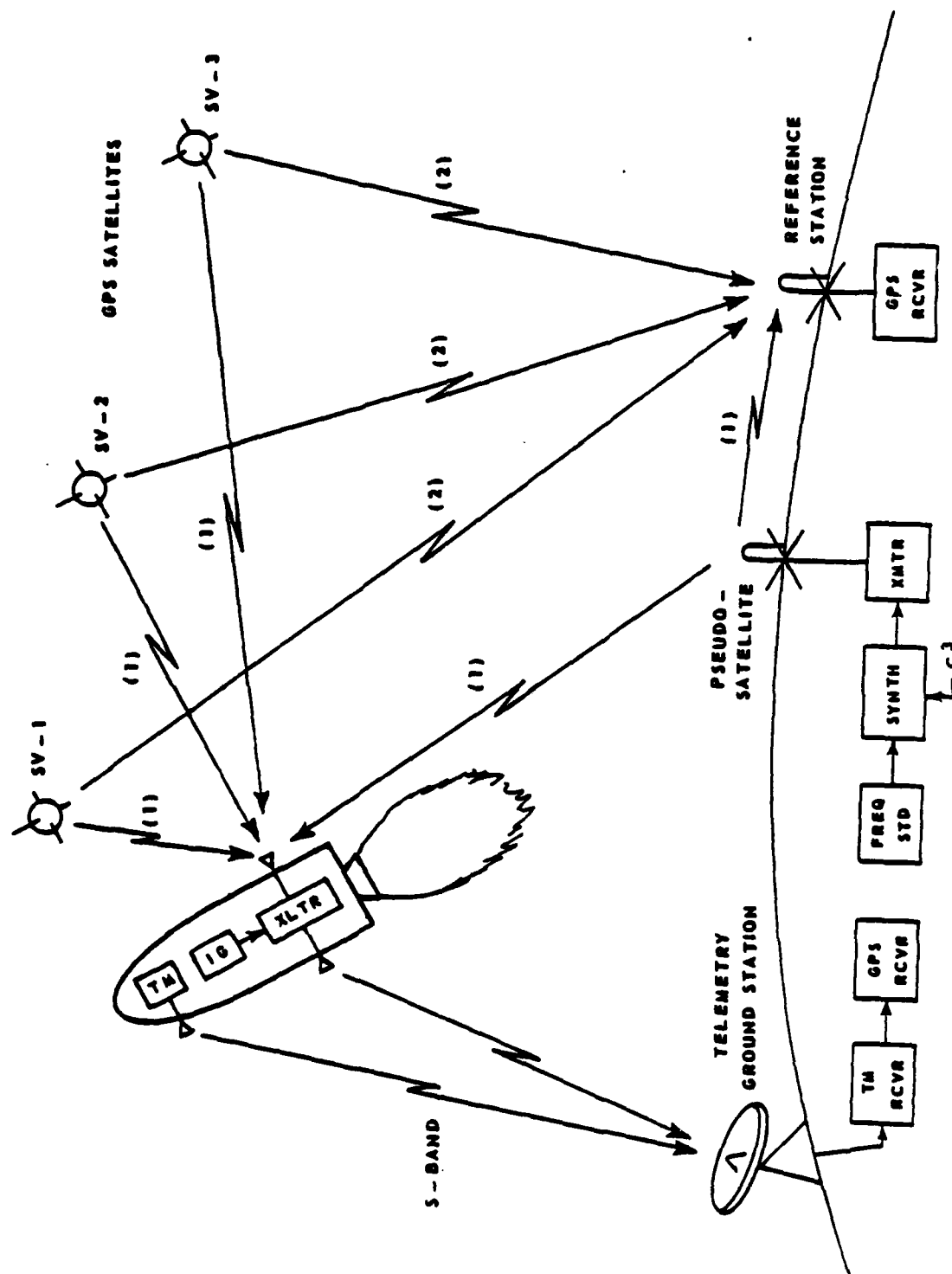


FIGURE 4.5.1 ICBM PSEUDO-SATELLITE OPERATION

satellites might be necessary for geometrical considerations or for supplementing satellite coverage in situations where survey locations are not available. Use of a pseudo-satellite on or near a target would optimize relative data. For targets in danger of being destroyed a less expensive translator configuration could be evaluated; for example, GPS satellite and pseudo-satellite signals relayed through the target translator to an attack vehicle translator signal receiver.

4.6 Effects of Vehicle Dynamics on Receiver Operation

In addition to the "steady state" errors (discussed in Section 2) inherent in the GPS system, the dynamics of the vehicle containing the GPS User Equipment introduces additional problems and errors in the operation of GPS navigation. In fact, the ability to even acquire and/or maintain track of the GPS signals depends on the dynamics (velocity, acceleration and jerk) of the vehicle as well as the user's equipment configuration and operational environment. This section presents a general discussion of the elements of the GPS user equipment which are affected by the dynamics and the nature in which they are affected.

4.6.1 Receiver Configuration

The basic design of the GPS receiver (See Fig. 1.1) consists of from one to five channels, each in turn incorporating:

- 1) A Delay Lock Loop (DLL) for the purpose of determining the pseudo-range from the user to a specific GPS satellite. The DLL achieves this by measuring the time delay that must be introduced to an internally generated Pseudo-random Noise (PN) code so as to achieve correlation with the PN code (either the C/A or P) on the received signal (see Table 1.1). This DLL will be referred to as the code loop.
- 2) A second loop involving a Costas (or similar) mechanization to lock the received, Doppler shifted, carrier signal (L_1 or L_2) with an internally generated oscillator frequency; the Doppler shift (thus measured) is used to determine the pseudo-range rate of the user relative to an SV. This loop is called the carrier loop.
- 3) A stable crystal oscillator used for generating the internal signals.

The time position of the internally generated PN code must be continually shifted as the pseudo-range changes in time, and the frequency of the internally generated "carrier" must be constantly shifted as the Doppler shift of the received signal changes in time. Only when both these loops are "locked" can the navigation data contained in the GPS signal be used. The process of

acquiring lock will be termed "acquisition" and the process of maintaining the lock once it has been achieved will be termed "tracking". The problems of acquiring and maintaining track due to vehicle dynamics will be discussed first followed by a brief look at the errors in the GPS measurements due to the dynamics.

4.6.2 Acquiring and Maintaining Track

Once the desired constellation of four GPS satellites has been selected the problem of acquisition of the signals arises. If the GPS receiver has four or more channels the acquisition of signals from four or more satellites can be carried on simultaneously and reacquisition will only be necessary when track cannot be maintained (either a failure of lock or changing the selected constellation). For receivers with less than four channels the acquisition must be carried out over and over as the satellite signals are processed sequentially. The problems that vehicle dynamics cause in the acquisition and tracking will be discussed first since they are always present and will simply be compounded in receivers with less than four channels.

Basic elements used in the tracking loops are; 1) a Phase Detector (PD) used to detect the phase error between the received signal and internal signal generated by 2) a Voltage Controlled Oscillator (VCO), and 3) a filter (normally of second order or higher) whose output of the filtered error signal regulates the VCO. The entire loop demonstrates a natural frequency with a characteristic loop bandwidth. Lock is typically indicated when a small phase error is achieved (high correlation between the received and internal signal). There are several mechanizations that are used to achieve lock but all depend on obtaining a frequency (or time delay) difference between the received signal and VCO generated carrier (or PN code) that is small compared to the bandwidth of the loop. A search for the appropriate frequency (or time delay) may be made, but if acquisition time is to be relatively short then the search must be restricted to frequencies (and delays) relatively close to the right one. In the case of the code loop this translates into the need for knowing an approximate pseudo-range so that the delay induced in the internally generated PN code is close to the pseudo-transit time. In the carrier loop it is necessary to know an approximate value of the relative velocity between the user and the satellite so as to calculate the Doppler shift expected on the

received signal. For a stationary or slowly moving user the acquisition problem can be solved just by using approximate knowledge of his position and the almanac data stored in his GPS receiver. However, for a highly dynamic user the acquisition problem can become acute (or take an unacceptable time) unless some other source of information, such as from an inertial navigation system, is available.

The wider the bandwidth of the loop the faster the acquisition but unfortunately the probability of slipping cycles increases also (due to the worsened system signal to noise ratio caused by the wider bandwidth). Once both loops have locked up, the tracking of the code loop is aided by delta pseudo-range information from the carrier loop. The narrower the loop bandwidths the better the system signal to noise ratio; however, the ability to maintain lock in the face of dynamics increases with wider bandwidths. Thus the design objective for a particular application takes the user's dynamics into account by choosing the minimum bandwidths consistent with the maximum dynamics expected. Reference [16], (page 104) details this trade-off and shows that the carrier loop loses lock before the code loop.

Only approximate formulas for the time required to acquire track have been derived for any practical GPS receiver loops. Thus, quantitative statements on acquiring and tracking are peculiar to each set of User Equipment. Generally the acquisition is accomplished by locking on the C/A code first; then, as the carrier loop locks up and begins aiding the code loop a transfer is made to lock on the P code. The reason for this method is that the C/A code is only 1023 bits repeating every 1 msec and thus much easier to lock onto than the one week period P code. In virtually all applications both the 50 bps data stream as well as the hand-over-word must be read to acquire the P code. In addition the C/A code track is easier to maintain on lock than the P code in cases of high dynamics (due partially to the fact that the L_1 C/A code has a 3 dB higher signal to noise ratio than the L_1 P code).

In addition to the problems of acquiring loop lock it would appear that an additional problem due to vehicle dynamics would be performing the navigational computations. Most formulations use an iterative approach to the navigation solution requiring an initial approximation of the position and velocity of the user. Depending on the degree of dynamics and the computational cycle period the initial position and velocity used in the iteration

could be greatly in error and thus require far more time to converge. No discussion of this problem was noted in the literature; although it is possibly reflected in the "time-to-first-fix" in the data sheets of the specific GPS User Equipment packages.

GPS receivers with fewer than four channels must sequentially acquire each of four satellite signals thus acquisition problems due to vehicle dynamics are greatly magnified unless the dynamics are so low (e.g., a man on foot) that acquisition can repeatedly be made very quickly.

4.6.3 Tracking Errors

Generally speaking being locked in a loop (hence tracking) is defined as the condition of small phase difference between the received signal and the internally generated signal. Practical loops can be demonstrated (Ref [55], Ch. 4) to maintain lock as long as the Doppler shift of the received signal is constant in time (the relative velocity of the receiver and GPS satellite must be constant); obviously this is virtually never a realizable case. As the Doppler shift changes in time the loop will attempt to adjust so as to make the phase difference small again but there will be a time lag in the adjustments being made. These lags translate themselves into pseudo-range measurement errors in the code loop and delta pseudo-range errors in the carrier loop. Ref. [56], (Ch. 18) gives a detailed mathematical treatment of acquisition and tracking limits for a delay lock loop as functions of acceleration. No mathematical derivation of errors in pseudo-range and pseudo-range rate due to acceleration and jerk was found in the available literature. One could and should be developed along the lines of Ref [69], (Section C.3).

The effects of acceleration on the frequency of the GPS crystal oscillator can cause tracking errors which appear as errors in pseudo-ranges. Unless crystal oscillators with very low sensitivities to acceleration are used (or the effects compensated for) the errors for high dynamics aircraft and missiles with GPS receivers can become excessive (Ref [70]). Finally, what might be considered a vehicle dynamics problem is the need to keep the GPS user antenna oriented (or beam pointed) so as to receive the GPS signals throughout maneuvers for applications of non omni-directional antennas.

GPS receivers with less than four channels must measure pseudo-range to four satellites sequentially. Since an unaided GPS receiver doesn't measure acceleration, any relative acceleration in the period between measurements is unaccounted for and creates errors in the navigated position and velocity. (Ref [2], pp 12, 13) states that the position and velocity errors due to this effect are:

$$\Delta S = 1/2 at^2$$

$$\Delta V = 1/2 jt^2$$

where:

ΔS = position error

ΔV = velocity error

a = vehicle/satellite relative acceleration

j = time rate of change of acceleration

t = computation time.

4.6.4 External Aids

In light of the acquisition and tracking problems and errors for highly dynamic user test vehicles, most GPS applications for these vehicles are envisioned as a complementary combination with other navigation systems (or other information sources) in order to obtain a more accurate and reliable navigation solution than any one system by itself. This section briefly describes several such aiding systems and how they can overcome the problems described previously.

4.6.4.1 Inertial Navigation System (INS) Integration

Inertial Navigation Systems (INS) have long been used as stand alone guidance systems. Recently the technological gains made in their accuracies as well as miniaturization and cost reduction has led to extensive use in both commercial and military aircraft as well as both large and small missiles. The errors in these systems are well understood and modeled. When two navigation systems such as GPS and INS are integrated together many of the weaknesses of both systems may be overcome.

A very simple example of the complementary nature of these two systems can be seen by recalling that one difficulty in rapidly acquiring track in GPS receivers is knowing an approximate position and velocity of the receiver;

the INS can supply this data to aid acquisition. Further, the acceleration measurements made by the INS's accelerometers can be used to aid the tracking loops in high dynamics; thus, allowing the loop bandwidths to be narrowed which improves the system signal to noise ratio which in turn decreases the probability of skipping cycles or otherwise losing track. The GPS can in turn be used to update INS error estimates in an integrated GPS-INS Kalman filter (see Section 4.10). In addition the INS can accurately navigate by itself during reasonable periods of GPS outage due to the slowly varying nature of INS errors even under high dynamics.

In addition to aiding acquisition and maintenance of GPS track, the loop tracking aids supplied by the INS can effectively eliminate the pseudo-range measurement errors due to loop lags. In order to optimize the tracking loops' performance, a process known as adaptive tracking may be performed in which the tracking loops' parameters (e.g., bandwidth) are changed dynamically in order to adapt to changing environments (e.g., jamming); the INS inputs can greatly facilitate this adaptive process. Finally, the attitude data derived from the INS can aid the control of the beam-pointing antenna so as to maintain sight of the GPS satellites (Ref [16], pp 144-153).

The pseudo-range errors due to high acceleration effects on the frequency of the GPS crystal oscillator can be compensated for, to some degree, by the use of an accelerometer (Ref [71]) thus an INS system should be capable of eliminating some of these errors also.

Of course many other measurements (e.g., altitude, air speed, etc.) may supplement the GPS when a Kalman filter is used.

4.6.4.2 A Priori Information Aiding

In some cases it is practical to aid the tracking by using a priori information stored in the GPS processor. An example of this is a missile borne receiver using a nominal acceleration profile for the pre-determined trajectory. References [46] and [47] describe a missile borne GPS receiver operation using a priori aiding, and the "mother-daughter" concept discussed in Section 4.9 would make use of a similar aiding.

4.7 The GPS Receiver versus Translator For Mobile and/or Stationary Applications

4.7.1 Background

Key performance objectives of the GPS system which distinguish it from other satellite and landbased navigation systems include the capability to provide continuous and worldwide three dimensional navigation coverage to users with relatively high dynamics. With the advent of this system it becomes practical to measure the position and velocity of high dynamic vehicles such as ballistic missiles, reentry bodies etc., with the precision and accuracy heretofore obtainable only through the use of metric radar systems. However, one major objection to this system has been the requirement for some type of onboard receiver to process and telemeter the position and velocity data to a recording facility. This has been accomplished in the past at the WTR by the installation of an onboard receiver (MBRS-Missile Borne Receiver Set)(see Ref [46] and [47]) interfaced to the telemetry system which relayed the position and velocity data to ground recording sites. Although this system proved to be very accurate, it also proved to be very expensive and subject to malfunction. The ETR currently uses a "bent pipe" arrangement (SATRACK) designed to only relay the received GPS signals to off-board data processing sites where it is processed either in near real-time or post-flight to provide the position and velocity data. This system has proved highly reliable and at a significantly lower cost since all of the processing equipment remains on the ground and is not lost at the completion of the flight.

The WSMC has funded the Johns Hopkins University/Applied Physics Laboratory (JHU/APL) to develop a GPS-Sonobuoy Missile Impact Location System (GPS-SMILS) for scoring weapons systems reentry vehicle impacts on a worldwide datum. The principal component of this system is an expendable sonobuoy which uses a GPS signal translator/digitizer and relay system to provide data to accurately estimate the position of the SMILS array. In this system, digitized acoustic and GPS data are multiplexed and transmitted to an aircraft for recording, processing and relay to the post mission processor for further data reduction.

4.7.1.1 Review of GPS C/A Code Signal Transmission and Reception

Before considering design considerations for translating, receiving, recording and processing GPS signals, it is useful to review relevant signal characteristics.

4.7.1.2 Signal Transmission

The technique used for GPS satellite CA Code signal generation is illustrated in Figure 4.7.1. Note that the transmitted signal is at 1.5 GHz (nominal) and the modulation is PCM-PSK at a 1.023 MHz bit rate with 50 bps data embedded in the PN Code. (PSK modulation induces a 180° phase change of the carrier each time the PN Code changes state.) The RF main lobe signal spectrum is 2.048 MHz wide.

4.7.1.3 Signal Reception

A simplified block diagram of a GPS analog receiver channel is shown in Figure 4.7.2. Received GPS signal levels may typically be -30 dB S/N in a 2 MHz bandwidth. Each GPS satellite transmits on the same "carrier" frequency, so the received signals are separated only by Doppler offset. Therefore, the GPS signal spectra overlap. In order for a receiver channel to lock up on one signal, a code generator in the receiver with the same code as generated in a satellite is clocked into a double balanced mixer. For initial lockup, the receiver's clock is set somewhat higher (or lower) than the satellite clock's known rate, and each time the code generator changes state a 180° phase shift is induced in each GPS signal. (See Appendix A.) When the receiver's code generator approaches time synchronism with one particular signal's code, the 180° phase shifts which were induced on that signal by the transmitter are shifted another 180° for a total shift of 360° , thus restoring the carrier. Code lock is then maintained by a tau dither loop which introduces a very small amount of amplitude modulation on the signal.

Simultaneously with code lockup, the receiver's down converter must be swept to place the IF signal within the receiver's IF band pass filter. The IF filter bandwidth required to accommodate 50 bps data recovery is 100 Hz. By collapsing the spectrum from 2 MHz to 100 Hz, the S/N is raised from -30 dB

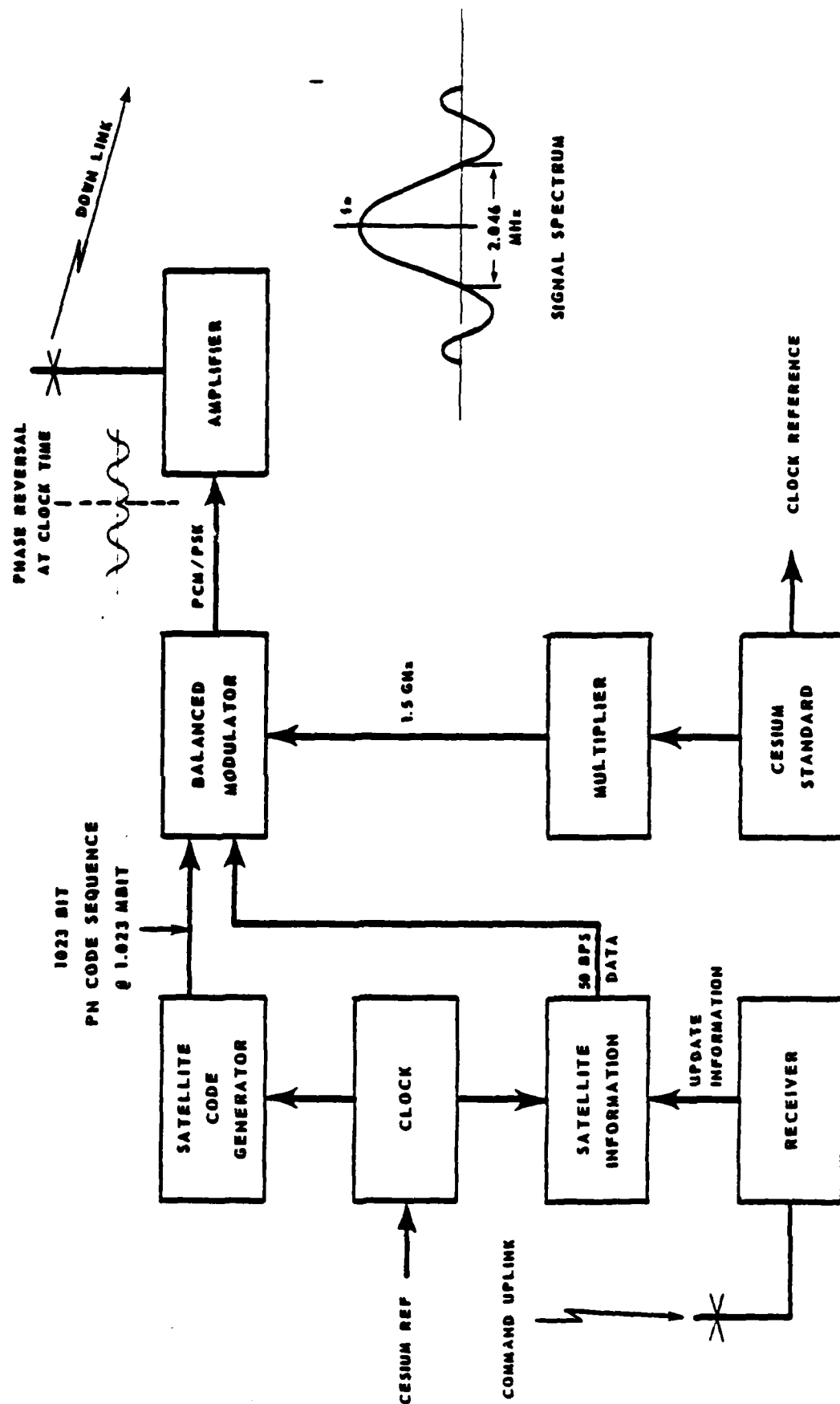


FIGURE 4.7.1 GPS SATELLITE C/A CODE SIGNAL GENERATION SIMPLIFIED BLOCK DIAGRAM

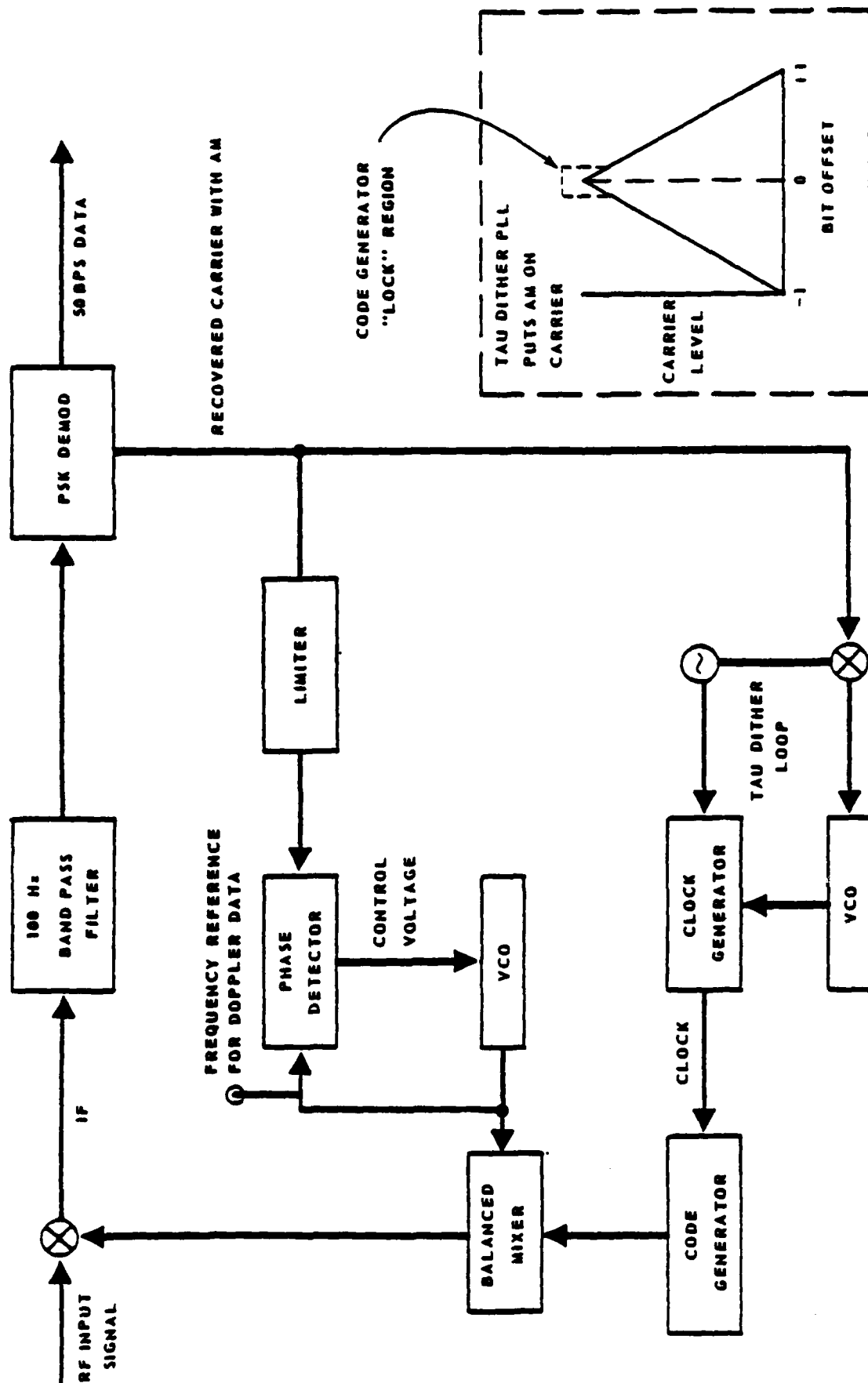


FIGURE 4.7.2 SIMPLIFIED SPREAD SPECTRUM RECEIVER BLOCK DIAGRAM

in a 2 MHz bandwidth, typical, to +23 dB in a 100 Hz bandwidth. After initial lockup, lock is maintained by standard phaselock techniques.

4.7.1.4 Points of Special Interest

From the preceeding discussion of signal reception, several points of specific interest to this note can be made. First, consider a hypothetical case when two of the GPS signals have carriers which are offset in frequency, but with identical codes in time synchronization. When the receiver locks to one of these signals, the spectrum of the second signal is also collapsed as 180° shifts are induced in both signals. This presents no particular problem if the carrier spacing is sufficient to allow the 100 Hz IF filter to pass one signal and reject the second. Carrier spacings of a few kilohertz can easily be accommodated. This feature allows GPS signals to be down converted to a very low IF frequency and then upconverted for input to a standard GPS receiver.

A second point of note is that the GPS receiver local oscillator need not be derived from a high stability reference. This is because local oscillator drift is common to all receiver channels and therefore the restored carrier frequency differences are not affected. Similarly, the translator's local oscillator drift is common to all signals relayed through the translator. A local oscillator stability of 1 part in 10^6 is compatible with receiver lockup and ranging requirements.

Finally, it should be noted that interfering signals are spread during signal reception. A CW signal, for example would be PSK modulated at 1.023 Mbit and would have a 2 MHz spectrum as shown in Figure 4.7.1. This feature provides excellent jamming protection. This is especially important in relay applications as spurs generated by the relay transmitter are less troublesome in terms of receiver desensitization.

4.7.1.5 Receiving, Recording of GPS Signals

GPS signals can be received, recorded and played back using conventional IRIG telemetry pre-detect equipment and techniques. Referring to Figure 4.7.3

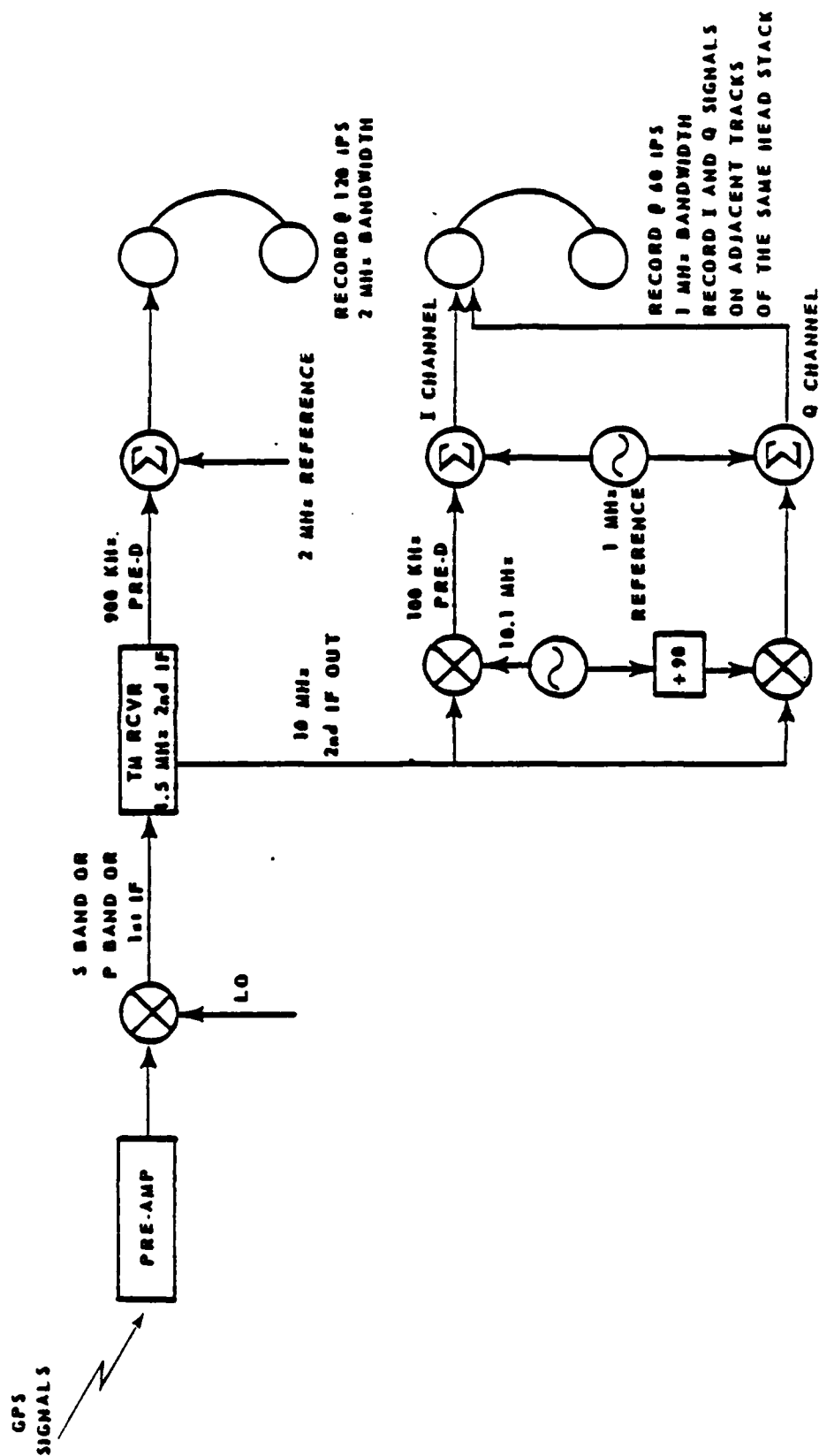


FIGURE 4.7.3 RECEIVING AND RECORDING GPS SIGNALS USING STANDARD TELEMETRY EQUIPMENT

the L-band signals can be received and up converted to S-band or down converted to P-band or to a receiver's first IF. The conversion allows the use of conventional telemetry receivers with IRIG standard 1.5 MHz IF's. . The output of these receivers is an IRIG standard pre-detect signal centered at 900 kHz which can be patched to an IRIG standard telemetry analog recorder running at 120 ips to provide a 2 MHz frequency response. A 2 MHz reference tone is also recorded on the data track in order to reduce recorder time base error during playback.

Recording at half speed can also be accomplished by down converting the signals to a very low IF such as 30 kHz. Referring to Figure 4.7.3, both in-phase and quadrature signals are recorded on adjacent tracks of the same record head. A 1 MHz reference tone is utilized.

4.7.1.6 Playback of GPS Signals

Playback of the signals for input to an analog receiver is accomplished as shown in Figure 4.7.4(a). The time base error corrector is an off-the-shelf IRIG standard unit which samples the signal in synchronism with the 90° crossings of the reference signal giving a sampling rate four times higher than the reference tone. The amplitude of the signal is represented by an 8 bit word. These 8 bit samples are then read out at a rate set by a stable reference, and a digital-to-analog converter restores the original signal with sufficient stability to allow the receiver phase lock loops to acquire and maintain lock. There is no appreciable increase in noise due to the 8 bit samples taken at an 8 MHz rate, but the total degradation of recording and playback with the suggested method has not yet been measured. It is expected that there will be a small degradation due to residual recorder time base error.

If a digital receiver is utilized, it is not necessary to re-construct the analog signal. Rather, the sample rate can be set to any convenient multi-digital processor as shown in Figure 4.7.4(b). This is convenient with signals recorded at 60 ips as both in-phase and quadrature signals can be simultaneously processed at a reduced sample rate.

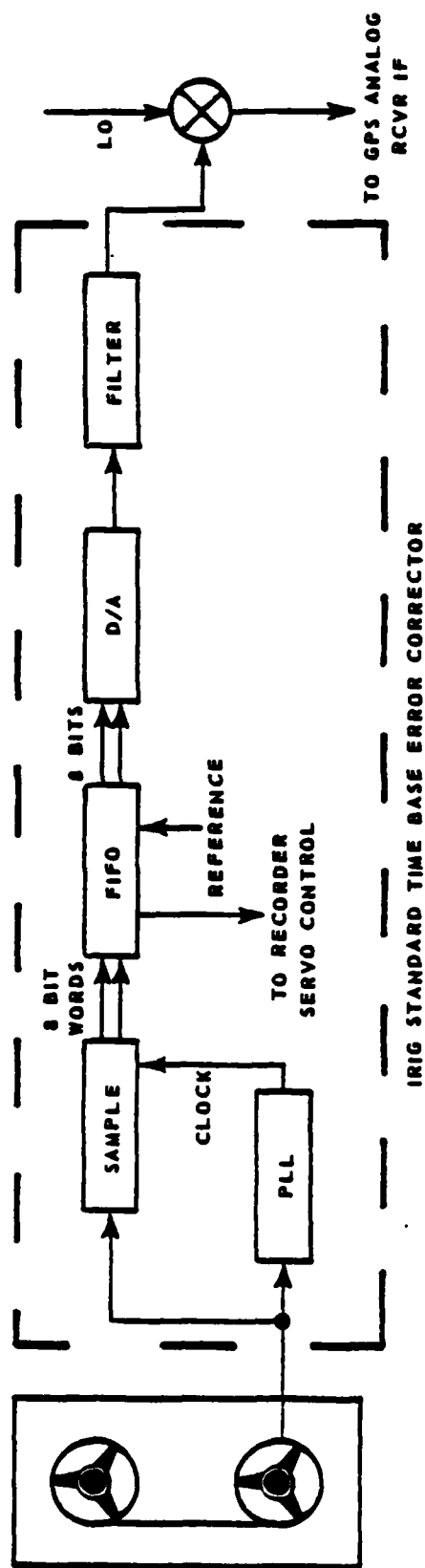


FIGURE 4.7.4(a) ANALOG PLAYBACK

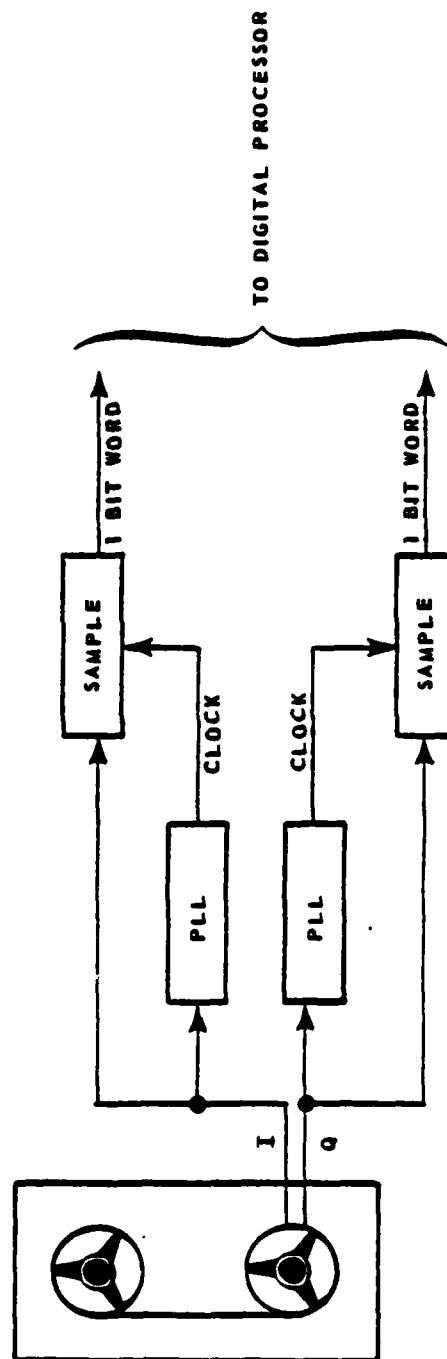


FIGURE 4.7.4(b) DIGITAL PLAYBACK

There are two principal categories of remote position determining systems: (1) the onboard receiver system is characterized by a relatively high cost and real-time total position processing capability. This system is designed to completely process the received GPS signals and provides as an output its vehicle position and velocity with respect to time. (2) The second system is characterized by low cost and almost total lack of GPS signal processing capability, it acts only as signal relay equipment. These relayed signals are processed for the vehicle position and velocity data at a remote data processing center, either near real-time or tape recorded for post operation processing. A comparison of the two categories is shown in Table 4.7.1 (Ref [16]).

As can be seen from Table 4.7.1, the full GPS receiver system requires a method of tracking loop aiding, normally derived from an onboard guidance or inertial system, facilitate the tracking loops during high dynamic maneuvers of the transporting vehicle. In addition to the simplicity of the translator/relay systems, aiding may not be required in these systems if the data is to be processed post-flight. Real-time processing of relayed data is complicated if timely acceleration data is not available as an aid.

The onboard GPS receiver may output its position/velocity solution to an existing telemetry system or to an independent transmitter relay. In either case, the RF bandwidth required to relay the data is relatively narrow, in the order of a few kilohertz and at a relatively low power penalty. The translator/relay system on the other hand would require an RF bandwidth equal to or greater than the bandwidth requirements of the GPS satellite. Thus the translator/relay may require in excess of 2 MHz RF bandwidth for the C/A code relay and 20 MHz for the P code relay. This requirement somewhat limits the relay data to the C/A code and further limits the number of links relayed at any one time due to the excessive bandwidth. A sequential sampling of the multiple link would be a possible solution but would require a scheme of coding unique to each relay.

TABLE 4.7-1 COMPARISONS OF RELAY AND RECEIVER SYSTEMS

PARAMETER	RECEIVER SYSTEM (HDUE)*	RELAY SYSTEM
Cost	high (\approx 25K) (HDUE)	low (\approx 5K)
Weight (lbs)	77	<5
Power (watts)	>200	<50 (Depends on relay trans- mitter class & power)
Size (cu ft)	3.5	<0.5
Time to first fix (sec)	152	152 (A rough position fix may be derived from less than 1 sec of cont. data through computer analysis of the relayed signals)
Code Demodulation	P, C/A	C/A
Pseudorange accuracy (1σ)	1.5 meters	10 meters
MTBF (Hrs)	500	>2000
Loop tracking aid	Inertial aids required	No aid required for post Op data reduction-Aids required for near realtime-May be der- ived from telemetry, radar or Doppler data.
RF bandwidth	2 kHz or less depending on update rate	2 MHz (C/A code) (P Code NA)
Transmitter power	Very low	Up to 20 watts depending on range (C/A code relay)
Probability of acquisition	0.95 (MBRS)	>0.95 if data reduction is post-flight.

*HDUE - High Dynamic User Equipment

4.7.3 Receiver/Translator Techniques/Designs

Having reviewed the basic techniques of generating, receiving, recording and playback of GPS signals, it is possible to readily understand the operation of several types of translators which may be used to relay GPS signals from a moving vehicle to a receiving site and which are compatible with IRIG standard receive/record equipment. Four techniques are illustrated in Figure 4.7.5 and are discussed below.

4.7.3.1 Onboard Receiver Relay

For the onboard receiver relay, a GPS receiver is placed on the vehicle and the computed positions, velocity, and raw measurement data may be relayed on a conventional telemetry link. It may be necessary to provide Doppler steering to accommodate vehicle motion and assist the onboard receiver in locking to the satellite signals. A 1 kHz data rate is typically required on high dynamic vehicles. Tabel 4.7.2 (Ref [16]) is a comparison of major performance requirements for GPS systems.

4.7.3.2 Translator Systems

GPS translator systems may be grouped into two major categories, the "bent pipe" design which performs no operations on the GPS signals other than to translate them to a second carrier frequency then relay to a processing/recording site, and those which alter the signals by digitizing, remodulating, etc., then relaying. In either system, it is possible but usually not practical to relay the P code due to the extremely wide bandwidths involved.

4.7.3.2.1 Bent Pipe Linear Relay

The bent pipe translator approach is used on the SATRACK system associated with the TRIDENT program. The received signal is converted to another frequency and re-radiated. It is necessary to radiate enough power to the receiving site to maintain the S/N ratio achieved at the vehicles receiver input. It is also necessary to retain amplitude and phase linearity of the transmitted signal which is typically accomplished with a linear output amplifier. A linear final amplifier introduces a 5 dB penalty in battery power

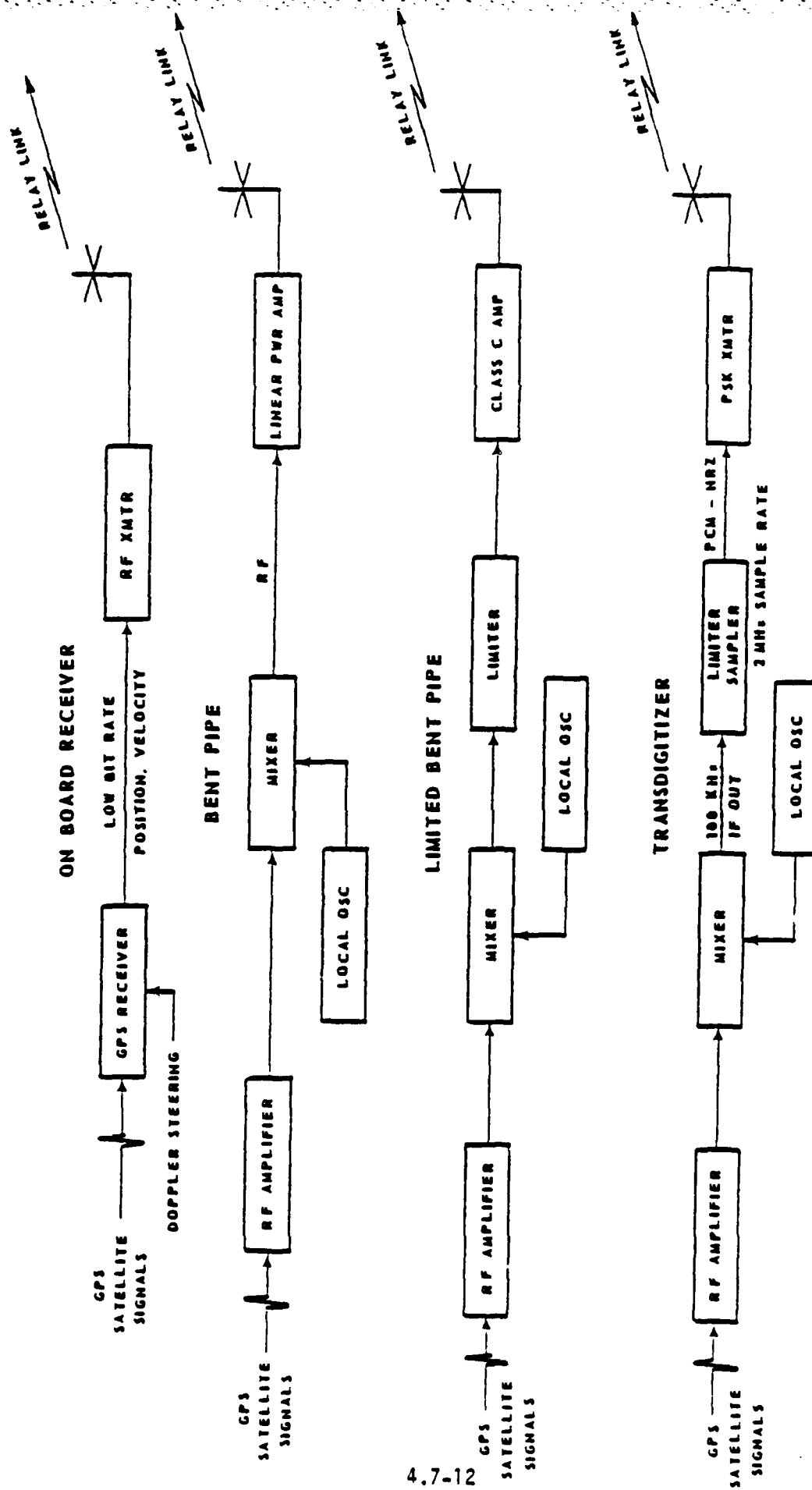


FIGURE 4.7.5 GPS RELAY TECHNIQUES SIMPLIFIED BLOCK DIAGRAM

TABLE 4.7.2 GPS RECEIVER REQUIREMENT COMPARISONS

PARAMETER	MBRS*	HDUE**	MVUE***
Code demodulation	P,C/A Code	P,C/A Code	P,C/A Code
User velocity max. (meters/sec)	7,620	1,100	25
User Acceleration max (meters/sec ²)	100	80	6
User jerk max. (meters/sec ³)	9	50	NA
Jamming levels J/S (dB) Acquisition Track/lock Weak signal	25 40 60	24 (C/A) 40 (P) 47 (P)	25 (C/A) 40 (P) NA
Time to first fix (seconds)	120	152	240
Pseudo-range accuracy at (C/N ₀) (1σ)	1.34m (25dB-Hz) 2.4m (20 dB Hz)	1.5m (30dB-Hz)	10 m (30 dB Hz) (position)
Pseudo-range rate (1σ) accuracy (meters/sec)	.012	.2	.3
Time	< 1 μs	50 ns	1 ms
MTBF (Hrs)	P _s = 0.995	500	2,000
Size (ft ³)	3.5	1.6	0.75
Weight (lbs)	77	61	25
Power (watts)	208	200	45

* MBRS - Missile Borne Receiver Set (Minuteman III)

** HDUE - High Dynamic User Equipment

*** MVUE - Manpack/Vehicular User Equipment

as compared to systems which employ class C amplifiers as the final.

4.7.3.2.2 Transdigitizer Relay

The C/A code transdigitizer is being developed by APL/JHU for GPS-SMILS. In this system, the received signals are down converted to a 30 kHz, nominal, intermediate frequency. Since the Doppler shift may be as great as ± 15 kHz, and local oscillator uncertainty as high as 1.5 kHz, the down converted GPS "carriers" may lie between 13.5 kHz and 46.5 kHz. Following the down conversion, the composite signal (GPS signals embedded in noise) is hard limited. Unfortunately, non-linear operations such as limiting, drive the weaker GPS signals further into the noise. The effect is equivalent to reducing the S/N on the received link.

After limiting, the signal is sampled at a 2 MHz rate providing a PCM-NRZ wavetrain. JHU/APL reports that the combined limiting and sampling actions cause an effective S/N degradation on the received link of 7 dB. The sampled signal is used to modulate a PSK transmitter, the signal spectrum of the transmitted signal is approximately 2 MHz wide. QPSK modulation of this signal would reduce the spectrum to 1 MHz. The primary advantages of the transdigitizer approach are the class C output stage which utilizes battery power efficiently and the capability to digitally encrypt the relayed data.

4.7.3.2.3 Nonlinear Relay Systems

Nonlinear relay systems are somewhat more complicated than the "Bent Pipe" linear relay system in that they require some additional signal processing, however power efficiency of these systems is greatly improved at the expense of some loss in signal-to-noise ratio as compared with the "Bent Pipe" design but considerably better performance than the transdigitizer.

The received GPS signal is down converted to the relay transmission frequency, limited and filtered to conserve transmission bandwidth, then amplified and used to directly drive a class C final amplifier. The signal-to-noise ratio loss due to the limiting action is approximately 1 dB. The transmission bandwidth required is slightly greater than 2 MHz.

Bandwidth of the retransmission link may be conserved by down converting the received GPS signals to approximately 30 kHz, limiting and filtering then transmitting at the desired frequency. The bandwidth required for this system is approximately 1.1 MHz but, some loss ($< 3\text{dB}$) is encountered due to the low down conversion frequency and the resultant spectrum foldover.

4.7.3.3 Signal-to-Noise Considerations

The translator serves the basic function of receiving the GPS satellite signals and transmitting the signals to a remote site. The transmitted signal "sidebands" will "feed back" into the receive channel as the transmit and receive antennas and electronics are, of necessity, located in close proximity. The relay transmitter emits "sidebands" which are essentially distributed noise that falls within the L-band receive spectrum thus adding noise to the receive channel. Therefore, there is little advantage to using a low noise L-band pre-amp unless the transmitter induced noise at (L-band) can be reduced to about the same level as the receiver's pre-amp noise. An L-band notch filter on the transmitter may be required to reduce the noise to an appropriately low level. With regards to sinusoidal spur interference from the transmitter, prudent design would require that spurs be moved outside the L-band receive bandwidth. In any case, it is important that the L-band receiver noise figure be determined in the operational configuration with the relay transmitter at full power.

Keeping the relay transmitter from interfering with the relay receiver favors a design wherein the transmit frequency is significantly higher than the receiver channel. Small commercial units which translate from L-band to S-band are available. These units are useful when the signal-to-noise ratio on the transmitter link can be maintained by high gain receiving antennas at the remote site. However, in some applications, the receiving site may have a low gain antenna, and it may be necessary to utilize a transmit frequency which is as low as practical to avoid excessive space loss. In either case, it is usually advantageous to radiate the minimum amount of power to establish a reliable link in order to conserve the vehicle's battery power.

When several translators are used in the same vicinity, care must be used in setting the relay link power to ensure that sidebands from one translator do

not interfere with the mainlobe signal of another transmitter. Where received levels cannot be conveniently matched, guard bands must be employed.

4.7.3.4 Translator Link Signal-to-Noise Ratio Considerations

The typical GPS satellite receive signal level is -160 dBW from a 0 dBi antenna. The received signal-to-noise ratio in the translator RF amplifier, S/N_{RF} , is therefore:

$$S/N_{RF} = \frac{P_R A_R}{KT_S B} \text{ or in dB, } -160 - 10\log_{10} A_R + 228.6 - 10\log_{10} T_S - 62, \text{ dB.}$$

Where P_R = received power from a 0 dBi antenna, -160 dBW

A_R = L-band receive antenna gain

K = Boltzman's constant, -228.6 dBW/K° Hz

T_S = L-band receive noise temperature including transmitter induced noise degradation, K°

B = GPS signal processing bandwidth, 1.3 MHz.

The signal-to-noise ratio of the transmitted signal, S/N_t is:

$$S/N_t = S/N_{RF} \cdot \frac{1}{F}$$

Where $\frac{1}{F}$ represents the signal-to-noise ratio degradation due to translator "processing".

For the linear bent pipe, $10\log_{10} \frac{1}{F}$ is 0 dB, while for the limited bent pipe, it is -1 dB and for the transdigitizer it is -5.5 dB.

The relayed signal spectra for the transdigitizer, bent pipe and limited bent pipe techniques can be characterized as band limited noise. As the GPS signal

power is very small compared with the noise power, the signal-to-noise ratio of the relayed signal, S/N_R received at the remote site is:

$$S/N_r = S/N_t \frac{P_r}{P_r + P_n}$$

Where

P_r is the signal power of the relayed signal at the remote site receiver input and

P_n is the noise power of the remote site receiving system referenced to the receiver input.

4.7.3.5 Translator Comparisons

The four translator techniques discussed in this note are all compatible with IRIG standard receive/record/playback techniques. The on-board receiver technique requires the smallest data spectrum, typically a few kilohertz, and is therefore useful in an arena where many translators will be used simultaneously. It is especially advantageous when relay from the vehicle to another vehicle (such as a satellite) via a standard narrowband communications channel is needed. However, the complexity and cost as well as the requirement for on-board Doppler steering may well preclude widespread use of the on-board receiver in many test range applications. In addition, the on-board receiver battery and transmitter power penalties are typically 10 dB because of the requirement to maintain a 10 dB signal-to-noise ratio in a bandwidth equal to the data bit rate.

With regards to the linear bent pipe, limited bent pipe and transdigitizer techniques, all three should be similar in terms of complexity, cost and spectral requirements. However, the transdigitizer suffers from severe transmitter power penalties as shown in Figure 4.7.6*. The limited bent pipe offers the potential for a 3 dB battery power savings if a 3 dB signal-to-noise ratio

*When both telemetry data and GPS signals are to be simultaneously radiated from the same vehicle, however, the transdigitizer becomes a viable option.
See 4.7.3.6

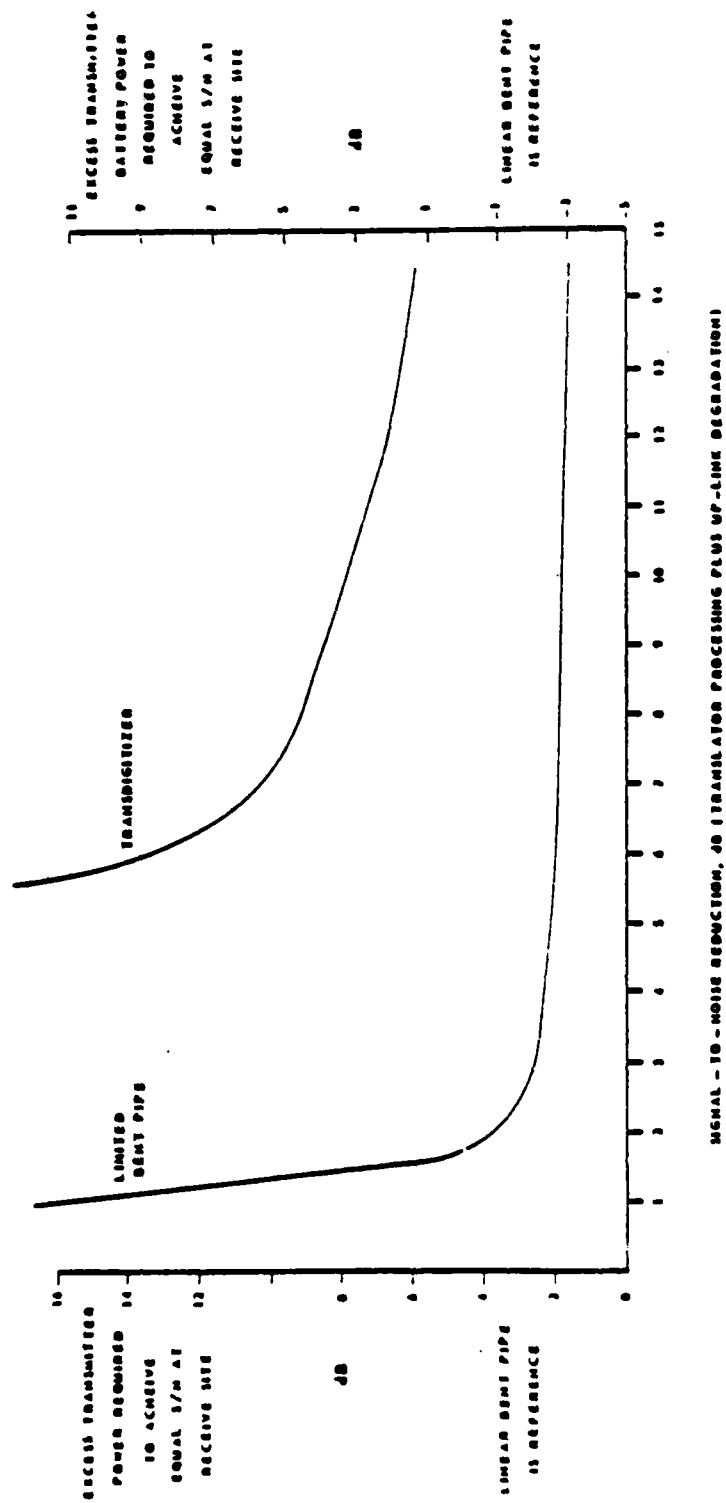


FIGURE 4.7.6 TRANSMITTER POWER AND TRANSMITTER FINAL BATTERY PENALTIES FOR EQUIVALENT SIGNAL-TO-NOISE PERFORMANCE AT THE RECEIVE SITE

degradation is tolerable. In general, however, when the vehicle's L-band receive antenna has low gain (perhaps -10 dBi or lower), it may be necessary to utilize the linear bent pipe in order to minimize the up-link degradation without having to overpower the link. A comparison of the important characteristics of each relay system is outlined in Table 4.7.3.

4.7.3.6 Telemetry Data Relay

In many range support applications, the vehicle may be designed to carry a telemetry transmitter and antenna, and it may be planned to add a GPS translator to the vehicle. However, such an addition may be impractical because of size, weight or spectrum constraints. In such cases, consideration should be given to developing a package of the same size and weight as the telemetry package alone but which provides both telemetry transmission and GPS translation. Many schemes can be conceived to transmit both GPS and telemetry data on a common link using a single transmitter final. When the telemetry data is PCM, a convenient approach is a QPSK transmission scheme wherein the trans-digitizer stream is clocked at 2 MHz and the PCM data rate is set to 1 Mbit or a convenient sub-multiple of 1 Mbit. With QPSK, one-half the transmitted power is in the telemetry stream, and one-half is in the GPS stream, and a 10 dB S/N is required by the QPSK receiver demodulator (in a bandwidth equal to the telemetry data rate). All other co-channel transmission techniques considered to date require the same or greater data spectral occupancy, as the QPSK technique, and several other techniques can potentially be used to reduce the transmitter power required by nearly 3 dB. However, the possibility of providing secure GPS and secure telemetry transmission makes the QPSK approach an attractive option. *

4.7.4 Multi Vehicle Interference

In most cases where there are only a few vehicles (≈ 10) whose positions must be determined, the wide transmission bandwidth required by the translator systems would pose few problems; however, in situations such as military field maneuvers, where possibly hundreds of vehicles would require positioning, the problem of bandwidth becomes more complex and alternate arrangements may be

* When links are secured, a 10 dB S/N ratio must be maintained in a 2 MHz bandwidth.

TABLE 4.7.3 COMPARISON OF RELAY SYSTEM CHARACTERISTICS

PARAMETER	Bent Pipe	Transdigitizer	Non Linear Relay
RF Bandwidth required (code)	2.1 MHz (C/A) 10.1 MHz (P)	1.1 (C/A) 5.1 (P) (QPSK Modulation)	2.1 MHz (C/A) 10.1 MHz (P)
Type of relay Transmitter	Linear	Class C	Class C
Remodulation Loss (dB)	0	7	1 to 3 dB
Battery power drain	High (Due to class A final)	Low	Low
Compatible with existing range receive/record equipment	No	Yes P Code - No (bandwidth limit)	C/A Code - yes P Code - No (bandwidth limit)
Compatible with standard GPS Receiver	Yes	Yes	Yes
Susceptibility to jamming on relay link	Low (Same as down link)	High	Low (Same as downlink)
Susceptibility to interception	High	Low IF Encrypted	High

required. In low vehicle dynamic situations, translator center frequencies may be spaced as close as 1 kHz. This close spacing causes the transmitted spectrums to overlay, however, due to the narrow bandwidths (≤ 100) employed in the processing center GPS receivers, the overlapping spectrums will not interfere. Since onboard receiver systems require only very narrow bandwidths to relay their information, spectral occupancy is not a problem.

4.7.5 Same Examples of Potential Translator Applications

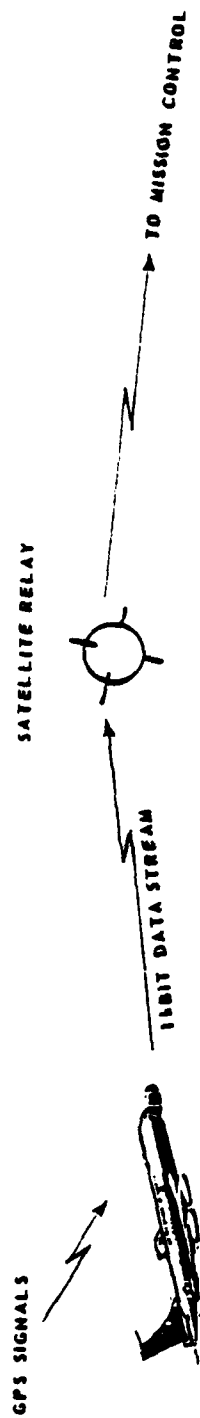
Figure 4.7.7 illustrates several potential translator applications. As shown, "Worldwide" aircraft testing can be accomplished using an on-board receiver relaying to a communications satellite.

Cruise missile type vehicles can be supported worldwide using a tracking aircraft as an intermediate relay to a communications satellite.

Ballistic vehicles can be supported by relaying to telemetry tracking sites.

Broad ocean scoring can be accomplished by relaying to the telemetry support aircraft.

Note that each application tends to favor the use of a particular kind or kinds of GPS signal relay because of the mission peculiar vehicle features and/or mission requirements.



- NO SPACE/WEIGHT/POWER CONSTRAINTS
- ON-BOARD COMPLEXITY NOT AN ISSUE BECAUSE TRANSLATOR CAN BE REUSED.
- DOPPLER STEERING AVAILABLE FROM AIRCRAFT NAVIGATION.

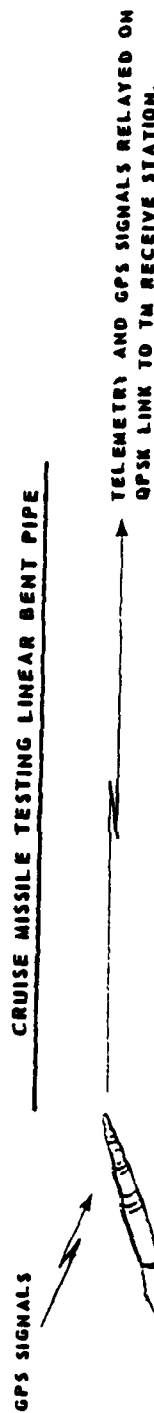
AIRCRAFT TESTING USING ON-BOARD GPS RECEIVER



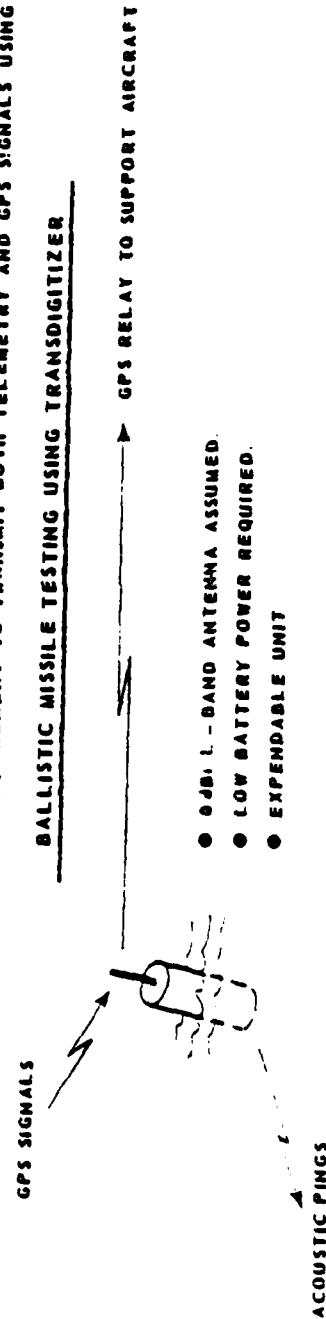
NOTE: IF AIRCRAFT IS EQUIPPED WITH A GPS RECEIVER, IT CAN RELAY CRUISE MISSILE POSITION VIA SATELLITE.

- POOR L-BAND RECEIVE ANTENNA GAIN ASSUMED.
- BATTERY POWER AVAILABLE
- LOW COST EXPENDABLE TRANSLATOR REQUIRED.

CRUISE MISSILE TESTING LINEAR BENT PIPE



- REQUIREMENT TO TRANSMIT BOTH TELEMETRY AND GPS SIGNALS USING 1 LINK
- #### BALLISTIC MISSILE TESTING USING TRANSDIGITIZER



- 6DBI L-BAND ANTENNA ASSUMED.
- LOW BATTERY POWER REQUIRED.
- EXPENDABLE UNIT

BROAD OCEAN SCORING USING LIMITED BENT PIPE

FIGURE 4.7.7 EXAMPLES OF POTENTIAL TRANSLATOR APPLICATIONS

4.8 Access to Raw Data Considerations

This section describes the type of data that may be available from a GPS receiver and the potential effect on processing. As an example the Missile Borne Receiver Set (MBRS) receiver flown on Minuteman III output pseudo-range, range rate (delta range), computed position, velocity and acceleration, ephemeris information and receiver status data. These data allowed for real-time evaluation using the on board GPS computed position and velocity output, and flexible post-flight processing using pseudo-range, range rate and ephemeris data. This receiver did not exercise the dual frequency ionospheric refraction capability forcing data users to apply an a priori refraction model or externally supplied correction (from Aerospace Corp.) or else neglect this term.

In contrast the Missile Accuracy Evaluation (MAE) receiver, that was to have been flown on the MX missile, was to have had a wide variety of raw data and receiver performance data as well as dual frequency output. The potential user would have been required to obtain GPS ephemeris data from a ground receiver (for real-time applications) or wait for corrected ephemeris data to be supplied for post-flight use. Use of the MAE data in real-time would have required far more ground based equipment/software than MBRS but, for post-test applications, the MAE data would probably have yielded a more accurate trajectory reconstruction. Subsequent subsections will detail these issues further.

4.8.1 Raw (R, R) Versus Processed (P, V) Data

"Raw" data (pseudo-range and pseudo-range rate) is somewhat of a misnomer as these data are calculated by a GPS receiver and represent the basic data for subsequent processing. The sample rates of these data vary but can be as high as 50 sps. In the case of an onboard receiver (such as MBRS) it is required that these data be multiplexed into a down link (usually S-band) for acquisition and subsequent processing. Care must be taken to ensure that all measurement samples are recoverable. Under some situations where the down link contains other data, such as INS parameters, it is possible that the down link frame rate is asynchronous with the raw data rate resulting in the potential loss of some data.

The availability of raw data allows the user to apply processing algorithms tailored to his requirement and computer capability. These requirements may be quite different as to real-time versus post-test.

Most military GPS receivers output position and velocity data, in various coordinate systems, for either visual CRT display or input to a navigation system. Extensive use of microprocessors are made for internal data processing in these receivers with the effect of limiting the parameters output to a minimum. This category of receivers cover most "off the shelf" equipment with the exceptions being the R&D receivers (such as MBRS and MAE) and some high dynamic receivers. It should be stressed that for most Range applications a receiver providing flexible parameter output (and possibly aiding inputs - due to the many high dynamic applications) will be required. In low and some medium dynamic field environments where real-time positioning is desired, off the shelf receivers (such as the manpack) are suitable. It should also be noted that many test range application receivers operate in a controlled environment with technical support and maintenance thus reducing the need for stringent reliability requirements.

4.8.2 Code and Carrier Loop Error Signals

In order to acquire a GPS signal it is necessary to obtain code correlation with a receiver generated replica code (sometimes aided by an anti-jamming T code). Once code lock has been achieved, a carrier loop is used to collapse the spectrum for the 50 bps data acquisition block (1500 bits) and to further recover the carrier to aid the code correlation function. The bandwidth of the carrier loop (and its design) becomes a trade off between higher carrier SNR and dynamic tracking performance (see Section 4.6). It should be noted that the carrier loop will only lock as long as code correlation is maintained so the net effect is to have a carrier aided code tracking loop and not continuous carrier tracking (see Section 4.6).

The common code loop contains early, late and prompt (or punctual) outputs that determine the status of the correlation. The input to the code loop is either a VCO or DCO that drives the replica PN generator. It may be desirable to have status indications of the mode of this loop such as C/A or P code track; early, late, and prompt status and the PN generator clocking rate.

The narrow band carrier loop may consist of a phase lock loop and a frequency lock loop. The carrier loop control signals are provided from a Costas error generator. The error signals that are provided from this narrow band loop are similar to that of the wideband code loop but may also indicate carrier cycle slip. Other types of narrow band carrier lock loops are the non coherent delay lock loop and the π dither loop. The choice of design is generally dependent on the expected dynamics and sequential/parallel channel design.

All of these signals, for both loops, can be used for analysis purposes and for possible aid in post-test data reduction.

4.9 Standard User Hardware Characteristics

Although there are numerous different GPS user hardware units already available and under development, the consideration here will be mainly restricted to those currently in the full scale engineering development phase for the GPS JPO. Magnavox and Collins were contracted to perform the Phase II Full Scale Development. The previous four years were devoted to Phase I, Concept Validation development and testing and involved Texas Instruments as well. This section will describe the overall design concepts of the user hardware being developed and tested in Phase II as well as a few more specialized GPS units which may be useful for Range applications.

The design philosophy has been dictated by the concept of using GPS equipment on hundreds of different vehicles whose dynamics vary from a stationary user to high velocity and acceleration aircraft and missiles. In order to produce this range of units at a reasonable cost the design goal was to produce the minimal number of unique hardware (as well as software) modules which, through various combinations, could meet all the performance and host vehicle requirements. The "System Segment Specification for the User System Segment, NAVSTAR Global Positioning system, Phase II," (United States Air Force, SS-US-200, 31 January 1979) should be consulted for details. Most of what follows borrows heavily from Ref [37].

4.9.1 Phase II Hardware Design Overview

The modularization can be broken into Line Replaceable Units (LRU) which are plug-in compatible units which can be used in various combinations to meet several requirements. Many more variations can be formed (and cost savings achieved) at the level of the Shop Replaceable Unit (SRU); for instance, the circuit boards used in a single channel receiver can be replicated to form a multichannel receiver. A description of the basic LRU's and an indication of the type of applications which would dictate their use follows.

4.9.1.1 Antenna/Antenna Electronics

A user obviously must have an antenna capable of receiving the signals transmitted from the GPS satellite. The simplest of these are omni-directional

antennas suitable for a user unlikely to encounter jamming and whose vehicle dynamics combined with antenna placement insures no shading of the antenna; the design may vary but all are referred to as Fixed Reception Pattern Antennas (FRPA). For applications requiring more complexity there are Controlled Reception Pattern Antennas (CRPA) which have control electronic modules associated with them. The most prevalent type of CRPA senses jamming energy arriving from certain directions and adjusts the antenna pattern so as to create nulls in those directions.

4.9.1.2 Receiver/Processors

The GPS receiver/processor consists of hardware and software necessary to acquire and track a GPS signal, demodulate the navigation message, and compute the navigated position and velocity of the user. The receiver section might be considered the signal processing sections comprising the tracking loops, etc.; while the processor generates the appropriate PN code, performs control functions, has a memory containing the almanac, and performs navigation computations, etc..

- a. The simplest receiver has only a single channel; hence, it must sequentially track four satellites to obtain the data necessary for navigation. Phase I tests revealed that such a receiver can meet the combined jamming, dynamics, accuracy, and time-to-first fix specifications for troops and land vehicles.
- b. For medium dynamics vehicles (e.g., helicopter) a two channel receiver is adequate. This cycle functions much like the one channel but reduces measurement cycle time.
- c. High dynamics aircraft and missiles (as well as submarines which need to have a very short time to first fix) requires a five channel receiver and in some applications aiding will be necessary. The five channel receiver can be tracking five satellites simultaneously so that changing constellations (of four) need not interrupt the navigation solution.

4.9.1.3 Flexible Modular Interface (FMI)

These units, where required, contain the hardware and software necessary to integrate the GPS set into the specific host vehicle. Since these units are the most applications specific, the flexibility must be at the SRU level. The different developers seem to have very flexible concepts of what the FMI comprises; for instance, some contain CPU's themselves with resident programs that the processors may pull in. This unit can serve as the interface with "aiding" measurements from inertial navigation systems, altimeters, etc..

As indicated in Ref [72] the number and type of output channels has been left up largely to the discretion of the manufacturer; this may be the way by which Test Ranges may gain access to the "raw" GPS data which would greatly aid post-test processing.

4.9.1.4 Control and Display

This unit, where needed or desirable, serves to display the GPS data, such as position and velocity, and to allow manual input of data. This unit is not needed in applications where navigation control panels already exist.

4.9.2 Special Applications GPS Hardware

Although the Phase II designs will cover most applications, there are specific uses where cost savings can be realized using simpler hardware.

4.9.2.1 Frequency Translator

For vehicles which are expendable a simple, inexpensive frequency translator is being developed. The translator, located on the vehicle whose position and velocity is to be determined, simply receives all the GPS signals it can and retransmits them on S-band. A surface (or an auxiliary vehicle) based GPS receiver (modified to receive S-band) decodes the signal and computes the location of the vehicle. Thus, a four channel ground based receiver/processor can determine the position and velocity of the vehicle with almost the same accuracy as a four channel receiver/processor on the vehicle while saving the electronics that would necessarily be destroyed (see Section 4.7).

4.9.2.2 Tactical Mid-Course Guidance

Another, slightly more complicated, unit designed for expendable use (i.e., tactical missiles) is based on a so called "mother-daughter" concept. The missile (the "daughter") contains a simplified receiver which need only extract the pseudo-range data which it uses in conjunction with its inertial navigation system. The launching vehicle ("mother") contains a complete GPS receiver and preselects the constellation, initializes, aligns, and calibrates the daughter receiver prior to launch. This technique is for relatively short flight tactical missiles.

4.9.3 Configurations for Test and Training

Following Ref [2] it is assumed that, with some modifications, the hardware just described could be used for test and training ranges also. Primarily, some provision to transmit the GPS data to a ground site must be made; it would also seem desirable to transmit some of the raw data (see Section 4.8). It should be stressed that this author has no knowledge of whether the designs, say on the SRU level and in the software, have any requirement to make this transmission option available.

For purposes of classifying the types of vehicles to be equipped with GPS units, Ref [2] defines the following four categories.

- A. High velocity with high acceleration - This is the class of vehicles with velocities over 200 kts and accelerations over 5 g; hence, it includes many missiles and the high performance aircraft.
- B. High velocity with medium acceleration - These vehicles have velocities over 200 kts but accelerations below 5 g; examples are tactical aircraft and helicopters.
- C. Low velocity with medium acceleration - Vehicles with velocities below 200 kts and acceleration less than 5 g such as ships and ground vehicles (perhaps representing moving targets for testing).

- D. Low velocity with low acceleration - This category is primarily for ground units which are basically stationary but move from time to time during an exercise.

Since these categories were defined in particular for Navy Test Range purposes, it is quite possible they will have to be modified and extended for a Triservices application. (Translators and pseudo-range receivers are examples.)

Again following Ref [2], five basic GPS hardware configurations (with aiding where necessary) will now be described to cover the four test and training categories. For most of them a down link transmitter and antenna for transmitting raw and processed data to a ground (or airborne) receiving site would be necessary for test purposes.

Type I - High performance/airborne - This configuration consists of an integrated inertial guidance system and a two frequency (L_1 and L_2), five-channel GPS receiver. This type is for use with category A user aircraft.

Type II - High performance/expendable - For category A vehicles which are not recoverable one of the special applications units may be used. One example would be a ballistic missile equipped with an INS and a GPS translator. The ground station would receive the translated GPS data as well as the INS acceleration data (so as to maintain lock under high dynamics maneuvers). Another example would be the tactical missile case using the "mother-daughter" configuration. The data that would be needed to be transmitted to a ground station is not clear though.

Type III - High speed/airborne - This configuration is intended for use with category B vehicles and with category C vehicles that require high accuracies. It consists of a two frequency, five channel GPS unaided unit with at least a 10 Hz update rate.

Type IV - Low speed/airborne - This is intended for category C vehicles that can tolerate a relatively low accuracy and with category D vehicles. The unit is a two frequency, two channel unaided GPS unit.

Type V - Manpack - This configuration of a two frequency, single channel unit will give accuracies sufficient only for category D users.

In addition there should be a sixth category to cover the possible use of translators for applications such as GPS-SMILS.

Table 4.9.1 (reproduced from Ref [2]) illustrates the accuracies expected from the five configurations.

4.9.4 Specifications of an Existing Hardware Configuration

For concreteness, an example of an existing configuration and its specifications will be described. This is drawn from Collins (Ref [45]); similar data from Magnavox was not at hand.

Type I configuration/attack aircraft - This GPS unit is capable of stand alone or aided navigation solutions for position, velocity, and time for a high performance aircraft. The antenna system consists of a bottom mounted FRPA and a top mounted CRPA (with six auxiliary elements to provide spatially adaptive nulling for simultaneous jamming sources); both are capable of receiving both the L_1 and L_2 frequencies. An antenna electronics module receives signals from both antennas simultaneously and does the null steering process for the CRPA. The receiver/processor module has five channels and consists of a central processing unit which, along with distributed microprocessors, performs the signal processing and navigation tasks. There is a twelve element Kalman filter for the integrated processing of GPS measurements and host vehicle aiding sensors (inertial navigation, Doppler radar, altimeter, heading/roll/pitch sensor, and true airspeed sensor). Fix updates are once a second and can be propagated up to 20 times a second. The FMI subassembly is connected to the receiver/processor unit and serves as the interface with the aircraft's other related systems. It contains a second CPU for weapons delivery computations using the navigation solution. There is an optional data loader subsystem for bulk loading host vehicle and mission unique data and an optional control/display unit.

The GPS unit's accuracy in a stand alone mode is quoted as: Position - 10 m; Velocity - .1 m/s; and time - 50 ns. These are for dynamics up to:

TABLE 4.9.1 ACCURACY EQUATIONS FOR GPS RECEIVER TYPES
(BASED ON 18 SATELLITE CONFIGURATION)

CONFIGURATION	ALL VALUES STANDARD DEVIATION					
	POSITION, FT. ABSOLUTE		POSITION, FT. RELATIVE TO LOCAL REFERENCE		VELOCITY, FPS (C)	DATA UPDATE RATE, HZ
	x, y	z	x, y	z		
TYPE 1	19	45	10	22	.5	1.3
TYPE 2	19	45	10	22	.5	1.3
TYPE 3	19+1.8n (B)	45+4.3n (B)	10+1.8n (B)	22+4.3n (B)	.5	1.3
TYPE 4	19+36n	45+36n	10+36n	22+36n	.016+36n (B)	.05+36n (B)
TYPE 5 (D)	19+145n	45+145n	10+145n	22+145n	.008+145n	.024+145n

(A) For position accuracy from player to player, multiply position accuracy relative to the surface by $\sqrt{2}$.

(B) Where n is the maximum amount of acceleration, in g's, to be experienced and A, the maximum number of j's (the time rate of change of acceleration (jerk)). For n values greater than 15, a loss of data may result, due to a loss of code loop lock.

(C) This is an average velocity, taken over the period of the update rate.

(D) Based on an update rate of 1/2 Hz for the two-channel receiver, and 1/4 Hz for the one-channel receiver.

(E) Source: Table 5

Velocity	1200 m/s
Acceleration	118 m/s/s
Jerk	180 m/s/s/s
Yaw	± 1 rad/s, ± 3 rad/s/s
Pitch	± 1 rad/s, ± 6 rad/s/s
Roll	± 5.5 rad/s, ± 17.5 rad/s/s

When significant jamming is present these accuracies can be maintained only with aiding.

This unit requires 4.5 minutes from power on to first accurate solution. Its Time-To-First-Fix (TTFF) after initialization is 1.5 minutes.

Examples of configurations suitable for the lesser dynamic applications can be found in References [39] through [44].

4.9.5 GPS Receiver and Translator Sources

In addition to the JPO contracted companies (Magnavox and Collins), the following are possible sources of User Equipment for range applications.

- a. Texas Instruments - In addition to TI's work developing a sequential, time multiplexed single hardware channel receiver for commercial use; they are developing a "mother-daughter" configuration for the Tomahawk missile.
- b. Stanford Telecommunications Inc. - STI has a C/A-L₁ receiver design under development for commercial use.
- c. Interstate Electronics Corp. - IEC has designs for an "all digital" full C/A-P, L₁, L₂ receiver as well as a C/A - L₁ receiver.
- d. RCA - Designs for a SATRACK translator.
- e. Cubic Corp. - Designs for a SATRACK translator.
- f. Applied Physics Lab - Designing a translator for GPS-SMILS.

4.10 Filtering and Smoothing

The problem of processing a set of measurements to produce "optimal" estimates of selected random variables has been of some interest since at least the early nineteenth century (Ref [65]). In recent years the widely successful application of linear estimation algorithms has been most notable (Ref [66], [67], [68]).

Linear estimation algorithms have generally been either of the "batch" or the "recursive" type. In the former, all measurements are operated upon at once, while in the latter, measurements are processed a few at a time, generally in time sequence. The Bayesian Weighted Least Squares (WLS) method is the most general batch processing algorithm; and the Kalman Filter/Smoothing (KFS) method is the most general recursive algorithm.

While there exist many similarities and much commonality of application between the WLS and KFS methods, the KFS method actually is applicable to a larger class of problems than the WLS method. For this reason, the KFS method is considered exclusively in the sequel.

The problem of processing measurements to obtain optimal estimates of selected variables of interest is a fundamental one. In the general case, the problem is formulated by expressing the variable of interest together with augmented auxiliary variables, collectively called state variables, as dependent variables in a set of stochastic differential equations in which time is the independent variable. The measurements are then expressed as stochastic functions of the state variables and time.

A brief mathematical treatment in Appendix A demonstrates the application of the KFS method to the estimation problem formulated above.

In order to apply the KFS algorithm, it is necessary to formulate a state variable representation for the quantities of interest. In GPS applications these variables generally include position and velocity. Moreover, measurement errors either in pseudo-range or from auxiliary sources such as inertial sensors, which are not sequentially uncorrelated (i.e., non-"white") must

be modeled in terms of augmented Markovian state variables to achieve optimality. In fact, in post-test applications, in which refined ephemeris and clock data for each SV are available, it may yet be worthwhile representing errors in these quantities as state variables, although realistically, there is little improvement expected in the estimate of these quantities. This is an example of a common principle — augmentation of states of little or no interest to improve the estimates of those states which are of primary interest.

In the error budgets presented in Section 2.0, errors were categorized as either slowly or rapidly varying with time. The rapidly varying errors are treated as white noise in the KFS. The slowly varying errors must optimally be modeled as biases or Markovian random processes.

Applications of KFS to GPS are widely reported in the literature. A few of these will be briefly discussed below.

A variety of applications can be readily envisioned in which vehicle navigation is performed using a combination of INS and GPS. Two examples will serve to illustrate most of the points of interest; namely, a real-time cruise navigation example and a post-test ballistic missile guidance accuracy analysis example.

An INS designed for long term real-time application will benefit considerably from GPS (Ref [16], pp 144-153). These systems normally are used to provide vehicle position and velocity as well as vehicle attitude (i.e., heading, pitch and roll) relative to a locally level frame of reference. Without some form of velocity reference these systems are subject to Schuler oscillations in the horizontal plane; and without an independent altitude (geodetic height) indicator, they are unstable in the vertical channel. Moreover, because of instrument noise, the position and velocity errors slowly diverge, resulting in the requirement for frequent position reset.

GPS is an inherently more accurate navigation system than the INS, but the INS provides attitude sensing and is more responsive to maneuvers than GPS. When measurements from the two systems are combined in a real-time Kalman Filter, very accurate position, velocity and attitude can result. Moreover, the INS can aid GPS tracking during high dynamic conditions, and the INS can

maintain high accuracy for brief intervals when GPS is not available.

The Inertial Guidance Systems (IGS) which are deployed on ballistic missiles are very similar in some respects to the inertial navigation systems previously discussed. The significant difference is in the duration of the navigation interval, which for ballistic missiles is sufficiently short that damping of Schuler oscillations and the vertical channel are unnecessary.

During ballistic missile tests, inertial guidance data is collected by telemetry systems for post-test analysis purposes. If GPS data is collected and telemetered during the missile flight, from either a receiver or translator onboard the missile, this data can be used as a basis for guidance system analysis in much the same fashion as ground based sensors have been used in the past (Ref [69]).

By combining telemetered GPS and IG data in a KFS, it is possible to estimate initial alignment, accelerometer and gyro instrument error parameters for the IGS. Estimates of these parameters can be used to isolate hardware and software problems which can then be corrected in future flights. Furthermore the KFS procedure produces an estimate of the missile trajectory and provides the basis for an accuracy analysis of the weapon system.

Perhaps the most widespread application of GPS is that of fixed-point surveys. In such applications, one has the luxury of collecting data over extended periods of time. Data reduction via KFS (or WLS) can be employed to achieve absolute accuracies which are potentially in the sub-meter range (Ref [6], p 85).

4.11 Doppler Preprocessing

This subsection deals with Doppler signal processing options which can be exercised prior to inputting GPS measurements into the post-test estimator. This section is based on analysis detailed in Ref [18] which should be consulted for more details.

The measurements of interest are the code and carrier loop outputs of pseudo-range and delta-range. The pseudo-range measurement is given by

$$\tilde{R} = R + R_S + R_T + R_I + R_M + R_N \quad ,$$

where R is the true range from the SV to the receiver, R_S is a systematic term which includes SV and user clock errors, R_T is tropospheric delay, R_I is ionospheric delay, R_M is multipath noise, and R_N is receiver noise and quantization error. In similar fashion, the delta-range measurement is given by

$$[\tilde{r}]_{t_0}^t = [R]_{t_0}^t + [R_S]_{t_0}^t + [R_T]_{t_0}^t - [R_I]_{t_0}^t + [r_m]_{t_0}^t + [r_n]_{t_0}^t \quad ,$$

where upper case letters denote the same quantities as before, and lower case letters denote quantities which apply only to the delta-range measurements.

From a purely theoretical viewpoint, the pseudo-range and delta-range measurements can be input directly to an optimal estimator, provided stochastic state variable representations can be formulated for each term (except white noise) in the measurement equations. State variable representation for R_S is straightforward. It is probable that state variable representation of R_T is possible also, but may not be worth the additional estimator complexity. It is questionable whether adequate state variable representation of R_I is possible. In any case, if state variable representations for R_S , R_T , and R_I are introduced, the measurements can be input directly to the estimator.

In the case of delta-range, an additional state must be introduced for $R(t_0)$, but this is easily done, since $R(t_0)$ is a perfectly correlated function of SV and receiver position states. Thus the a priori estimate of $R(t_0)$ and the a priori covariance of $R(t_0)$ are simple functions of the a priori estimates and covariances of SV and receiver position states.

In practice, R_T and R_I are not typically modeled in terms of state variables. Instead R_T is generally estimated from local measurements of atmospheric conditions (viz, temperature, pressure, relative humidity), and R_I is estimated from dual frequency ranging measurements.

The ionospheric delay terms R_{I1} and R_{I2} at the respective frequencies f_1 and f_2 are related by

$$\frac{R_{I2}}{R_{I1}} \approx \frac{f_1^2}{f_2^2} ,$$

where the approximation improves with increasing frequencies and is excellent at L-band. The above relation is the basis for dual frequency ionospheric delay compensation.

When continuous measurements (i.e., no dropouts or cycle slips) exist simultaneously on L_1 and L_2 for both pseudo-range and pseudo-Doppler, a very accurate means of ionospheric delay compensation is possible. For this purpose the following measurements are available.

$$\tilde{R}_1 = R + R_S + R_T + R_{I1} + R_M + R_{N1} ,$$

$$\tilde{R}_2 = R + R_S + R_T + R_{I2} + R_M + R_{N2} ,$$

$$\begin{aligned} [\tilde{r}_1]_{t_0}^t = & [R]_{t_0}^t + [R_S]_{t_0}^t + [R_T]_{t_0}^t \\ & - [R_{I1}]_{t_0}^t + [r_M]_{t_0}^t + [r_{N1}]_{t_0}^t , \end{aligned}$$

$$\begin{aligned} [\tilde{r}_2]_{t_0}^t = & [R]_{t_0}^t + [R_S]_{t_0}^t + [R_T]_{t_0}^t \\ & - [R_{I2}]_{t_0}^t + [r_M]_{t_0}^t + [r_{N2}]_{t_0}^t . \end{aligned}$$

It now follows that

$$\tilde{R}_2 - \tilde{R}_1 = R_{I2} - R_{I1} + R_{N2} - R_{N1}$$

and

$$[\tilde{r}_2]_{t_0}^t - [\tilde{r}_1]_{t_0}^t = [R_{I1}]_{t_0}^t - [R_{I2}]_{t_0}^t + [r_{N2}]_{t_0}^t - [r_{N1}]_{t_0}^t .$$

Now if $[t_0, t_f]$ is the interval over which the above measurements are available and if $T = t_f - t_0$, then using the notation

$$\langle X \rangle \equiv \frac{1}{T} \int_{t_0}^{t_f} X(t) dt ,$$

it follows that

$$\begin{aligned} & \langle \tilde{R}_2 - \tilde{R}_1 + [\tilde{r}_2]_{t_0} - [\tilde{r}_1]_{t_0} \rangle \\ &= R_{I2}(t_0) - R_{I1}(t_0) + \langle R_{N2} + [r_{N2}]_{t_0} - R_{N1} - [r_{N1}]_{t_0} \rangle . \end{aligned}$$

Thus, with

$$K = \frac{f_2^2}{f_1^2 - f_2^2} ,$$

we take as an estimate of $R_{I1}(t_0)$:

$$\begin{aligned} \tilde{R}_{I1}(t_0) &\equiv K \langle \tilde{R}_2 - \tilde{R}_1 + [\tilde{r}_2]_{t_0} - [\tilde{r}_1]_{t_0} \rangle \\ &= R_{I1}(t_0) + K \langle R_{N2} + [r_{N2}]_{t_0}^t - R_{N1} - [r_{N1}]_{t_0}^t \rangle . \end{aligned}$$

It can also be shown that an estimate of $[R_{I1}]_{t_0}^t$ is given by:

$$\begin{aligned} [\tilde{R}_{I1}]_{t_0}^t &= K \{ [\tilde{r}_1]_{t_0}^t - [\tilde{r}_2]_{t_0}^t \} \\ &= [R_{I1}]_{t_0}^t + K \{ [r_{N1}]_{t_0}^t - [r_{N2}]_{t_0}^t \} . \end{aligned}$$

Combination of the last two expressions yields an estimate for $R_{I1}(t)$, namely

$$\begin{aligned}\tilde{R}_{I1}(t) = & R_{I1}(t) + K < R_{N2} + r_{N2} - R_{N1} - r_{N1} > \\ & + K [r_{N1}(t) - r_{N2}(t)] .\end{aligned}$$

Now, $\tilde{R}_{I1}(t)$ can be used to compensate \tilde{R}_1 and $[\tilde{r}_1]_{t_0}^t$ for ionospheric delay, and an estimate of $R(t_0)$ can be obtained by a Doppler smoothing technique.

Thus

$$\begin{aligned}\tilde{R}(t_0) = & < \tilde{R}_1 - [\tilde{r}_1]_{t_0} - 2 \tilde{R}_{I1} + \tilde{R}_{I1}(t_0) > \\ = & R(t_0) + R_S(t_0) + R_T(t_0) \\ & + < R_M + R_{N1} - [r_M]_{t_0} - [r_{N1}]_{t_0} > \\ & + K < R_{N1} - [r_{N1}]_{t_0} - R_{N2} + [r_{N2}]_{t_0} > \\ = & R(t_0) + R_S(t_0) + R_T(t_0) \\ & + < R_M + (1+K) R_{N1} - K R_{N2} > \\ & - < [r_M]_{t_0} + (1+K) [r_{N1}]_{t_0} - K [r_{N2}]_{t_0} > .\end{aligned}$$

Also an estimate of $[R]_{t_0}^t$ can be obtained by compensating $[\tilde{r}_1]_{t_0}^t$ with $[\tilde{R}_{I1}]_{t_0}^t$. Thus

$$\begin{aligned}[\tilde{R}]_{t_0}^t = & [R]_{t_0}^t + [R_S]_{t_0}^t + [R_T]_{t_0}^t + [r_M]_{t_0}^t + [r_{N1}]_{t_0}^t \\ & + K ([r_{N1}]_{t_0}^t - [r_{N2}]_{t_0}^t) .\end{aligned}$$

Finally, combination of the last two equations yields

$$\begin{aligned}\tilde{R}(t) &= R(t) + R_S(t) + R_T(t) + \langle R_M + (1+K) R_{N1} - K R_{N2} \rangle \\ &\quad - \langle r_M + (1+K) r_{N1} - K r_{N2} \rangle \\ &\quad + r_M(t) + (1+K) r_{N1}(t) - K r_{N2}(t) .\end{aligned}$$

The last equation provides a pseudo-range measurement which has been fully compensated for ionospheric delay. Except for the systematic error term R_S and the tropospheric error term R_T , the only errors are a bias (due to initialization @ t_0) and ultra-low phase noise terms. The bias term

$$\begin{aligned}R_B &= \langle R_M + (1+K) R_{N1} - K R_{N2} \rangle \\ &\quad - \langle r_M + (1+K) r_{N1} - K r_{N2} \rangle\end{aligned}$$

is approximately

$$R_B = \langle R_M + (1+K) R_{N1} - K R_{N2} \rangle ,$$

since the RMS values of R_M , R_{N1} , R_{N2} are greater than the corresponding values for r_M , r_{N1} , r_{N2} by at least a factor of 100.

Furthermore, the RMS value of R_B is simply

$$\sigma_B = \sqrt{\frac{\tau_R}{T}} (\sigma_{RM}^2 + (1+K)^2 \sigma_{RN1}^2 + K^2 \sigma_{RN2}^2)^{1/2} ,$$

where τ_R is the correlation time of the code receiver ($\tau_R = 1/B_R = 1$ sec).
If $T \gg \tau_R$, then

$$\sigma_B \ll (\sigma_{RM}^2 + (1+K)^2 \sigma_{RN1}^2 + K^2 \sigma_{RN2}^2)^{1/2} .$$

The last expression for $\tilde{R}(t)$ represents the most practical combination of pseudo-range and delta-range measurements with dual frequency ionospheric delay compensation. It is this value of $\tilde{R}(t)$ which, after compensation for tropospheric delay, should be input to the optimal estimator to obtain maximum navigation accuracy.

The pseudo-range measurement developed above contains unavoidable systematic error, R_S , tropospheric delay compensation error, δR_T , an initialization bias with RMS value proportional to $1/\sqrt{T}$, and an ultra-low noise error which is serially uncorrelated at a 10 Hz rate ($B_D = 1/\tau_D$, where $\tau_D = 0.1$ sec is the Doppler receiver correlation time).

In contrast to the above, there exists a similar processing technique in which Doppler smoothing is employed over discrete intervals of specified length, but only the initial condition on each interval is input to the estimator algorithm. In this case, the expression for $\tilde{R}(t_i)$, where t_i denotes the initial time of each discrete interval, is approximated by

$$\begin{aligned} \tilde{R}(t_i) \approx & R(t_i) + R_S(t_i) + R_T(t_i) \\ & + \langle R_M + (1+K) R_{N1} - K R_{N2} \rangle_i \end{aligned}$$

where now

$$\langle X \rangle_i = \frac{1}{t_{i+1} - t_i} \int_{t_i}^{t_{i+1}} X(t) dt$$

and phase noise terms have been neglected. With $\Delta t \equiv t_{i+1} - t_i$, it follows that the RMS noise error in the measurement sequence $\tilde{R}(t_i)$, $i = 0, 1, \dots$, is given by

$$\sigma_N = \sqrt{\frac{\tau_R}{\Delta t}} [\sigma_{RM}^2 + (1+K)^2 \sigma_{RN1}^2 + K^2 \sigma_{RN2}^2]^{1/2}$$

In this method the data rate is $1/\Delta t$, and the noise level is determined by the code noise. Thus in comparison to the previous method, this method is deficient both with respect to data rate and noise level. Quantitatively this deficiency can be expressed by a product of ratios. Thus

$$\left\{ \sqrt{\frac{\tau_R}{\Delta t}} \sigma_{RN} / \sigma_{rn} \right\} \times \sqrt{\frac{\Delta t}{\tau_D}} = \frac{\sigma_{RN}}{\sigma_{rn}} \sqrt{\frac{\tau_R}{\tau_D}} = \sqrt{10} \frac{\sigma_{RN}}{\sigma_{rn}} .$$

In reality, this latter method is equivalent to processing only the code measurements in the presence of a smooth trajectory constraint. Hence, the latter method does not make very effective use of the high precision and high data rate inherent in the pseudo-Doppler range measurements.

5.0 CONCLUSIONS AND RECOMMENDATIONS

This document orients the Range analyst toward use of GPS technology for meeting Test and Training Range TSPI requirements. The highly accurate GPS navigation capability has potential benefits of improved accuracy and lower costs for Range instrumentation. The Range analyst is aided in evaluating accuracy by the definition of error budgets and accuracy measures. Development of GPS compatible configurations is aided by discussions of system and data processing applications considerations. Use of GPS technology in Range instrumentation is a manageable problem involving the development of configurations meeting Test and Training Ranges requirements.

In order to expedite availability of this document at this time, it is not possible to develop each of the topics to the in-depth detail it might deserve. Additional work should supplement other projects such as the GPS evaluation tests at Yuma, the Triservices GPS Ranges Applications study, and development of the GPS-SMILS. It is assumed that the Triservices Study will provide generic GPS compatible range instrumentation configurations and requirements for receivers, translators and pseudo-satellites. The configurations should include data flow/processing diagrams.

This document addresses technical aspects of evaluating use of GPS technology in range instrumentation but not cost considerations. The Triservices study will develop cost information for selected generic ranges which can be used by the Range analyst to develop cost comparisons for specific situations.

Recommendations for follow-on work are:

- 1) Utilize the Yuma inverted GPS facility to determine near/far effect constraints.
- 2) Develop lag error models and calibration techniques for dynamic targets carrying various receiver and translator configurations.
- 3) Determine applicability of the translocation approach to ionospheric delay correction for various target flight paths, accuracy requirements, and time and distance separation.

- 4) Initiate a continuing effort to monitor GPS error budgets and refine accuracy estimation techniques for real-time and post-test modes using relative and absolute techniques.
- 5) Investigate use of operational GPS receivers for meeting range requirements: real-time result accuracy and timeliness, incorporation of a recorder or data link in the vehicle, and availability.
- 6) Identify and categorize test range raw data output requirements for real-time and post-test processing.
- 7) Develop GPS receivers, translators and pseudo-satellites for use in Range instrumentation.
- 8) Design and perform experiments to allow determination of fast and slow error sources and magnitudes for refinement of GPS data processing error correction.
- 9) Investigate the use of C/A code vs P-code for meeting Range TSPI requirements.
- 10) Evaluate the uses of C/A and P-code on combinations of L_1 and L_2 links and L_1 and L_3 links for estimating ionospheric delay.
- 11) Develop optimal estimation algorithms for GPS applications.

BIBLIOGRAPHY

1. Erb, Hinely, Seiders and White, Assessment of Enhanced TSPI Capability Requirements at Navy T&E and Fleet Training Ranges, Technical Report 7205-81-TR-115, July 1981, SRI International, Menlo Park, Calif.
2. J. N. Fredericksen, Applicability of NAVSTAR GPS to Test and Training, May 1980, The MITRE Corp., McClean, Virginia.
3. Principles of Error Theory and Cartographic Applications, ACIC Technical Report No. 96, February 1962, United States Air Force, St. Louis, Missouri.
4. SS-GPS-300B, System Specification for the NAVSTAR Global Positioning System, Code Ident 07868, 3 March 1980.
5. R. B. Pickett, F. L. Matthews and G. D. Trimble, Use of GPS and Telemetry Doppler in Trajectory Measurement Applications, Technical Note AS300-N-81-40, August 1981, Federal Electric Corporation-ITT, Vandenberg AFB, California.
6. Paul D. Perreault, Civilian Receivers Navigate by Satellite, January 1981, Microwave Systems News, Pgs 61-93, Stanford Telecommunications, Inc.
7. Wayne F. Brady and Paul S. Jorgenson, Worldwide Coverage of the Phase II NAVSTAR Satellite Constellation, The Aerospace Corp., El Segundo, California.
8. A. J. MacMillan, NAVSTAR Global Positioning System Flight Test Program Overview, The Aerospace Corp., El Segundo, California.
9. S. P. Teasley, W. M. Hoover, and C. R. Johnson, Differential GPS Navigation, Texas Instruments, Inc.
10. Phil Ward, Advanced NAVSTAR GPS Multiplex Receiver, Texas Instruments, Inc., Lewisville, Texas.
11. Kenneth Putkovitch, USNO GPS and TRANSIT Programs, U. S. Naval Observatory, Washington, D. C.
12. S. A. Book, W. F. Brady, and Mazaika, The Nonuniform GPS Constellation, Mazaika, The Aerospace Corp., El Segundo, California.
13. Paul S. Jorgenson, Combined Pseudo Range and Doppler Positioning for the Stationary NAVSTAR User, The Aerospace Corp., El Segundo, CA
14. W. C. Melton, Global Positioning System Measures Time of Arrival, Stanford Telecommunications, Inc., Microwave Systems News, January 1982, Vol. 12, No. 1, pgs 136-142.
15. Phase I NAVSTAR/GPS Major Field Test Objective Report, Ephemeris and Space Vehicle Clock Prediction Accuracy, 4 May 1979, NAVSTAR/GPS Joint Program Office, SAMS0, Los Angeles, California.

16. Vol. 25, No. 2, Global Positioning System, Reprint of Summer 1978 Institute of Navigation Journal, 1980.
17. Caroline F. Lerory, The Impact of GRS 80 on DMA Products, Defense Mapping Agency, Washington, D. C.
18. Dr. R. A. Brooks, Ionospheric Refraction Compensation in GPS Applications, Technical Note AS300-N-82-07, January 1982, Systems Performance Analysis Department, Federal Electric Corp.-ITT, Vandenberg AFB, California.
19. P. B. Levine and H. L. Jones, GPS Range Instrumentation Equipment Issues and Applications, 30 January 1982, The Analytic Sciences Corp., Reading, Massachusetts.
20. P. S. Jorgenson, Ionospheric Measurements from NAVSTAR Satellites, December 1978, The Aerospace Corp., El Segundo, California.
21. A. J. Mallinckrodt, Group and Phase Phenomena in an Inhomogeneous Ionosphere, Santa Ana, California.
22. Phase I NAVSTAR/GPS Major Field Test Objective Report, Tropospheric Correction, 4 May 1979. Navstar/GPS Joint Program Office, Los Angeles, California.
23. Phase I NAVSTAR/GPS Major Field Test Objective Report, Ionospheric Refraction, 4 May 1979, NAVSTAR/GPS Joint Program Office, Los Angeles, California.
24. V. L. Pisacane and M. M. Feen, Ionospheric Effects on Transionospheric Measurements of Range and Range Difference TG 1267, October 1974, Johns Hopkins University, Applied Physics Laboratory, Silver Spring, Maryland.
25. J. A. Klobuchar, M. A. and J. A. Pearson, A Preliminary Evaluation of the Two-Frequency Ionospheric Correction for the NAVSTAR-Global Positioning System, Air Force Geophysics Laboratory, Hanscom AFB, The Aerospace Corp., Los Angeles, Calif.
26. J. A. Klobuchar, Ionospheric Time Delay Corrections for Advanced Satellite Ranging Systems, Air Force Geophysics Laboratory, Hanscom AFB, MA.
27. J. A. Klobuchar and J. M. Johnson, Correlation Distance of Mean Daytime Electron Content, AFGL-TR-77-0185, Air Force Surveys in Geophysics, No. 373, 22 August 1977, Air Force Geophysics Laboratory, Hanscom AFB, MA.
28. John A. Klobuchar, A First-Order, Worldwide, Ionospheric, Time-Delay Algorithm, AFCRL-TR-75-0502, Air Force Surveys in Geophysics, No. 324, 25 September 1975, Air Force Geophysics Laboratory, Hanscom AFB, MA.
29. E. G. Blakwell, J. S. Cline, E. A. Erb, and J. R. Olmstead, GPS-SMILS Concept Definition, WSMC TR 80-1, March 1980, SRI International, Menlo Park, California.
30. John H. Painter, Designing Pseudorandom Coded Ranging Systems, Motorola, Inc., Scottsdale, Arizona.

-
31. S. C. Gupta and J. H. Painter, Correlation Analysis of Linear, Processed Pseudo Random Sequences, December 1966, Motorola, Inc., Scottsdale, AZ.
 32. Rodney J. Boehm, Simulation of a Kalman Filter for GPS, June 1979, Texas A&M University, College Station, Texas.
 33. Steven B. Hyde, A NonLinear Technique to Compensate for Range Bias Error in a Low Cost GPS Set, TCSL Memo # 8009, August 1980, Texas A&M University, College Station, Texas.
 34. Rodney J. Boehm, An Adaptive Gain Technique for the GPS Extended Kalman Filter, TCSL Memo 7910, November 1979, Texas A&M University, College Station, Texas.
 35. M. D. Eggers and D. M. Ballock, Computer Simulation of Ionospheric Wave, Propagation for Detection of Range Error for Satellite Navigation Systems, TCSL Research Memorandum 81-06, May 19, 1981, Texas A&M University, College Station, Texas
 36. Col. Donald W. Hederson, Joseph A. Strada, Lt. Com., NAVSTAR Field Test Results, MX-TM-3316-80A, July 20, 1980, USAF Space Division, El Segundo, CA.
 37. L. J. Jacobson, and V. Calbi, Engineering Development of NAVSTAR GPS User Equipment, April 1981, Magnavox Advanced Products and Systems Company, Torrance, California
 38. Richard Enossen, Low-Cost GPS Navigation Receiver for General Aviation, February 1980, Magnavox Government and Industrial Electronics Company, Torrance, California
 39. Technical Data Sheet, Collins GPS User Equipment Manpack/Vehicular Application, Rockwell International, Collins Government Avionics Division.
 40. Technical Data Sheet, Collins GPS User Equipment Surface Ship Application, Rockwell International, Collins Government Avionics Division.
 41. Technical Data Sheet, Collins GPS User Equipment Submarine Application, Rockwell International, Collins Government Avionics Division.
 42. Technical Data Sheet, Collins GPS User Equipment Rotary Wing Aircraft Application, Rockwell International, Collins Government Avionics Division.
 43. Technical Data Sheet, Collins GPS User Equipment Transport/Patrol Aircraft Application, Rockwell International, Collins Government Avionics Division.
 44. Technical Data Sheet, Collins GPS User Equipment, Strategic Bomber Application, Rockwell International, Collins Government Avionics Division.
 45. Technical Data Sheet, Collins GPS User Equipment, Attack Aircraft Application, Rockwell International, Collins Government Avionics Division.

46. G. Trimble, R. Weigel and S. Cresswell, Analysis of the Ballistic Receiver Evaluation Wafer Flight Test, OP 7434 (PVM-19), June 1981 Technical Report Number AS300-T-81-27, Systems Performance Analysis Department, Federal Electric Corporation, ITT, Vandenberg AFB, CA.
47. G. Trimble, R. Weigel and S. Cresswell, Analysis of the Ballistic Receiver Evaluation Wafer Flight Test, OP1767 (PVM-18) Technical Report AS300-T-80-33, November 1980, Systems Performance Analysis Department, Federal Electric Corporation, ITT, Vandenberg AFB, California
48. Multi-Object Tracking, Range Instrumentation Symposium, 3-4 March 1981, Volume 1 - Unclassified
49. GPS-RTP, ICD-4, MBRS Functional Characteristics, Interface Control, June 3 1978 plus Revisions SAMSO AFSC, Norton AFB, CA.
50. Space Vehicle Nav Subsystem and NTS PRN Navigation Assembly/User System Segment and Monitor Station, August 1979, Rockwell International Corp., Space Division, Downey, CA.
51. R. L. Barkley, Jr., and R. T. Herzog, Global Positioning System Mobile Missile Tracking Platform Feasibility Study, 30196-6002-TU-00, 30 June 1977, TRW Defense and Space Systems Group, Redondo Beach, CA.
52. Nicholas Stilwell, Edward H. Martin, and Jack Moses, GPS Study for Range Instrumentation, Final Report for Space and Missile Test Center (XREA), 30 March 1977, Magnavox Government and Industrial Electronics Co., Advanced Products Division, Torrance, CA.
53. R. L. Bogusch, F. W. Guigliano, D. L. Knepp, and A. H. Michelet, Frequency Selective Propagation Effects on Spread-Spectrum Receiver Tracking, Mission Research Corp., Santa Barbara, CA; Proceedings of the IEEE, Vol 69, No. 7, July 1981, pgs 787-796.
54. W. R. Fried, A comparative Performance Analysis of Modern Ground-Based, Air-Based, and Satellite-Based Radio Navigation Systems, Hughes Aircraft Co., Fullerton, CA; Journal of the Institute of Navigation, Vol 24, No.1, Spring 1977, pgs 48-58.
55. Technical Digest, Johns Hopkins APL, Navy Navigation Satellite System (Transit) Issue; January-March 1981, Vol 2, No. 1.
56. Jack K. Holmes, Coherent Spread Spectrum Systems, John Wiley & Sons, New York, N. Y. 1982.
57. James J. Spilkor, Digital Communications by Satellite, Prentice Hall, Englewood Cliffs, NJ 1977.
58. John D. Cardall and Richard S. Crossen, Civil Application of Differential GPS, Oct. 1981, Magnavox Advanced Products and Systems Company, Torrance, CA.
59. Jacques Beser and Bradford W. Parkinson, The Application of NAVSTAR Differential GPS in the Civilian Community, Intermetrics, Inc., Huntington Beach, CA.

60. W. A. Eliot, Applicability of GPS as Range Instrumentation, 16 April 1981, The MITRE Corp., McLean, VA.
61. W. A. Eliot, GPS Performance Using Aircraft Pod-Mounted Antennas, 12 June 1981, The MITRE Corp., McLean, VA.
62. H. Leon Harter, Circular Error Probabilities, Aeronautical Research Laboratories, Wright-Patterson, Air Force Base.
63. 95GP05215, Navigating with the GPS, Rockwell International Space Division.
64. R. L. Harrington and J. T. Dolloff, The Inverted Range: GPS User Test Facility, General Dynamics Electronics Division, San Diego, California, pgs 204-211, IEEE PLANS 76.
65. Gauss, Karl F., Theory of the Motion of the Heavenly Bodies Moving About the Sun in Conic Sections, New York, Dover Publications Inc., 1963 (Reprint).
66. Kalman, R. E., "A New Approach to Linear Filtering and Prediction Problems", Journal of Basic Engineering, Transaction ASME, Vol. 82D, 1960, pp.35-50.
67. Meditch, J. S., Stochastic Optimal Linear Estimation and Control, McGraw-Hill, New York, 1969.
68. Carlson, N. A., "Fast Triangular Formulation of the Square Root Filter", AIAA Journal, Vol. 11, Number 9, September 1973, pp. 1259-1265.
69. Brooks, R. A., Trajectory Reconstruction Methodology, SAMTEC TR-79-1.
70. J. M. Przyjemski, P. L. Konop, "Limitations on GPS Receiver Performance Imposed by Crystal Oscillator G-Sensitivity", C. S. Draper Laboratory Report P-432, March, 1977 NAECON '77 Record, pp 319-322.
71. "A Compensation Technique for Acceleration - Induced Frequency Changes in Crystal Oscillators", C. S. Draper Laboratory Report P-606, NAECON '78 Record, May 1978.
72. J. I. Statman and W. J. Hurd, "Study Report on Applicability of NAVSTAR Global Positioning System to MAFIS", Jet Propulsion Laboratory Report 7011-31, July 2, 1982.
73. P. S. Jorgenson, "Normalized Accuracy of the NAVSTAR/Global Positioning System", The Aerospace Corporation, Report No. TOR-0078(3475-10)-2, 28 February 1978.

APPENDICES

A. LINEAR ESTIMATION

Consider a linear stochastic system described by

$$(1) \quad x_{i+1} = \Phi_i x_i + u_i, \quad i = 0, 1, \dots, N-1,$$

$$(2) \quad y_i = H_i x_i + v_i, \quad i = 0, 1, \dots, N.$$

In these equations x is the state vector, and y is the measurement vector. $\{u_i, i = 0, 1, \dots, N-1\}$ is a sequence of random vectors called the state noise process, and $\{v_i, i = 0, 1, \dots, N\}$ is a similar sequence called the measurement noise process. These processes are assumed to be zero mean, sequentially uncorrelated, and mutually uncorrelated with each other and x_0 . Mathematically these assumptions are expressed as follows:

$$E(u_i) = 0, E(u_i u_j^T) = Q_i \delta_{ij}; \quad i, j = 0, 1, \dots, N-1,$$

$$E(v_i) = 0, E(v_i v_j^T) = R_i \delta_{ij}; \quad i, j = 0, 1, \dots, N$$

and

$$E(u_i v_j^T) = 0, E(x_0 u_i^T) = 0, E(x_0 v_j^T) = 0;$$

where

$$\delta_{ij} = \begin{cases} 1, & i = j \\ 0, & i \neq j \end{cases}.$$

Q and R are the state noise and measurement noise covariance matrices, respectively. To complete the system description, it is assumed that the a priori mean and covariance of x_0 , denoted by \hat{x}_0 and P_0 , respectively, are also specified.

The estimation procedures to be considered in the remainder of this appendix will apply to the linear system given by (1) and (2).

A.1 Optimal Linear Estimation

For the system (1), (2), let $\tilde{x}(i|j)$ denote a function which is in the form of a constant plus a linear function of the measurement set y_0, \dots, y_j and which has the property $E[\tilde{x}(i|j)] = E(x_i)$. Such a function is said to be a linear unbiased estimate of x_i given y_0, \dots, y_j .

Let $\hat{x}(i|j)$ be a linear unbiased estimate of x_i given y_0, \dots, y_j , and suppose $\hat{x}(i|j)$ has the property*

$$E[||\hat{x}(i|j) - x_i||^2] \leq E[||\tilde{x}(i|j) - x_i||^2]$$

for all linear unbiased estimates $\tilde{x}(i|j)$ of x_i given y_0, \dots, y_j . Then $\hat{x}(i|j)$ is said to be an optimal linear estimate of x_i given y_0, \dots, y_j .

It can be shown that an optimal linear estimate of x_i given y_0, \dots, y_j always exists and is unique. The notation $\hat{x}(i|j)$ will be used exclusively to denote the optimal estimate defined above, and the notation $P(i|j)$ will be used to denote the error covariance of $\hat{x}(i|j)$ defined by

$$P(i|j) \equiv E[(\hat{x}(i|j) - x_i)(\hat{x}(i|j) - x_i)^T].$$

$P(i|j)$ is also called the state covariance of x_i given y_0, \dots, y_j .

A.2 Kalman Estimation

A recursive procedure for realization of the optimal linear estimator for the system (1), (2) has been developed by Kalman [3], [4]. The procedure consists of two stages. The first stage employs a filter algorithm, while the second uses a smoother algorithm**.

* The notation $||z||^2 \equiv z^T z$ denotes the ordinary Euclidean norm of z .

**The terminology employed here is due to N. Wiener and has been adopted by R. Kalman. An estimator which estimates x_i given measurements with indices up to and including j is called a filter if $i = j$; it is called a predictor if $i > j$, and it is called a smoother if $i < j$.

Application of the Kalman filter to the system (1), (2) yields $\hat{\bar{x}}(i|i) \equiv \hat{x}_i$ and $P(i|i) \equiv P_i$ by recursion. The algorithm is

$$(3) \quad K_i = P_i^{-1} H_i^T [H_i P_i^{-1} H_i^T + R_i]^{-1},$$

$$(4) \quad \hat{x}_i = \hat{\bar{x}}_i + K_i (y_i - H_i \hat{\bar{x}}_i),$$

$$(5) \quad P_i = P_i^{-1} - K_i H_i P_i^{-1}, \quad i = 0, 1, \dots, N,$$

$$(6) \quad \hat{\bar{x}}_{i+1} = \phi_i \hat{x}_i,$$

$$(7) \quad P_{i+1}^{-1} = \phi_i P_i \phi_i^T + Q_i, \quad i = 0, 1, \dots, N-1.$$

The smoother algorithm is initiated when the filter stage is complete. The smoother uses the filter outputs in a recursive process, which runs in reverse order to the filter recursion, to compute $\hat{x}(i|N)$ and $P(i|N)$, $i = 0, 1, \dots, N$. The algorithm for smoothing is given by

$$(8) \quad A_i = P_i \phi_i^T (P_{i+1}^{-1})^{-1},$$

$$(9) \quad \hat{x}(i|N) = \hat{x}_i + A_i [\hat{x}(i+1|N) - \hat{\bar{x}}_{i+1}],$$

$$(10) \quad P(i|N) = P_i + A_i [P(i+1|N) - P_{i+1}^{-1}] A_i^T, \quad i = N-1, \dots, 0.$$

GLOSSARY

ACRONYMS

SECTION

BET	=	Best Estimate of Trajectory	4.81
bps	=	Bits Per Second	4.8.2
C/A	=	Coarse or Clear Acquisition Code, 2 MHz	2.0
CEP	=	Circular Error Probable	3.0
CPU	=	Computer Processor Units	4.9.1.3
CRPA	=	Controlled Reception Pattern Antenna	4.9.1.1
CRT	=	Cathode Ray Tube	4.8.1
dB	=	Decibels	2.0
DBI	=	Decibels	2.0
DBW	=	Decibels Referred to 1 w	2.0
DCO	=	Digitally Controlled Oscillator	4.8.2
DOP	=	Dilution of Precision	3.0
ETR	=	Eastern Test Range	4.7.1
FMI	=	Flexible Modular Interface	4.9.1.3
FOM	=	Figure of Merit	3.0
FRPA	=	Fixed Reception Pattern Antenna	4.9.1.1
g	=	Unit of Gravity	4.9.3
GPS	=	Global Positioning System	2.0
GPS-SMILS	=	GPS-Sonobuoy Missile Impact Location System	4.7.1
HDUE	=	High Dynamic User Equipment	4.7.2
Hz	=	Hertz, Cycles per Second	2.0
ICBM	=	Intercontinental Ballistic Missile	4.0
IF	=	Intermediate Frequency	4.7.3.2.3
IG	=	Inertial Guidance	4.10
IGS	=	Inertial Guidance System	4.9.3
INS	=	Inertial Navigation System	4.9.3
JHU-APL	=	Johns Hopkins University-Applied Physics Lab	4.7.1
JPO	=	Joint Program Office	1.1
KFS	=	Kalman Filter/Smoother	4.10
kHz	=	KiloHertz	4.7.3.2.2
kts	=	Knots	4.9.3

GLOSSARY (Continued)

ACRONYMS		SECTION
L_1, L_2	=	Designations for GPS SV Signals 2.0
LEP	=	Linear Error Probable 3.0
LRU	=	Line Replaceable Units 4.9.1
MAE	=	Missile Accuracy Evaluation 4.8
MBRS	=	Missile Borne Receiver Set 4.7.1
MHz	=	Mega Hertz 2.0
MX	=	Missile X 4.8
P	=	Precision Code, 20 MHz 2.0
PCM-NRZ	=	Pulse Code Mod - Non Return To Zero 4.7.3.2.2
$P_C(R)$	=	Circular Error Probability 3.0
$P_E(K;3)$	=	Elliptical Error Probability in 3 Dimensions 3.0
$P_L(R)$	=	Linear Error Probability 3.0
PM	=	Phase Modulation 4.7.3.2.3
PN	=	Pseudo-Noise 4.8.2
PSK	=	Phase Shift Keyed 4.7.3.2.2
$P_S(R)$	=	Spherical Error Probability 3.0
QPSK	=	Quad Phase Shift Keyed 4.7.3.2.2
R&D	=	Research and Development 4.8.1
RF	=	Radio Frequency 2.0
RH	=	Right Hand (Polarization) 2.0
RMS	=	Root Mean Square 4.2.1
SEP	=	Spherical Error Probable 3.0
σ_C	=	Circular Standard Error 3.0
σ_S	=	Spherical Standard Error 3.0
SNR, S/N	=	Signal to Noise Ratio, dB 4.7.3.2.2
SPS	=	Samples Per Second 4.8
SRU	=	Shop Replaceable Units 4.9.1
SV	=	GPS Satellite "Space Vehicle" 2.0
TTF	=	Time to First Fix 4.9.4
USERE	=	User Equivalent Range Error 2.0
VCO	=	Voltage Controlled Oscillator 4.8.2
WLS	=	Weighted Least Squares 4.10
WSMC	=	Western Space and Missile Center PREFACE
WTR	=	Western Test Range 4.7.1

END

FILMED

7-83

DTIC